THE SCATTERING OF LOW ENERGY ELECTRONS FROM HYDROGEN, HELIUM, AND ARGON.

A Thesis

Presented for the degree of Doctor of Philosophy

in

The University of Adelaide

by

Peter J.O. Teubner, B.Sc.

Department of Physics

1967.

TABLE OF CONTENTS

SUMMARY

A modulated crossed beam apparatus has been used to study the angular distribution of elastically scattered electrons from helium, argon, atomic hydrogen, and molecular hydrogen. The energies of the incident electrons used in the investigation ranged from 50 electron volts to 200 electron volts, and the electrons were observed over the angular range from 25° to 130°.

Details are given of the high current density, multistage electron gun which produced the incident electron beam. A parallel plate electron spectrometer was used to analyse the energy of the scattered electrons.

The measurement of the angular distribution for elastic scattering of electrons from helium at incident energies of 50, 75, 100, and 200 electron volts is described. The results are compared with other measurements and are discussed in the framework of recent calculations.

A modulated argon beam has been used to obtain the angular distribution of 50, 100, 150, and 200 electron volt electrons elastically scattered from argon. The present results are compared with other results which were obtained using a different technique.

An investigation of the angular distribution of elastically scattered electrons from molecular hydrogen has been undertaken. These results, which play an important role in determining the elastic scattering from atomic hydrogen, are compared with other

measurements and with theoretical calculations.

A beam containing a high percentage of atomic hydrogen has been produced in a low pressure tungsten furnace. The percentage of atomic hydrogen in the beam was determined with a mass spectrometer. The beam has been used to determine the angular distribution of elastically scattered electrons from atomic hydrogen for incident energies of 50, 75, 100, and 200 electron volts. The results, which constitute a sensitive test of approximations in the quantum theory of scattering, are compared with several calculations.

ACKNOWLEDGEMENTS

I would like to thank Dr. E. Weigold for his encouragement during the early developmental stages of this work and Professor J.H. Carver for his guidance throughout the course of the project.

The apparatus was constructed by the Staff of the Physics Department Workshop. Their work and in particular that of Mr. E. Comnock and Mr. P. Schebella is gratefully acknowledged.

The modulated beam analyser was designed and constructed by Mr. K. Williams. I would like to thank Mr. Williams for his many fruitful suggestions.

Thanks are due to my wife, Jillian, for her help in the preparation of the manuscript of this thesis; to Dr.B.L. Scott for providing tables of values of the differential cross section for elastic scattering of 54 electron volt electrons from atomic hydrogen; to Dr. S.P. Khare for tables of values of differential cross sections for elastic scattering of electrons from helium and molecular hydrogen; and to Dr. K.H. Loken for his ready assistance whenever it was required.

I am grateful to the Commonwealth Government for the financial assistance provided by a Commonwealth Postgraduate Award.

STATEMENT

This thesis contains no material which has been accepted for the award of any other degree or diploma in any University.

To the best of my knowledge and belief it contains no material previously published or written by another person except where due reference is made in the text.

Peter J. Teubner,

November 1967.

CHAPTER I

THE SCATTERING OF LOW ENERGY ELECTRONS FROM ATOMS.

I.1 HISTORICAL REVIEW

1(a). General.

The importance of the use of low energy electrons as sensitive probes in the investigation of the physics of atomic collisions was first illustrated by Franck and Hertz (1914). Their experiments on the scattering of electrons by mercury vapour provided confirmation of the Bohr theory of quantised energy states.

This old quantum theory was unable to predict the diffraction of electron waves by atomic systems. The new quantum theory of Schrödinger removed the fault in the old theory and Born's theory of successive approximations (Born 1926) was capable of describing the scattering process. However the Born approximation had two important omissions. Firstly it did not allow for the distortion of the incoming and outgoing electron waves by the atomic field of the atom and secondly it did not take account of the effect of exchange of the atomic and incident electron.

By adapting a method used by Rayleigh in the treatment of the scattering of sound waves by obstacles, Faxen and Holtsmark (1927) described electron scattering by a static potential field and allowed for distortion.

Oppenheimer (1928) was able to account for the possibility of interference effects between atomic and incident electrons by the inclusion of exchange in Born's theory. The Born-Oppenheimer theory however neglected the possibility of distortion just as Faxen and Holtsmark neglected the effects of exchange.

Massey and Mohr (1932) took as the first approximation, not plane waves, but rather waves that had been distorted by the field of the atom. By the inclusion of exchange, satisfactory agreement between their prediction of large angle elastic scattering and experimental differential cross sections was obtained. The discrepancies between predicted and experimental low angle scattering were removed by the inclusion of a polarisation potential (Massey and Mohr 1934).

Thus by 1934 "it was widely felt that the field was completely understood in principle and that a limited number of then impossible experiments and calculations would tie up the entire matter" Fite and Gerjuoy(1965).

The general decline in interest in the field of electron atom collisions was due no doubt to this prevailing idea. However in the past decade the field has expanded to such an extent that interest is now greater than it ever was in the 1930's (Massey 1964).

The reasons for the upsurge are related to the corresponding rise in the fields of space physics, plasma physics, and upper atmosphere physics - all of which rely heavily on basic electron-atom

collision phenomena. Advances in experimental techniques and in the speed of digital computers have enabled electron-hydrogen atom collisions to be studied experimentally and have increased the range of theoretical work which has been attempted. Some of the impossible experiments and calculations have been performed and in general have presented more problems than they have solved. (Fite and Gerjuoy (ibid.)

1(b). Electron - Hydrogen Atom Interactions.

Since the wave functions for the hydrogen atom are known analytically and since the interaction between the electron and the hydrogen atom is known, it is not surprising that electron hydrogen collision processes have dominated the theoretical work not only in the 1930's but also in more recent times. Experimentally it has proven very difficult to work with atomic hydrogen. In fact before 1958, there were very few quantitative experiments performed involving electrons and atomic hydrogen. In 1958, Fite and Brackmann (1958) had developed the modulated crossed beam technique of Boyd and Green (1958) to such a stage that the absolute cross section for the ionization of hydrogen atoms by electrons from threshold to 700 electron volts was measured. These results did not give good agreement with the Born approximation calculations at energies below 200

electron volts.

Lichten and Schultz (1959), Stebbings et al. (1960) have measured the excitation cross section to the 2S state of atomic hydrogen for incident electron energies from threshold to 500 electron volts. When the results were compared with the sophisticated close coupling expansion of Burke, Schey, and Smith (1963) agreement was poorer than was expected. Hils, Kleinpoppen, and Koschmieder (1966) have remeasured this cross section. They have found reasonable agreement with the experimental results of Stebbings et al. thereby casting doubt on the close coupling calculation.

Measurements of the total cross section for the excitation of the 2P state have been made by Fite and Brackmann (1958a) and by Fite, Stebbings, and Brackmann (1959). The poor agreement with a close coupling calculation has subsequently been verified by the laboratory data of Smith (1965).

The total elastic scattering cross section for electrons from atomic hydrogen has been measured by Bederson et al. (1957), Brackmann, Fite, and Haynaber (1958), Haynaber et al. (1961) for incident energies from 1 electron volt to 10 electron volts. The discrepancy between the results of Bederson et al. and those of Brackmann et al. prompted Gilbody, Stebbings, and Fite (1961) to measure the angular distribution for elastic scattering of electrons

from atomic hydrogen for incident energies of 9.4 e.v., 7.1 e.v., 5.7 e.v., and 3.4 e.v. between 30° and 130°. Because of their experimental arrangement Gilbody et al. were restricted to energies below the excitation threshold.

Above 10 electron volts there are no laboratory measurements on the elastic scattering cross section either total or differential. Hence the only data which is available is that which has come from the various theoretical calculations. Clearly there is a need to extend the elastic scattering measurements so that the approximations involved in the theory can be tested.

The present investigations on electron-hydrogen atom collisions have been involved with the measurement of the angular distribution for elastic scattering at incident energies of 50, 75, 100, and 200 electron volts. The results of these investigations are presented in Chapter V.

1(c). Elastic Scattering of Electrons from Helium.

Because of the relative ease of working with helium and its relative simplicity from the theoretical point of view, much work has been done on elastic scattering from helium.

Hughes, McMillen, and Webb (1932) have made an experimental

study of the differential cross section for the elastic scattering of electrons from helium in the energy range from 25 electron volts to 912 electron volts whilst Bullard and Massey (1931) determined differential cross sections from 4 electron volts to 50 electron volts.

The calculations of Massey and Mohr (1934) which included exchange and polarization, greatly improved the agreement between theory and experiment. However Kingston, Moiseiwitsch, and Skinner (1960) and Kingston and Skinner (1961) have pointed out an inconsistency in the former approach. This inconsistency led Khare and Moiseiwitsch (1965) to investigate afresh the role of polarization in the electron-helium elastic scattering process. The results of the calculation were compared with the 1952 results of Hughes et al. The agreement of the theoretical calculations although very good indicated the need for confirmation of the Hughes et al. data using modern techniques.

A recent calculation of Banerjee, Jha, and Sil (1966) which disagreed both with the theoretical calculations and the laboratory data of Hughes et al. further emphasized the need for new measurements.

The present investigation on the electron-helium elastic scattering process has been concerned with energies between 50 electron volts and 200 electron volts. It is in this energy range

where the role of polarisation is expected to play its most important role in modifying the angular distribution predicted by the first Born approximation.

The results of the investigation are presented in Chapter IV.

1(d). Elastic Scattering from Argon.

The angular distribution of elastically scattered electrons from argon was first observed by Bullard and Massey (1931). Subsequent investigations by Arnot (1931), Hughes and McMillen (1932), Mohr and Nicoll (1932) and Webb (1935(a)) confirmed the general shape of the angular distribution curves.

Perteus (1964) has used a different technique to that used in the earlier measurements and has found discrepancies between his results and the measurements of Hughes and McMillen (ibid).

In view of the advantages offered by the modulated crossed beam technique over earlier techniques, a study of elastic scattering from argon has been undertaken in the energy range from 50 electron volts to 200 electron volts and in the angular range from 30° to 130°. The results of this investigation are presented in section IV.2.

1(e). Elastic Scattering from Molecular Hydrogen.

Arnot (1931) and Webb (1935(b)) have measured the angular distribution for the elastic scattering of electrons from molecular hydrogen in the energy range from 29 to 912 electron volts. The agreement between the two sets of results at an incident energy of 200 electron volts was very good.

The present measurements of the angular distribution for elastic scattering of electrons from molecular hydrogen were made because of the important role which elastic scattering played in the determination of the angular distribution of electrons elastically scattered from atomic hydrogen. The present elastic e-H_2 angular distributions are given in Chapter V.

I.2 Theory of Electron Atom Collisions.

In so far as the experimental work described in this thesis is concerned, the velocities of the electrons under investigation was not great compared with the velocities of the atomic electron. Thus the collision can be described as "slow". (Massey 1956)

The theory of elastic scattering of electrons by atoms has been the subject of many review articles. Massey (1956, 1956(a)); Burke and Smith (1962); Moiseiwitsch (1962); Massey (1964); Mott and Massey

(1965); Massey and Burhop (1952); Cerjuey (1965).

In this section, the main features of the several approximations which will be compared with the experimental results of Chapters IV and V will be described. The details of the use of these approximations will be left until the discussion of the results in the appropriate chapters.

For simplicity, the hydrogen atom will be discussed and the possibility of exchange in the equations will be neglected.

The Schrödinger equation for an electron in the field of a hydrogen atom is

$$\left[\frac{\hbar^2}{2m}(\nabla_1^2 + \nabla_2^2) + E - \frac{e^2}{r_{12}} + \frac{e^2}{r_1} + \frac{e^2}{r_2}\right]\Psi(r_1, r_2) = 0 \qquad \ldots(1.1)$$

where the subscripts 1 and 2 refer to the atomic and incident electrons respectively. If the wave number of the incident electron is expressed as k_o, the energy E of the system can then be expressed as

$$E = E_n + \frac{\hbar^2}{2m} k_o^2$$

where E_n describes the eigen energy of the state n.

Equation (1.1) can be simplified by expanding the total wave function $\Psi(r_1, r_2)$ in terms of the eigenfunctions of the target

Hamiltonian (Massey and Mohr (1932)).

i.e. $$\Psi(r_1, r_2) = \left(\sum_n + \int dn \right) \psi_n(r_1) F_n(r_2) \qquad \ldots (1.2)$$

The wave equation for the hydrogen atom is given by

$$\left[\frac{\hbar^2}{2m} \nabla_1^2 + E_n + \frac{e^2}{r_1} \right] \psi_n(r_1) = 0 \qquad \ldots (1.3)$$

The integral symbol in equation (1.2) allows for integration over the states of positive energy which form a continuum.

Substitution of equation (1.2) into (1.1) and using equation (1.3) gives a set of coupled equations for the expansion coefficients F_n - which can be expressed as

$$\left[\nabla_2^2 + k_n^2 \right] F_n(r_2) = \left(\sum_m + \int dm \right) U_{mn} F_m(r_2) \qquad \ldots (1.4)$$

where U_{mn} describes the matrix element between states m and n and the interaction potential $\frac{e^2}{r_{12}} - \frac{e^2}{r_2}$ and is given by

$$U_{mn} = \frac{2me^2}{\hbar^2} \int \psi_n^* \left(\frac{1}{r_{12}} - \frac{1}{r_2} \right) \psi_m \, dr_1$$

and

$$k_n^2 = \frac{2m}{\hbar^2} (E - E_n)$$

Solutions for F_n, which describes the relative motion of the incident projectile and the target atom in a quantum state specified by n, are required which, for axial symmetry, satisfy the boundary conditions

$$F_n(0) = 0$$

$$F_n(r) = \frac{e^{ik_n r_2}}{r_2} f(\theta) + e^{i\underline{k}_0 r_2}$$

The differential cross section for elastic scattering is given by

$$I(\theta)\, dw = \left| f(\theta) \right|^2 dw$$

Since it is not possible to solve equations (1.4) exactly it is necessary to make approximations in order that the equations for $F_n(r)$ can be uncoupled.

The simplest approximation is the first Born approximation which is obtained by setting

$$F_0(r_2) = e^{i\underline{k}_0 r_2}$$

and $\quad F_m(r_2) = 0 \quad$ for all $\quad m \neq 0$

in equation (1.4) which then becomes

$$(\nabla_2^2 + k_n^2) F_n(r_2) = U_{no}(r_1)\, e^{i\underline{k}_0 r_2}$$

and by using Green's function the elastic scattering amplitude to the first Born approximation $f_{B1}(\theta)$ results. Where

$$f_{B1}(\theta) = -\frac{1}{4\pi}\int e^{i(\underline{k}_o-\underline{k}_n).r_2} U_{oo}\, dr_2$$

where

$$U_{oo} = \frac{2me^2}{\hbar^2}\int |\psi|^2\left(\frac{1}{r_{12}} - \frac{1}{r_2}\right) dr_2$$

Thus the elastic scattering amplitude in the first Born approximation is the same as that by a structureless scatterer having a potential energy equal to the mean interaction energy between the electron and the atom, the atom remaining undisturbed in its ground state.

The Born-Oppenheimer approximation is obtained when exchange between the atomic and incident electron is considered.

The criterion for the use of the Born approximation is given by Massey (1956) as that which is satisfied when the energy of the incident electron is very much greater than the internal energy of the system, that is when

$$\frac{\hbar^2}{2m} k_o^2 \gg E_n$$

Since it is relatively simple to perform calculations using the first Born approximation it is important that the lower limit for

the validity of the approximation is known. To date the evidence on the validity has come from the comparison of the calculations of Massey and Mohr (1932) on helium. These calculations however show a marked dependence on the accuracy of the wave function which is used (Mott and Massey 1965). Thus any experimental check on the validity of the approximation based on electron-helium interactions must test a composite of the validity of the wave function as well as the approximation.

Another way of looking at the Born approximation is to regard the exact scattering amplitude as being expanded in powers of the interaction. The first Born approximation retains only those terms which are linear in the interaction.

The next level of approximation comes from considering terms which are quadratic in the interaction and yields the second Born approximation. The simplest form of this approximation arises from ignoring all the second order terms which correspond to excitation. The problem therefore is reduced to potential scattering where allowance is made for both the incident and scattered electron waves to be distorted by the effective field of the atom in its ground state.

As the energy of the incident particle decreases, it spends more time in the vicinity of the target atom and can suffer more

scatterings. Thus to represent the interaction accurately all possible scatterings must be taken into account.

At low energies it is clearly not correct to ignore the possibility of excitation completely. If the possibility of large changes in momentum between the incident and target electrons is allowed so that several elastic scatterings can occur, then clearly excitation must also take place. A description of the way in which the excitation of states can affect angular distributions of elastically scattered electrons has been given by Massey and Burhop (1952). If the incident electron velocity is small it may cause a transition in the atom whilst traversing the atomic field. When this occurs the electron will on average suffer only a slight deviation from its path. Before emerging from the atomic field, the atom may revert back to the ground state returning the energy to the original electron. The nett result of such a collision would be to produce an electron which has lost no energy and is only deviated slightly from its original path.

Massey and Mohr (1934) have shown that the inclusion of a polarization potential in the radial wave equation can account for such a double collision. At long range for the spherically symmetric ground state of a neutral target atom, the polarization potential is itself spherically symmetric and inversely proportional to the fourth

power of the radius vector.

It is possible to allow for excitation directly in the wave-function expansion (1.2) by writing

$$\Psi = \psi_0(r_1) F_0(r_2) + \psi_n(r_1) F_n(r_2)$$

If only S states are included in the expansion, the approximation suffers from two main defects. The first is that it completely ignores the polarisation potential and secondly, as has been noted by Hummer and Seaton (1961) and Krall and Cerjuay (1961) it is important to include all degenerate eigenfunctions in the initial and final states. Inclusion of the 2p state leads to the close coupling expansion of Burke and Smith (1962) and takes the polarizability into account since the 2p state contributes 65.77% of the hydrogen atom polarizability (Castillejo, Percival, and Seaton (1960)).

The 1s-2s-2p close coupling approximation leads to a set of three coupled equations.

The poor agreement between theory and the experimental determination of the total cross section for the 1s-2s transition referred to in section 1(b) has prompted Burke et al. (1966) to include the 3s, 3p, and 3d states in the close coupling expansion. Although the calculated position of the peak in the cross section at 11.8 electron volts is in good agreement with the measurement of

Hils, Kleinpoppen, and Kaschnider (1966) of 11.7 ± 0.3 e.v., the absolute value of the measured cross section at the peak was found to be a factor of 2 lower than the predicted value.

Burke, Schey, and Smith (1963) have suggested that if the disagreement between theory and experiment is caused by any fault in the close coupling expansion, it could be ascribed to large contributions from higher angular momentum states.

If this disagreement was also the case in elastic scattering, then the phase shifts associated with the higher partial wave contributions would affect any angular dependent quantity - such as a differential cross section - much more than they would the total cross section.

Clearly a measurement of the angular distribution for elastic scattering of electrons from atomic hydrogen at energies greater than the threshold for excitation will provide a sensitive test of the close coupling expansion.

CHAPTER II

THE MODULATED CROSSED BEAM TECHNIQUE.

Introduction.

It was noted in Chapter I that the differential cross section for elastic scattering of electrons from atomic hydrogen provides a sensitive test of the approximations used in electron-atom scattering theory. Many of the difficulties associated with experiments based on atomic hydrogen arise from production problems and, once formed, its chemical instability. The problem of instability can be solved by using a beam of atoms. However it will be shown below that the concentration of hydrogen atoms in such a beam is usually considerably less than the background. Hence a signal, which is at least an order of magnitude less than that arising from scattering from the background gas, must be detected. One way in which this problem can be overcome is to use the modulated crossed beam technique. The advantage which the technique has over the more conventional means of measuring differential cross sections for elastic scattering of electrons from helium will be discussed. The modulated beam analyser which was used in the present investigation is described.

II.1 Production of Atomic Hydrogen.

Several methods were available to produce atomic hydrogen. The most commonly used means of dissociating molecular hydrogen into

atomic hydrogen are by an R.F. discharge - as employed by Heynaber et al. (1961)( ) - or thermally in a low pressure, high temperature tungsten furnace - Lamb and Retherford (1950); Fite and Brackmann (1958); Lichten and Schultz (1959).

The latter method was chosen in the present investigations because the reported concentration of hydrogen atoms in a beam formed in a tungsten oven is greater than that which can be obtained in an R.F. discharge. For example Heynaber et al. (ibid) have obtained 30% atomic hydrogen in a beam using the former method whilst Fite and Brackmann quote figures of 96% atomic concentration.

In a tungsten oven operating at temperatures above that which is required for dissociation, the equation which governs the dissociative reaction is

$$H_2 \rightleftharpoons 2H$$

and the extent of the dissociation is governed by an equilibrium constant K(T) where

$$K(T) = \left[\frac{P(H)}{P(H_2)}\right]^2 \qquad (2.11)$$

where $P(H)$, $P(H_2)$ are the partial pressures of the atomic and molecular hydrogen respectively.

P, the total pressure in the source is

$$P = P(H) + P(H_2) \qquad (2.12)$$

and the degree of dissociation D is

$$D = \frac{P(H)}{P} \qquad (2.13)$$

By substituting (2.13) into (2.11) and using (2.12), D can be calculated from the equation

$$\frac{D^2}{1-D} = \frac{K(T)}{P}$$

The values of the equilibrium constant K(T) for different source temperatures T have been measured by Langmuir (1915) and more recently by Lockwood et al. (1964).

Figure (2.1) shows the relationship between D and the source temperature for different source pressures. It can be seen that highly dissociated beams can be produced in a tungsten furnace if the temperature is greater than 2500°K and the source pressure is less than 1 torr.

The beam formed by the effusion of the atoms through a slit in the wall of the source can be made to cross an electron beam giving rise to the crossed beam configuration. However by the time a collimated beam of atoms has been drawn sufficiently far

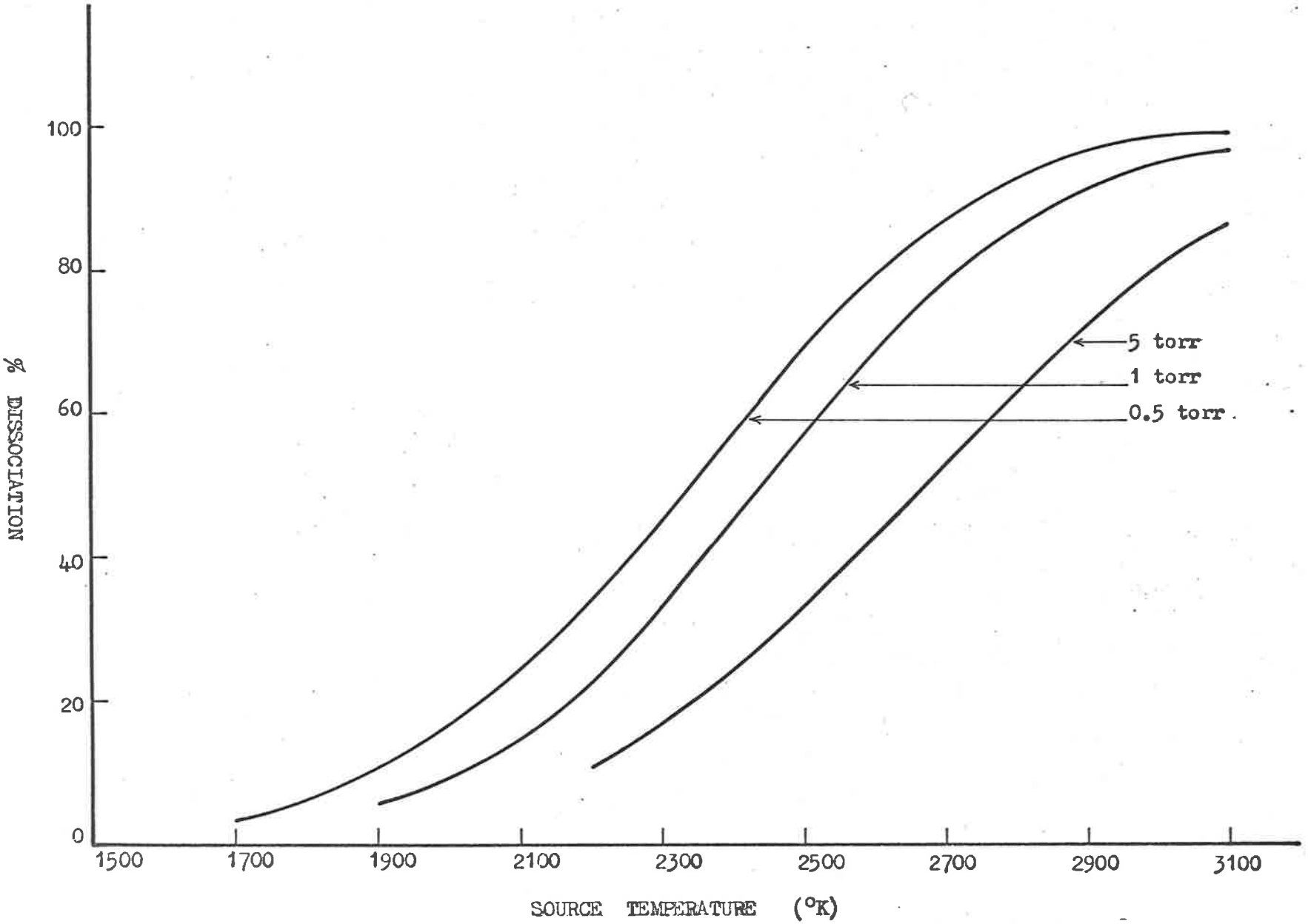

Fig. 2.1: Degree of dissociation of molecular hydrogen as a function of source temperature for several source pressures.

away for an experiment to be performed the partial pressure of atoms in the beam has dropped substantially. For example, in the single aperture oven employed in the present investigations the concentration had dropped to about 10^9 atoms/cc in the interaction region. With a typical operating pressure of 2×10^{-6} torr the density of molecules in the background gas was 7×10^{10}. Thus an elastic scattering experiment would require the separation of a signal from a background which was around 50 times greater. Since ordinary vacuum systems experience fluctuations and drifts which are much greater than a few percent, an elastic scattering experiment on atomic hydrogen would be impossible using D.C. and subtraction techniques.

II.2 Modulated Crossed Beam Technique.

In the context of the present discussion, signal is defined as the number of electrons scattered from the beam and noise, the number of electrons scattered from the background.

The way in which the problem of a poor signal to noise ratio, which is inherent in elastic electron - hydrogen atom collisions, can be overcome, is to modulate the beam at a definite frequency. The signal is then specified by its frequency and phase.

This is the modulated crossed beam technique which was first used by Boyd and Green (1958) to measure the ionization cross section of molecular hydrogen and by Fite and Brackmann (1958 a) in the measurement of the ionization cross section of atomic hydrogen.

Since then the technique has been used extensively in electron-hydrogen atom collision studies, in the investigation of proton-hydrogen collisions (Fite, Brackmann, and Snow, 1958) and in a mass spectrometric study of free-radical reactions (Foner and Hudson (1962)).

The crossed beam configuration is also useful in the measurement of the angular distributions of elastically scattered electrons from chemically stable atoms such as the inert gases. The conventional method of studying these angular distributions has been to scatter the electrons from a large volume of gas, the scattering volume being defined by the intersection of the electron beam and the solid angle subtended by the entrance aperture to the electron spectrometer. If θ is the scattering angle, the scattering volume varies as $\operatorname{cosec}\theta$ (Massey and Burhop (1952)). Hence to obtain the true scattered intensity per unit solid angle, the observed signal must be multiplied by $\sin\theta$. Thus a substantial correction must be made at small and large scattering angles where the distributions are most interesting theoretically.

If a circular cross section atomic beam is used, the scattering volume is independent of angle therefore no correction needs to be made to the observed intensity. Porteus (1964) has used the crossed beam configuration to investigate the angular distribution of elastically scattered electrons from argon. The discrepancies with the results of Hughes and McMillen (1932), taken with conventional techniques, have been ascribed to the correction factor mentioned above (Porteus (ibid)).

With a rare gas beam, where there is no limitation on the source pressure set by dissociation conditions, the partial pressure in the beam can be substantially increased over that quoted above for atomic hydrogen. If the arrival of the beam in the scattering region does not cause an increase in the background pressure, the signal to noise ratio can be improved to such an extent that the beam can be operated D.C. Porteus limited the rise in background pressure by condensing an argon beam on a liquid nitrogen cooled surface.

The technique of condensing the beam is not as readily applicable in the case of helium. However the crossed beam configuration can still be preserved if the pressure in the beam is reduced and the beam is modulated. The modulated beam technique has been used in the present experiments to measure the angular

distribution of elastically scattered electrons from helium. The results are given in section IV.1.

II.3 Modulated Beam Analysis.

As the energy range covered in the present electron-hydrogen experiments was greater than the energy required to excite the atom, it was necessary to analyse the energy of the scattered electrons with an electron spectrometer. In order to perform the energy analysis, fine slits were used which therefore reduced the solid angle of the detector. In the present case the solid angle was about 10^{-5} steradians. The predicted values of the differential cross sections for the elastic scattering of 50 electron volt electrons from hydrogen ranged between 0.1 and 0.01 πa_o^2 per steradian where a_o is the first Bohr radius (Scott 1965). Therefore small scattered electron fluxes were expected and a particle multiplier tube was used as the detector of the analysed electrons.

The output from a particle multiplier tube consists of a large number of pulses of varying pulse height which can be dealt with in either of two ways. The electron flux may be converted into an average current, and the component of this analogue signal which is synchroncus with the beam modulation frequency detected with a tuned amplifier and phase sensitive detector; or the individual

electrons may be preserved as pulses and handled with digital counting techniques. In the latter case the recording system is arranged to count in synchronism with the beam modulation.

In the analogue technique, such as that used by Gilbody et al. (1961), the individual charge pulses are converted into an average current by storing them on a condenser. The current level is proportional to charge delivered by the pulses. With the digital method, the pulses are fed to a discriminator which gives out a pulse of fixed height. As long as the input pulse height to the discriminator is greater than some threshold value, each pulse will be counted with the same efficiency regardless of the pulse height. Since small pulses contribute less to the average current than they do to a digital count, digital systems are inherently more sensitive than analogue systems.

In the electron hydrogen studies, sensitivity was of great importance therefore a digital system was used to analyse the modulated beam.

In a digital system of analysis, if N_1 events are recorded when the beam chopper is open and N_2 events are recorded when the beam chopper is closed, then N_1 represents the number of electrons scattered from the beam plus the background and N_2 represents the number of electrons scattered from the background. The difference

N_1-N_2 then represents the number of electrons scattered from the beam.

A similar method of analysis to that used in the present experiments has been used by Fomer and Hudson (1962).

II.4 The Modulated Beam Analyser.

Whereas Fomer and Hudson (ibid) used two separate scalers to perform the analysis of the modulated beam, the analyser employed in the present case consisted of one scaler which was designed to add pulses when the beam was on and subtract when the beam was off. Thus the beam signal was represented by the number of counts recorded in the scaler at the end of a preset time which represented a considerable advantage in data handling over the separate scaler method.

The block diagram shown in figure 2.2 is a schematic representation of the modulated beam analyser. Apart from the add-subtract scaler, a second scaler, the background scaler, was used to count the number of electrons scattered into the detector when the beam was off. Although the background scaler played no part in the analysis of the beam it proved very useful in the determination of counting rates which were used to correct for the dead time of the pulse amplifier. Since the background signal depended on the

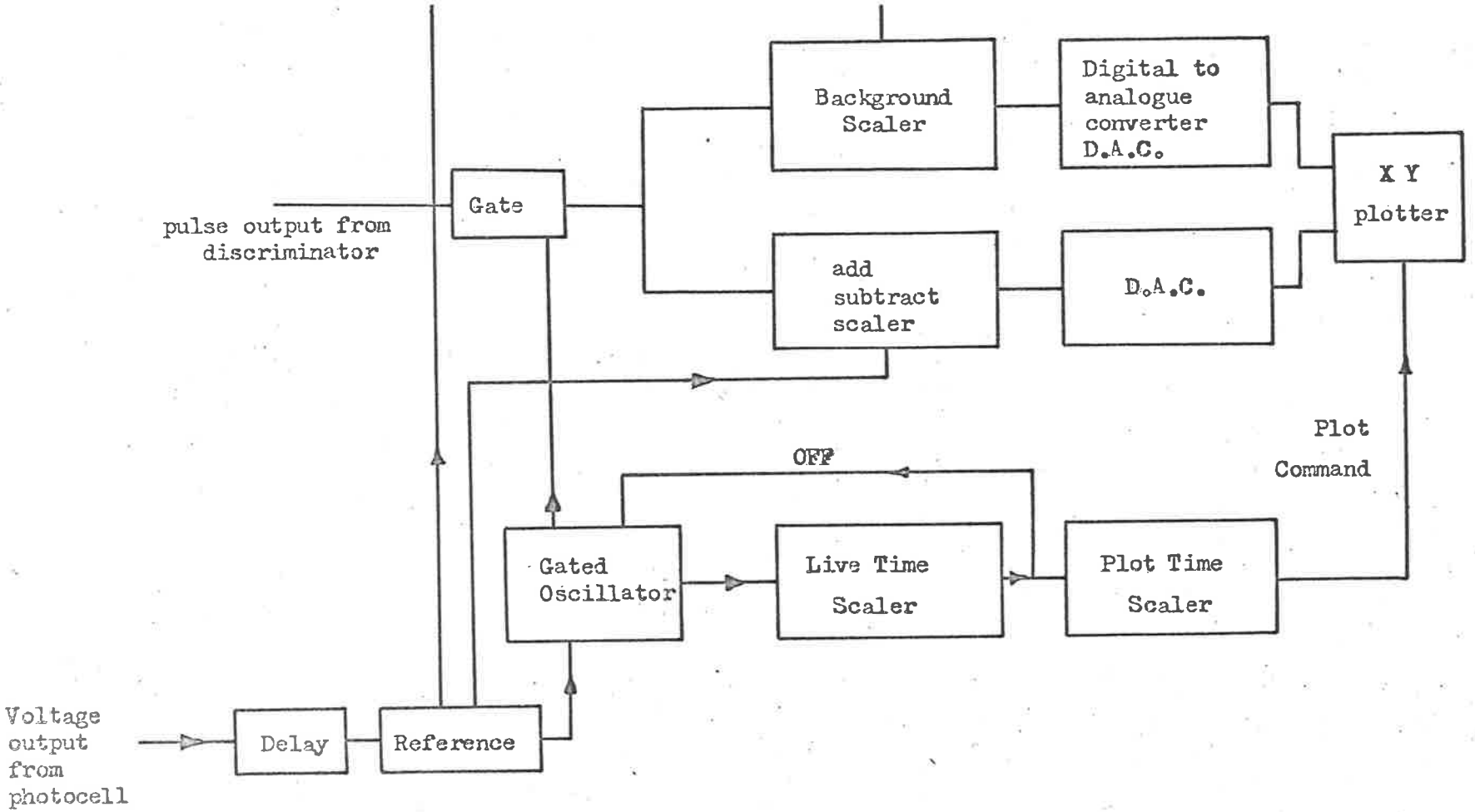

Fig. 2.2: Block Diagram of Modulated Beam Analyser.

product of electron beam signal and background pressure, the output of the background scaler gave an independent measure of these two factors.

4(a). Timing.

It was essential that the add-subtract scaler was switched from the add mode to the subtract mode at the correct time. The most straightforward means of switching was to use the voltage direct from the reference supply which monitored the mechanical chopper. It was found, however, that with this method the performance of the device was susceptible to chopping frequency fluctuations. Although these fluctuations could be averaged out electronically to about 1%, a significant source of error was introduced when working with signal to noise ratios of 1 : 100.

The susceptibility to variations in the chopping frequency was removed by making the analyser operate over a fraction of a half cycle. The time for which the device was operating - the live time - was controlled by counting pulses from a 100 kilocycles per sec. (kcs) crystal oscillator in a scaler - the live time scaler in figure 2.2. A live time of 1.7 milliseconds was derived by counting 170 pulses of length 10 microseconds.

The number of live times was recorded in another scaler -

the plot time scaler - by storing a digit every time the live time scaler was full.

4(b). Verification of Correct Timing.

Pulses were fed from a pulse generator into the analyser and the output of the add-subtract scaler was observed on a cathode ray oscilloscope. The criterion for correct timing was that there should be no nett addition or subtraction over typical integrating times used in the experiments.

With the timing procedure described above the maximum addition or subtraction over these integrating times was 1 part in 2000.

4(a). Data Recording.

The outputs from the add-subtract scaler and the background scaler were converted into voltage levels by a digital to analogue converter. These voltage levels were fed into the Y amplifier of an X-Y plotter* and were displayed so that one half of the Y axis was used for the background scaler and the other half was used for the add-subtract scaler.

---

* Moseley

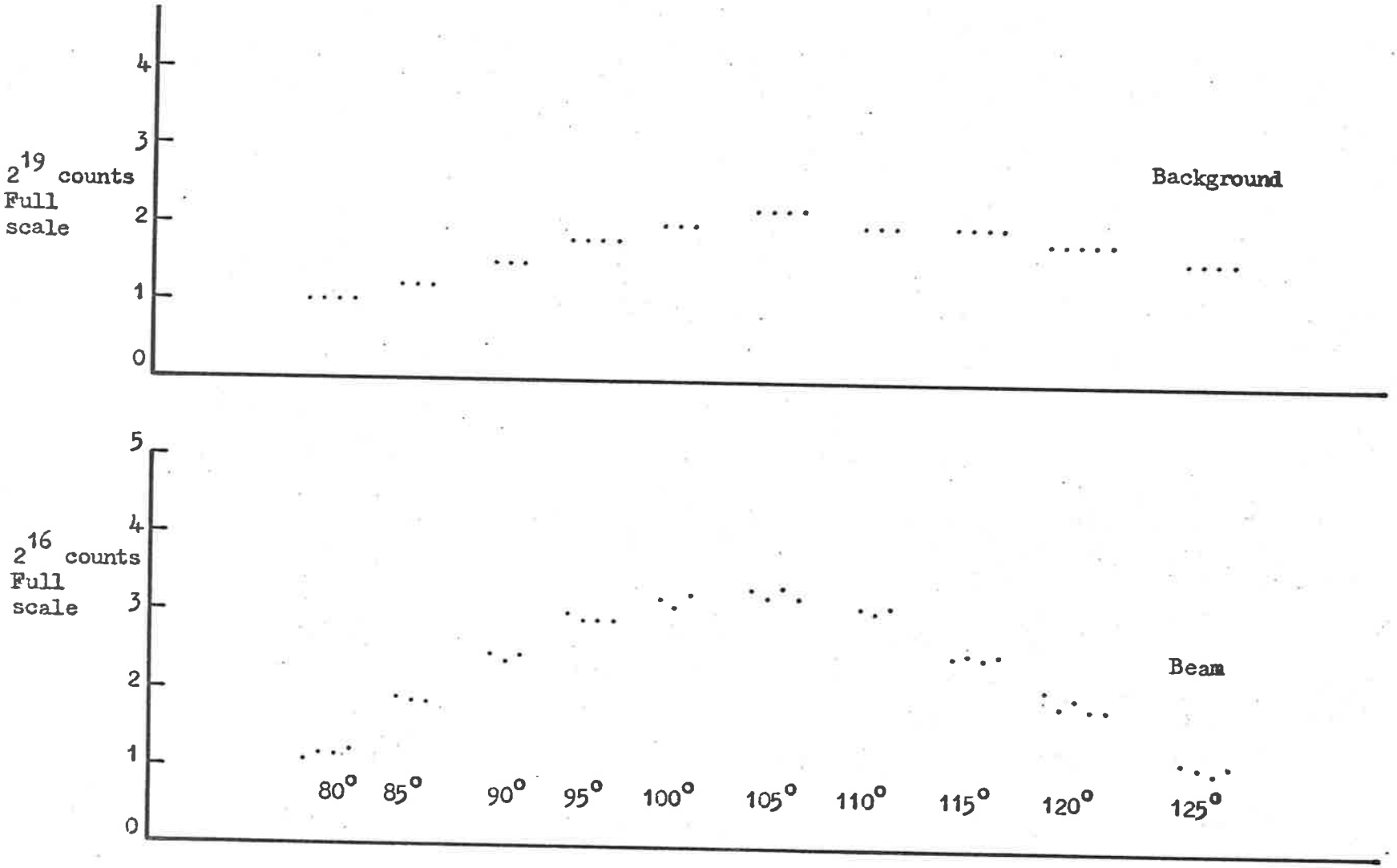

Fig. 2.3: Sample of raw data from modulated beam analyser. Scattering from argon.

Counts were accumulated in each scaler for a certain time after which the voltage level was plotted on the Y axis. The time between each plot - the plot time - could be preset externally by setting the number of live times which the plot time scaler could count.

The effect of doubling the plot time was to double the number of counts in the add-subtract scaler, and so long as the half period of the modulation was greater than the live time, the output of the add-subtract scaler remained independent of the chopping frequency.

The data recording system was linear to 0.04%.

Figure 2.3 is a sample of the raw data derived from the number of 50 electron volt electrons scattered elastically from argon at several angles around the maximum in the distribution.

4(d). Phase Delay.

The assumption that the signal from the beam reached the analyser at the same time as the reference would have been true if no phase changes were introduced by the electronics associated with the detector or the reference; if the beam atoms arrived simultaneously in the interaction region after they had been chopped and if the reference was switched at the same time as the beam was switched.

Although the use of pulse techniques minimised the possibility of large phase changes in the detecting stage, it was necessary to allow for the finite time taken for the beam atoms to travel the 9 cms from the chopper to the interaction region and also to check that the reference and beam were in synchronisation. Therefore the facility of varying the phase relationship between the signal and the reference was incorporated by delaying the reference voltage in time before switching the add-subtract scaler.

For a given beam-chopper geometry and for a given chopping frequency, the number of atoms arriving at the interaction region would be as indicated in figure 2.4(a). Figure 2.4(b) shows the effect on the beam signal of varying the time delay assuming that the shape of the modulated beam was as indicated in 2.4 (a). The effects of any lack of synchronisation between the reference and the signal would be to shift the flat portion shown in figure 2.4(b) in time.

Consequently the shape of the modulated beam could be determined and compensation for the effects of lack of synchronisation could be made by adjusting the time delay.

Figure 2.4(c), shows the effect on the beam signal of varying the delay. The beam signal was derived from the helium peak of the mass spectrometer - which will be described in Chapter

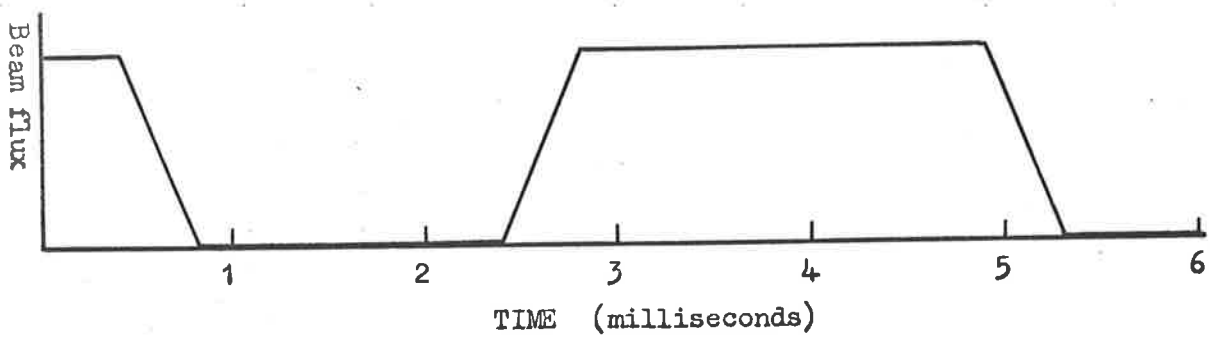

Fig. 2.4(a). Theoretical wave form of the modulated beam for a given beam chopper geometry and chopping frequency.

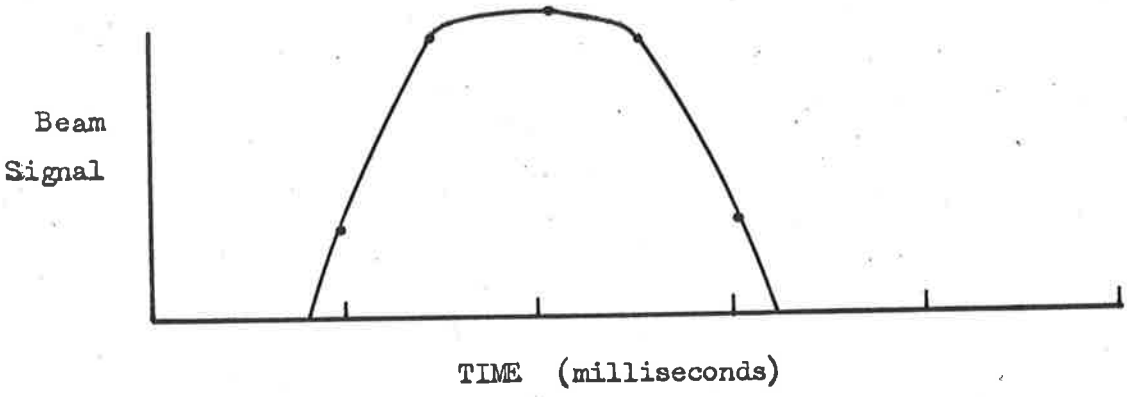

Fig. 2.4(b). Predicted variation of the beam signal with phase assuming wave form as shown in Fig. 2.4(a).

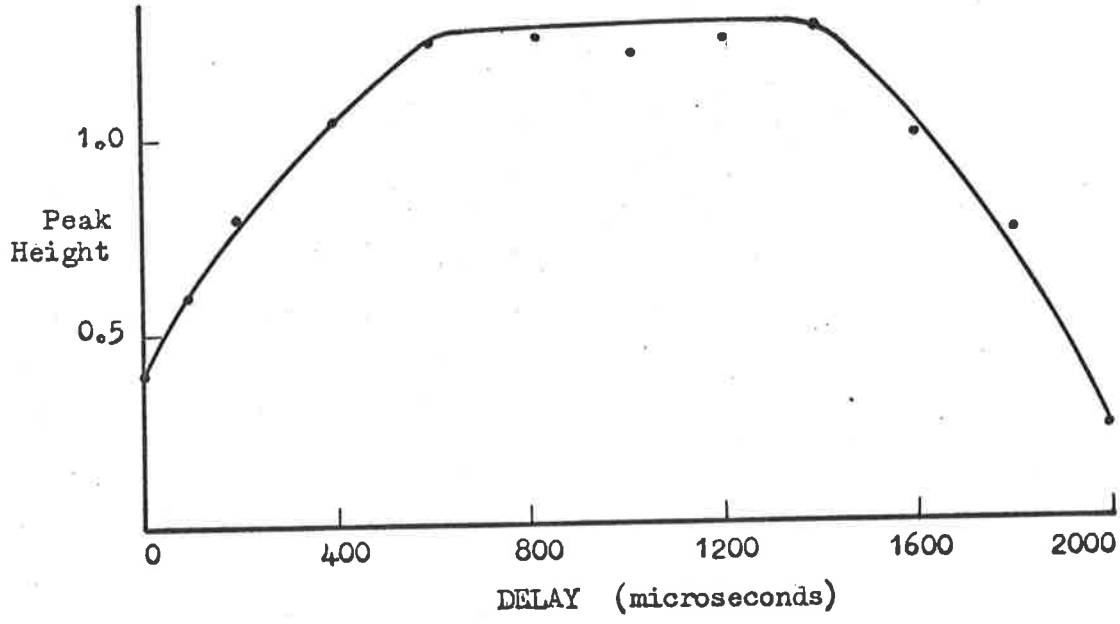

Fig. 2.4(c). Observed variation of modulated beam signal with delay of reference voltage. The signal was derived from the He^+ peak of the mass spectrometer using a helium beam.

V - with a helium beam. The wave shape as shown in figure 2.4(c) is consistent with the predictions of figure 2.4(b).

CHAPTER III

THE VACUUM SYSTEM AND THE ELECTRON GUN.

Introduction.

It has been pointed out in Chapter II that the modulated or seed beam technique can be used to measure the angular distribution of elastically scattered electrons from gases. Therefore in order to perform the present experiments a modulated atomic beam and an electron beam were required. The apparatus which was used to produce these two beams is described below.

III.1 The Vacuum System.

The vacuum system consisted of the three parts which are illustrated schematically in figure 3.1.

1(a). Source Section.

Although the beam source was designed specifically to produce beams of atomic hydrogen, it proved most satisfactory in the production of helium and argon beams.

Lamb and Retherford (1950) pioneered the use of tungsten ovens to produce beams of atomic hydrogen. Hendrie (1954) improved on the design but both types of ovens had the disadvantage that they were made from two ground half cylinders. The slit was formed by lapping a notch in one edge and fitting the two halves together.

The advantage of the source used in all of the experiments described in this thesis was that it was made from a single piece of

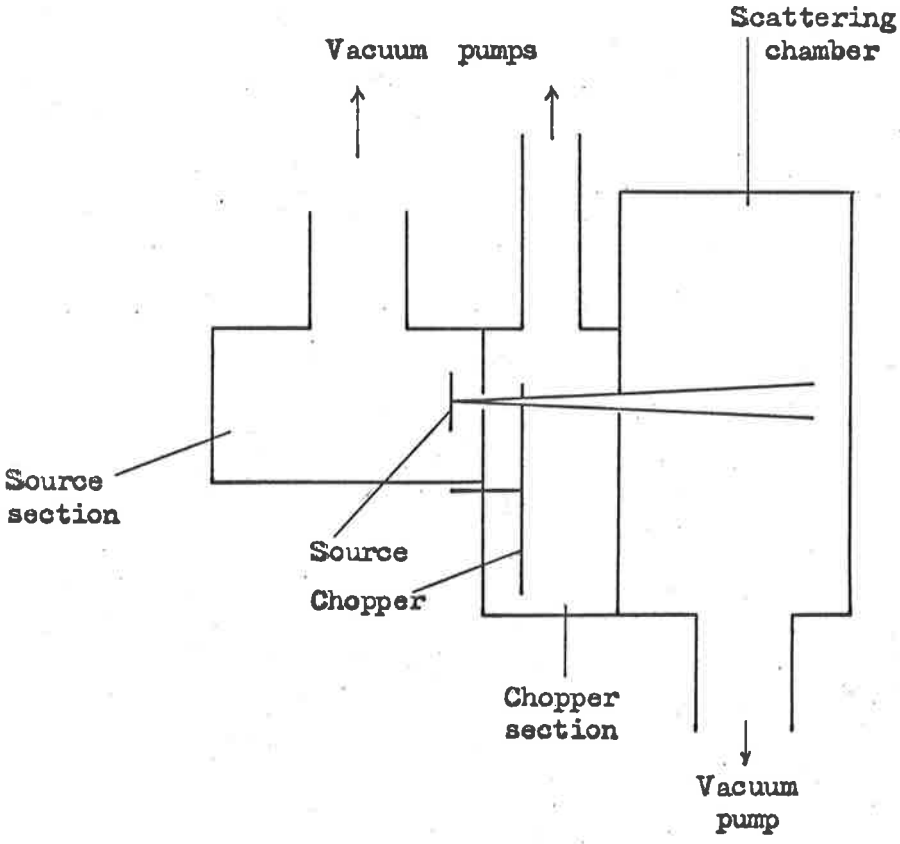

Fig. 3.1: Schematic diagram of vacuum system.

tungsten. Thus there were no problems of excess gas leakage around the join. The oven is illustrated schematically in figure 3.2(b). It was 1.5" long and a 0.060" hole was drilled up the centre to a depth of 1". The drilling was carried out with a spark erosion machine. The resistance of the central portion of the tube was increased by milling it to a diameter of 0.100". The ends of the tube were 0.25" in diameter. The spark erosion machine was used to punch a slit (0.008" by 0.125") in the wall of the cylinder.

The oven was supported from two water-cooled copper rods as indicated in figure 3.2(a). The lower rod was fixed to a brass plate. The upper rod was supported with sufficient flexibility to allow for approximately 0.010" linear expansion in the tungsten when it was heated.

The oven was sealed in the vacuum system by bolting the brass plate to a flange. The position of the source could be adjusted by moving the plate relative to the flange.

Gas was admitted to the source along the inlet pipe shown in figure 3.2(a).

The oven was heated by passing an alternating current through it. Currents of order 300 amps were required to raise the oven temperature to 2750°K. The oven supply is illustrated schematically in figure 3.3. The voltage drop across the oven was controlled by a variable

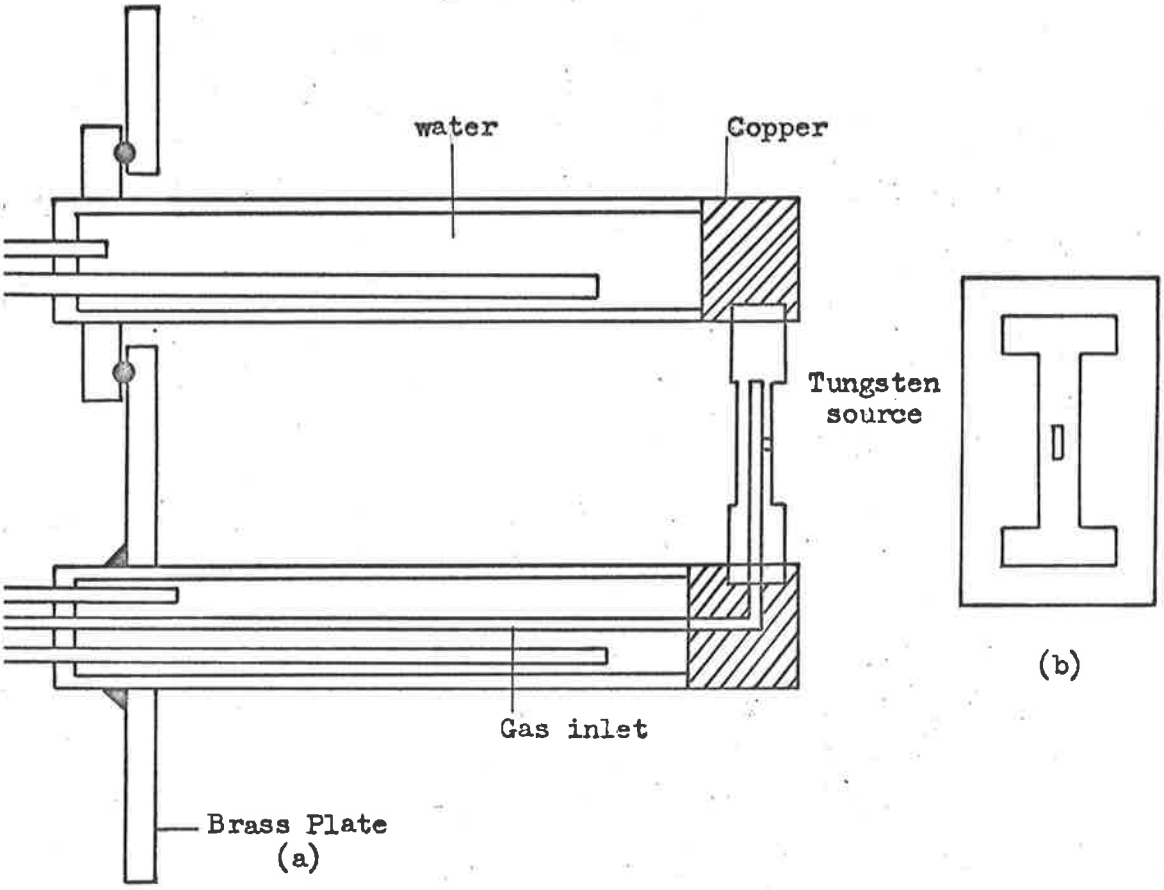

Fig. 3.2: (a) Schematic view of Oven support.

(b) Schematic view of Oven.

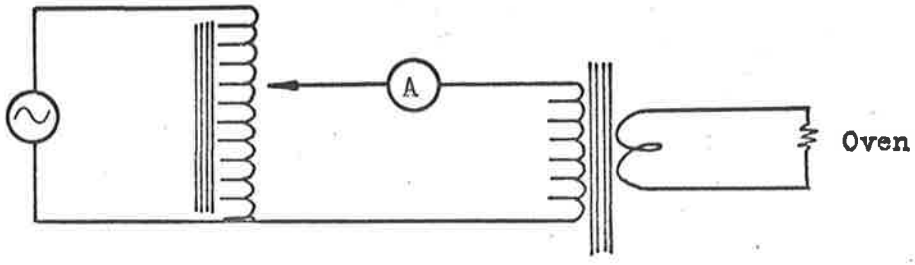

Fig. 3.3: Electrical Supply to Oven

voltage transformer* in series with the primary of a current transformer. The temperature of the oven was measured with a disappearing filament optical pyrometer.**

1(a)(i) Beam Geometry.

The width of the oven slit was chosen so that the molecular flow criterion was satisfied at pressures of approximately 1 m.m. This criterion states that the width of the slit should be less than the mean free path of the atoms in the source. (Dushman and Lafferty (1965).)

Since the ratio of slit width to length was 0.4:1, the beam was fairly well collimated after leaving the source. Further collimation, which defined the beam shape in the interaction region, was provided by two additional stops. The first was rectangular in shape and was manufactured from molybdenum. Its dimensions were calculated using the technique described by Ramsey (1956). The entrance aperture to the scattering chamber was circular in section since it was an advantage to work with a cylindrical beam in the scattering chamber.

---

* Berco Rotary Regavolt.

** Leeds and Northrop.

The chopper housing, structural features of the vacuum system and the incorporation of a differential pumping facility limited the distance from the source to the interaction region to 21 cms.

The oven chamber was pumped by a 6" oil diffusion pump* which was fitted with a liquid air trap and a water-cooled baffle valve. With a pressure of 1 torr of hydrogen in the source, the pressure read on an ionization gauge in the chamber, was of order 1×10^{-5} torr. Thus attenuation of the beam by scattering from the background gas was negligible.

1(b). Chopping Chamber.

The chopping chamber was a 9" diameter 2" long mild steel pipe which was welded to the base of the scattering chamber. Apart from housing the chopper mechanism, it provided an interface for differential pumping and enabled all leads terminating in the scattering chamber to be passed into the atmosphere via glass to metal seals.

1(b)(i). Chopper.

Two methods of modulating atomic beams have been reported in the literature. Foner and Hudson (1962), Gilbody and Ireland

---

* Edwards F603.

(1963) have used a vibrating reed type device whilst Fite and Brackmann (1958), Boyd and Green (1958), McGowan and Fineman (1965) have used a rotating toothed wheel.

The main reason for choosing the latter device was that it was anticipated that the magnetic fields associated with the vibrating reed mechanism may have influenced the electron paths in the interaction region.

The chopper was a 6" diameter aluminium disc which had twelve teeth evenly spaced about the circumference. The teeth were accurately machined so that the mark to space ratio between each castellation was unity to a tolerance of 0.001".

A gear box was used to couple the shaft, which supported the disc, to a main drive shaft. The main drive shaft was driven from outside the vacuum system through a rotary seal by an electric motor. The space between the two "O"-rings in the seal was pumped continuously.

1(b)(ii). Reference Signal.

As the toothed wheel rotated it interrupted the light from a small light source falling on an L.S. 400 phototransistor. The square wave voltage output derived in this way was amplified and fed in parallel to the modulated beam analyser and a cathode ray oscilloscope which enabled a constant check to be kept on the chopping frequency.

The upper limit on the chopping frequency was set by the lifetime of the "O"-rings in the rotary seal and the lower limit by the magnitude of the fluctuations in the chopping frequency.

By modulating the beam at 180 cycles per second (c.p.s.), the angular velocity of the disc was large enough to average out fluctuations caused by imperfections in the gears of the gear box to approximately 2% and the "O"-rings lasted for about three weeks. With a "live-time" (section II.4) of 1.7 milliseconds this frequency gave a duty cycle of 60% and prevented any harmonics of the 50 c.p.s. line frequency from influencing the analysis of the beam.

The chopping chamber was pumped with a liquid air trapped 2" oil diffusion pump, which was backed by the oven chamber diffusion pump so that pressure fluctuations could be reduced (Fite and Brackmann (1958)).

1(c). The Scattering Chamber.

The scattering chamber was 14" in diameter and 6" long and was manufactured from mild steel which acted as a shield against low level magnetic fields.

A 5 litre capacity liquid air trap was installed in the scattering chamber to reduce the partial pressure of water vapour thereby improving the performance of the electron gun.

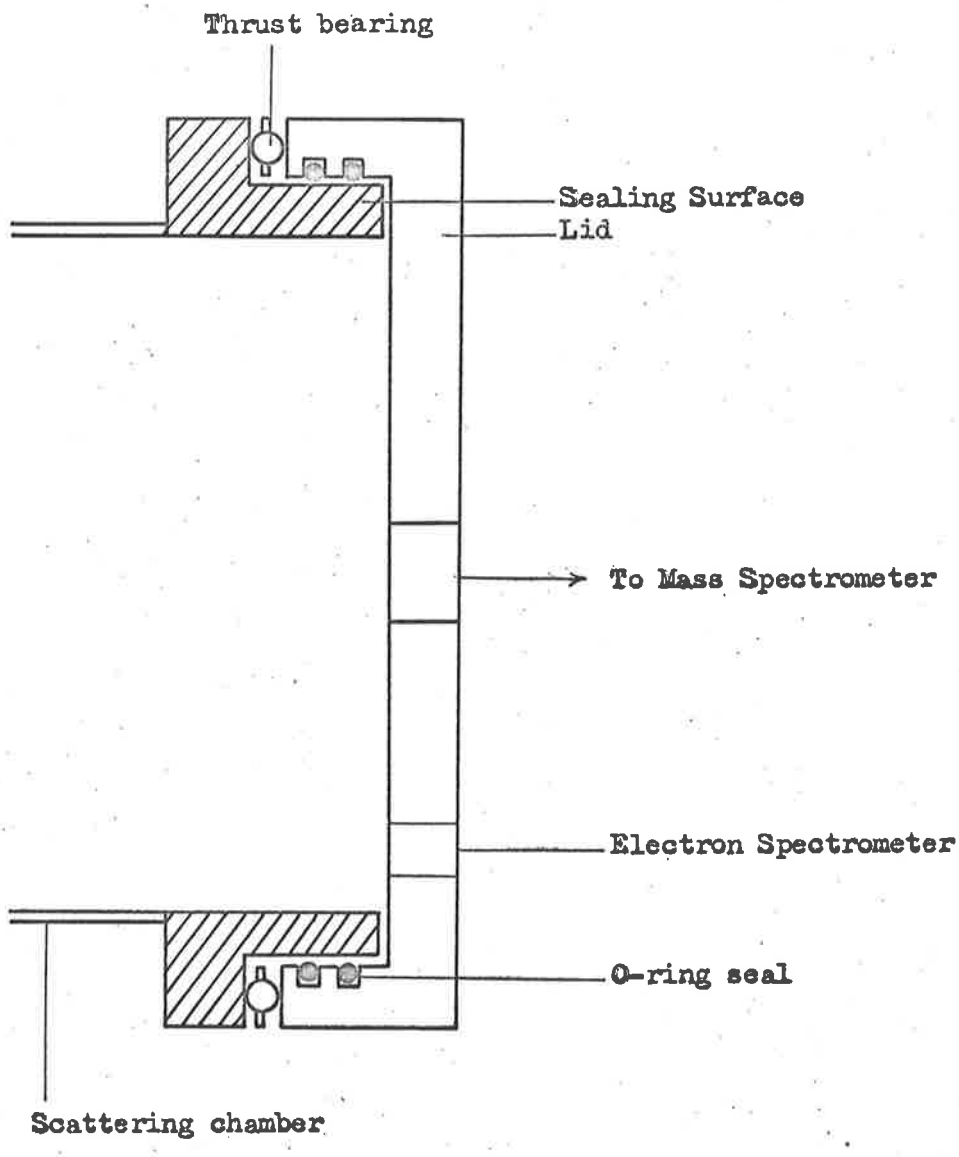

Fig. 3.4: Lid of the scattering chamber.

The lid of the chamber, sealed on the circumference in a manner indicated in the figure 3.4. The sealing surface was ground so that the maximum variation along the diameter was 0.001 inch in 15 inches. Hence the rim could be used as an accurate reference surface for alignment.

1(d). Background Pressure Effects.

During analysis of the modulated beam, it is assumed that the background remained constant over one cycle. Owing to the finite pumping speed of the chamber enclosing the interaction region, the background pressure will rise when the beam enters the chamber.

These fluctuations can be averaged out with a time constant which is given by (Fite 1962)

$$\tau = V/S$$

where V is the volume of the chamber and S the pumping speed of the pumps.

The pumping speed was chosen so that the time constant was long compared to the chopping period.

An additional requirement on the pumping speed was set by the time taken to reach the ultimate pressure of the system after it had been exposed to the atmosphere.

With a vacuum system time constant of 200 milliseconds, the time taken to pump the system down to an operating pressure of 2×10^{-6} torr was about 15 hours.

Variations in background pressure caused by irregular boiling in the 6" oil diffusion pump which pumped the scattering chamber were removed by increasing the heater wattage by 10%.

1(e). Alignment.

The collimators described in III.1(a)(i) were positioned so that they were collinear with a hole in the centre of the lid to an accuracy of 0.005" over the 8". By viewing the oven slit through these three apertures, the position of the oven could be adjusted so that the beam entered the scattering chamber along the axis of rotation of the gun.

III.2 The Electron Gun.

2(a). Requirements.

The difficulties associated with the measurement of the angular distribution of elastically scattered electrons from atomic hydrogen at energies in excess of 10 electron volts stem from two causes. First, as has been noted in section II.1, the concentration of atomic hydrogen in a beam which has been produced in a tungsten oven is of the order of 10^9 atoms/cm^2 and secondly, as was pointed

out in section II.2, the energy analysis of the scattered electrons greatly reduces the solid angle of the detector. Therefore it was important that the electron gun should produce an intense beam of incident electrons. Since the energy of the electrons was low, the requirement of a high beam current at low voltage meant that a high perveance gun was required. The perveance is defined as the ratio of beam current to the 3/2 power of the beam voltage. High perveance guns are those for which the ratio is of the order of 1×10^{-6}. (Frost et al. 1962.)

As the gun was to be used to study angular distributions it was necessary for it to rotate through an angular range of at least 100°.

To prevent the penetration of electric fields from the gun into the interaction region, the last electrode was run at earth potential. Thus the beam energy was set by the cathode potential. A dispenser cathode was used because the gun had to be exposed to the atmosphere when alterations were made to the apparatus and because these cathodes have good emission characteristics at temperatures of $1100^{\circ}C$. Therefore the thermal spread in electron energies produced by such a source was less than that produced by a normal tungsten emitter.

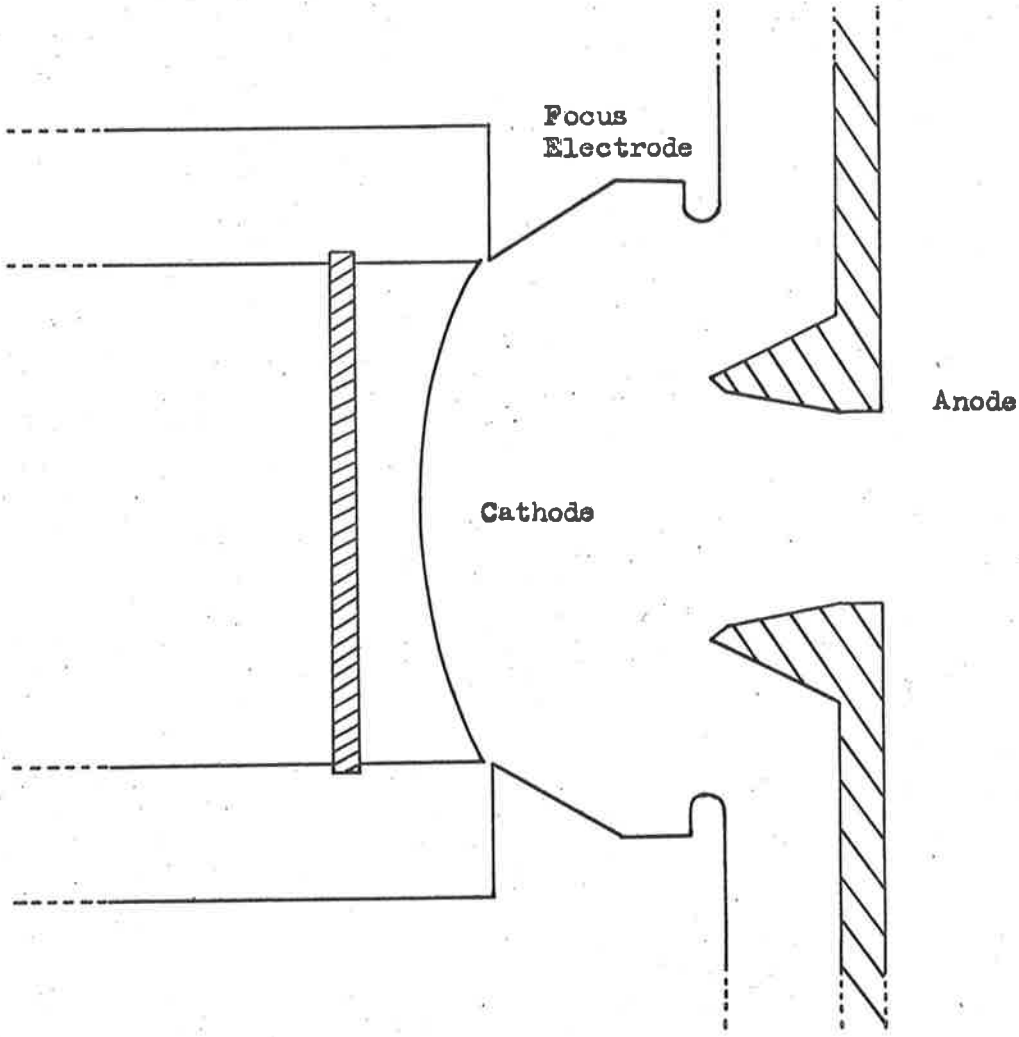

Fig. 3.5: First Stage Electrode Shapes after Frost et al. (1962).

It was an advantage to have the electron beam diameter greater than the atomic beam diameter so that the scattering volume was independent of angle.

2(b). Description.

The simplest way of satisfying the above requirements was to design a gun based on the multistaging principle. The advantages of this principle have been discussed by Simpson and Kuyatt (1963). The technique seems to have originated on purely empirical grounds and was first reported by Danielson, Rosenfeld, and Saloom (1956); Currie (1958). It involves the production of an electron beam at high energies and subsequently decelerating the electrons in a second stage.

2(b)(i). Production Stage.

The basic design of this stage was adapted from the gun design of Frost, Furl, and Johnson (1962). The perveance was high - and it produced a solid beam of electrons. That is the current density across the beam was uniform. The electrode shapes are shown in figure 3.5.

Figure 3.6 illustrates the way that the electrodes were supported. Pressed boron nitride was used as the main insulating material because it could be easily machined; it could withstand

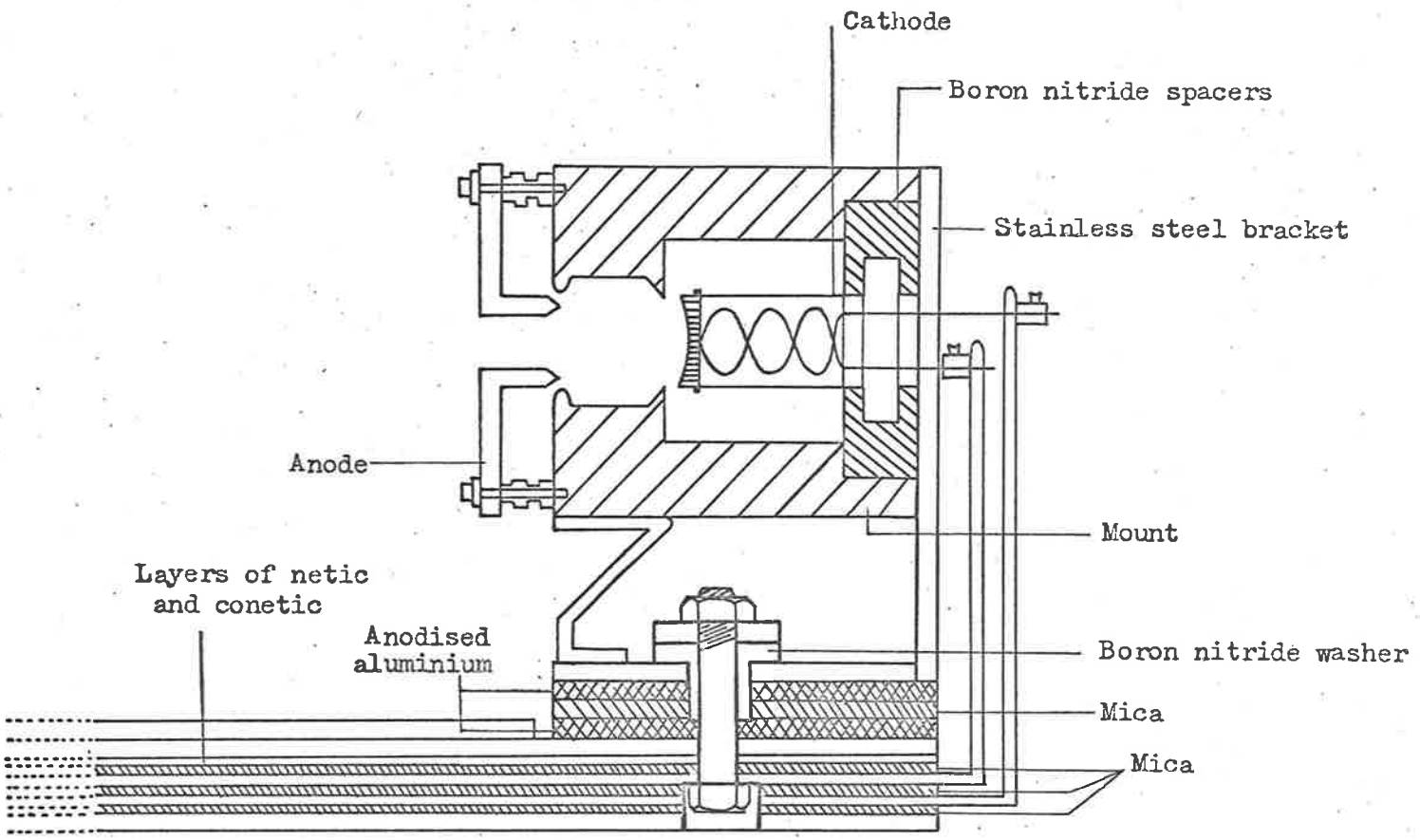

Fig. 3.6: First stage of the electron gun.

temperatures in excess of 600°C and because its resistance did not degrade with use.

The stainless steel bracket in figure 3.6 was insulated from the earthed base of the gun by laminations of mica and anodised aluminium. The bracket supported the production stage so that the bore of the anode hole was parallel to the base to a tolerance of 0,001 inches.

Cathode.

The cathodes were of the dispenser type and were made to fit the requirements indicated by Frost et al.,* and consisted of a mixture of barium, calcium, and aluminium oxides impregnated in an 80% dense tungsten matrix.

Such cathodes have a long life, a high primary emission current density and can be reactivated many times after exposure to the atmosphere (Hughes and Coppola (1957)).

The cathodes were indirectly heated by the passage of an alternating electric current through non-inductively wound tungsten heaters. The insulation between the heater windings and the cathode was provided by a very thin (of the order of 0,002 inch) layer of aluminium oxide. It was found that much care had to be exercised

---

* Cathodes manufactured by Spectra-Mat Inc.

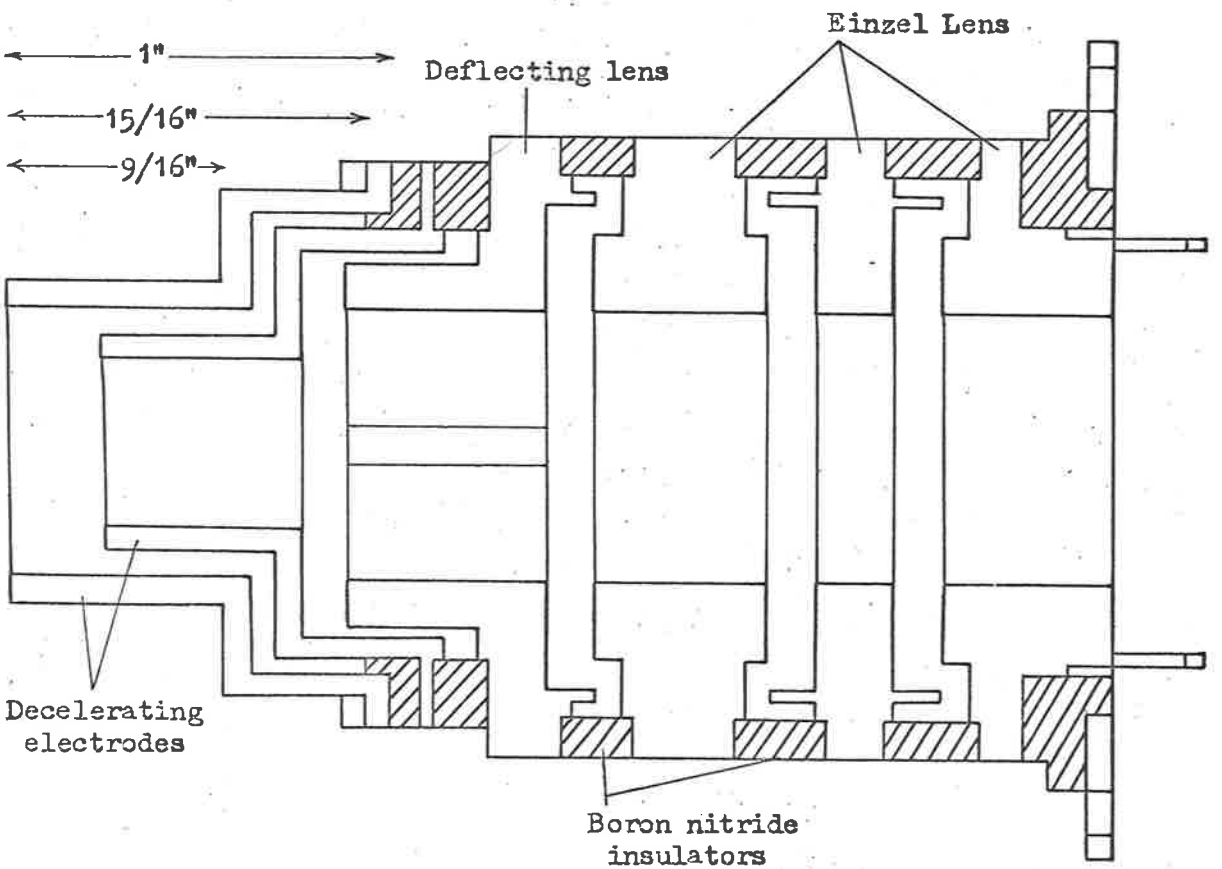

Fig. 3.7: Electrodes of decelerating stage.

when the heaters were fitted to the cathodes to avoid flaking off the insulating layer.

2(b)(ii). Decelerating Stage.

The decelerating stage consisted of an einzel lens, a deflecting lens and a final focussing stage and is illustrated schematically in figure 3.7.

The einzel lens was a three-electrode lens similar in design to that which has been investigated by Klemperer (1953). The electron velocity outside the lens was set by the potential V_1 on the two outer electrodes. The potential V_2 on the inner electrode was kept such that $V_2-V_1 < 0$. Pierce (1949) has shown that the device acts as a converging lens under these conditions.

The deflecting lens was composed of four 90° sectors. The basic potential of the lens was that of the outside of the einzel lens. The electron beam was deflected by varying the potentials on each sector about V_1.

The final stage was a two-electrode lens based on the design of Spangenburg (1948).

The electrodes were manufactured from copper and were gold-plated so that they could be easily cleaned. Each electrode was insulated by rings of boron nitride. The steps which located the insulating rings were machined in such a way that the electron

Fig. 3.8

The electron gun

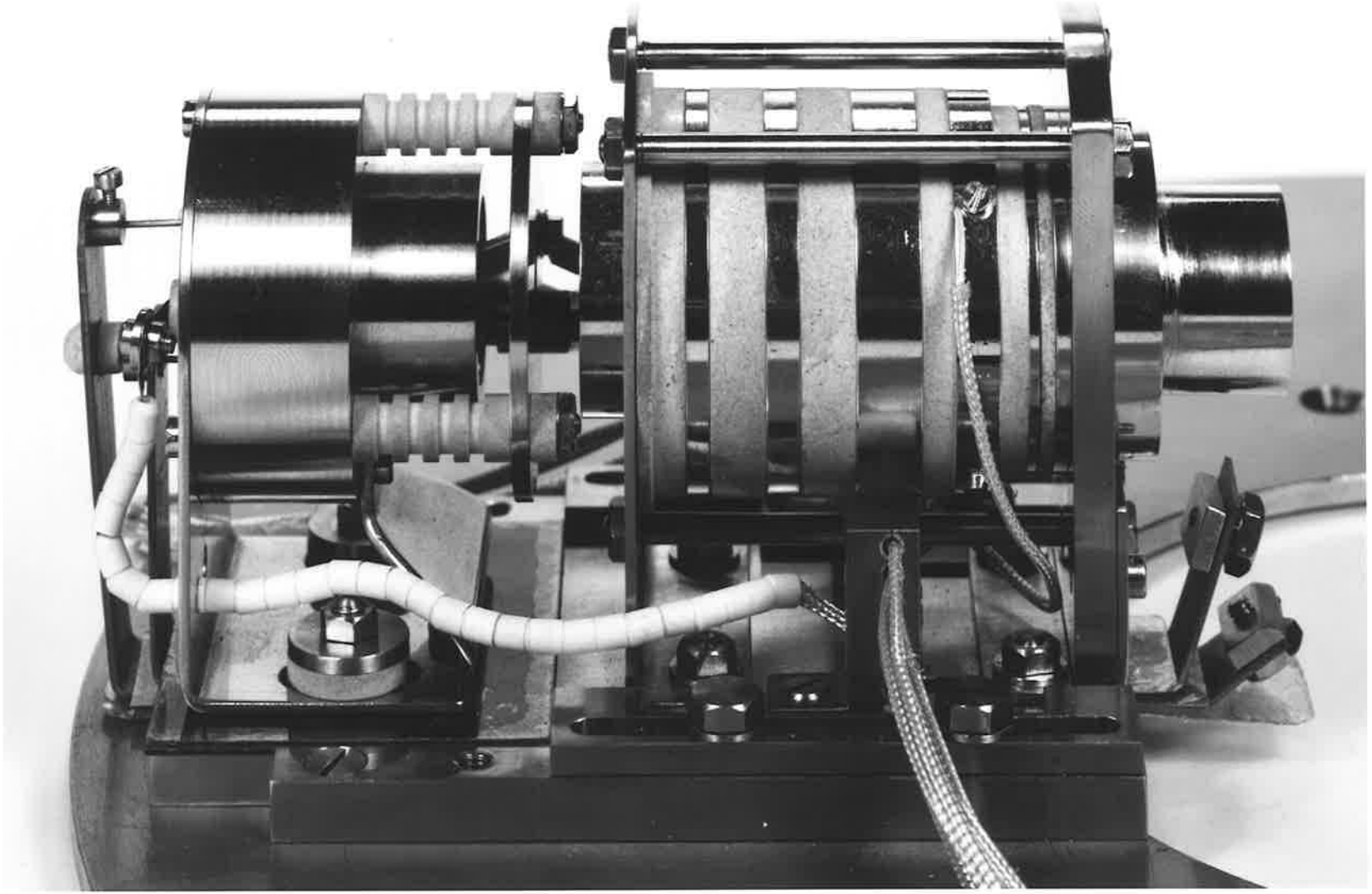

beam was shielded from the insulating surface. Thus any build-up of charge on this surface could not affect the electron beam.

Two stainless steel brackets were used to support the electrodes. The gun axis was parallel to the base to a tolerance of 0.003".

Flexible leads were used in the scattering chamber and were attached to the electrodes with mechanical joints.

Figure 3.8 is a picture of the assembled gun.

2(b)(iii). Magnetic Shielding.

Currents of the order of 20 amps. were used to heat the cathode to the operating temperature. Alternating currents were used to prevent the setting up of any standing magnetic fields which could have influenced the paths of the low energy electrons.

Since a 50 electron volt electron will travel 1 metre in about 20nanoseconds it was possible for the electrons to be influenced by the A.C. component of the magnetic field. Therefore the heater leads were kept close together and were encased in high permeability magnetic shielding material* to minimise the penetration of magnetic fields into the interaction region.

---

* Netic and Comatic

Fig. 3.9

An interior view of the scattering chamber. Magnetic shields are shown in the centre and surrounding the electron gun.

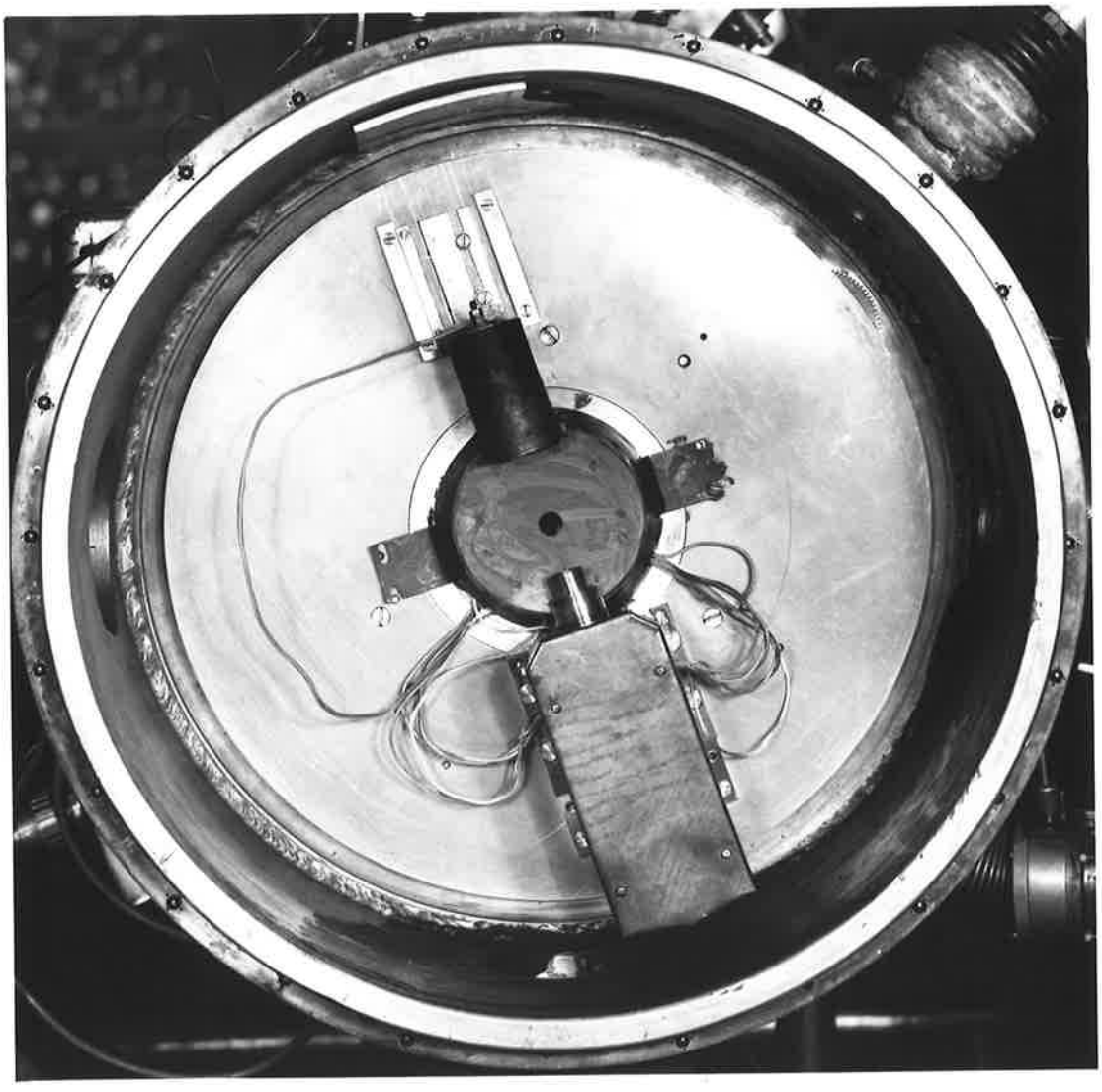

At large angles of scattering the back of the gun was close to the electron spectrometer. A box of metal which surrounded the gun prevented magnetic fields from interfering with the performance of the spectrometer.

Figure 3.9 shows the gun in position in the scattering chamber with the magnetic shields in place.

2(b)(iv). Alignment.

The gun was positioned so that its axis of rotation coincided with the atomic beam axis to a tolerance of 0.005". Thus no variation in scattering volume was introduced by rotating the gun.

Figure 3.10 shows a schematic diagram of the mechanism used to rotate the gun. The gun was mounted on a 12 inch diameter stainless steel plate, so that the electron beam axis was perpendicular to the atomic beam axis. By rotating the shaft K the scattering angle could be varied. The circumference of the plate was graduated in degrees which could be read through a window in the base of the scattering chamber.

2(c). Operation.

2(c)(i). Activation.

Before the cathode could be used, a layer of barium had to be prepared from the barium oxide. At temperatures of 1200°C the

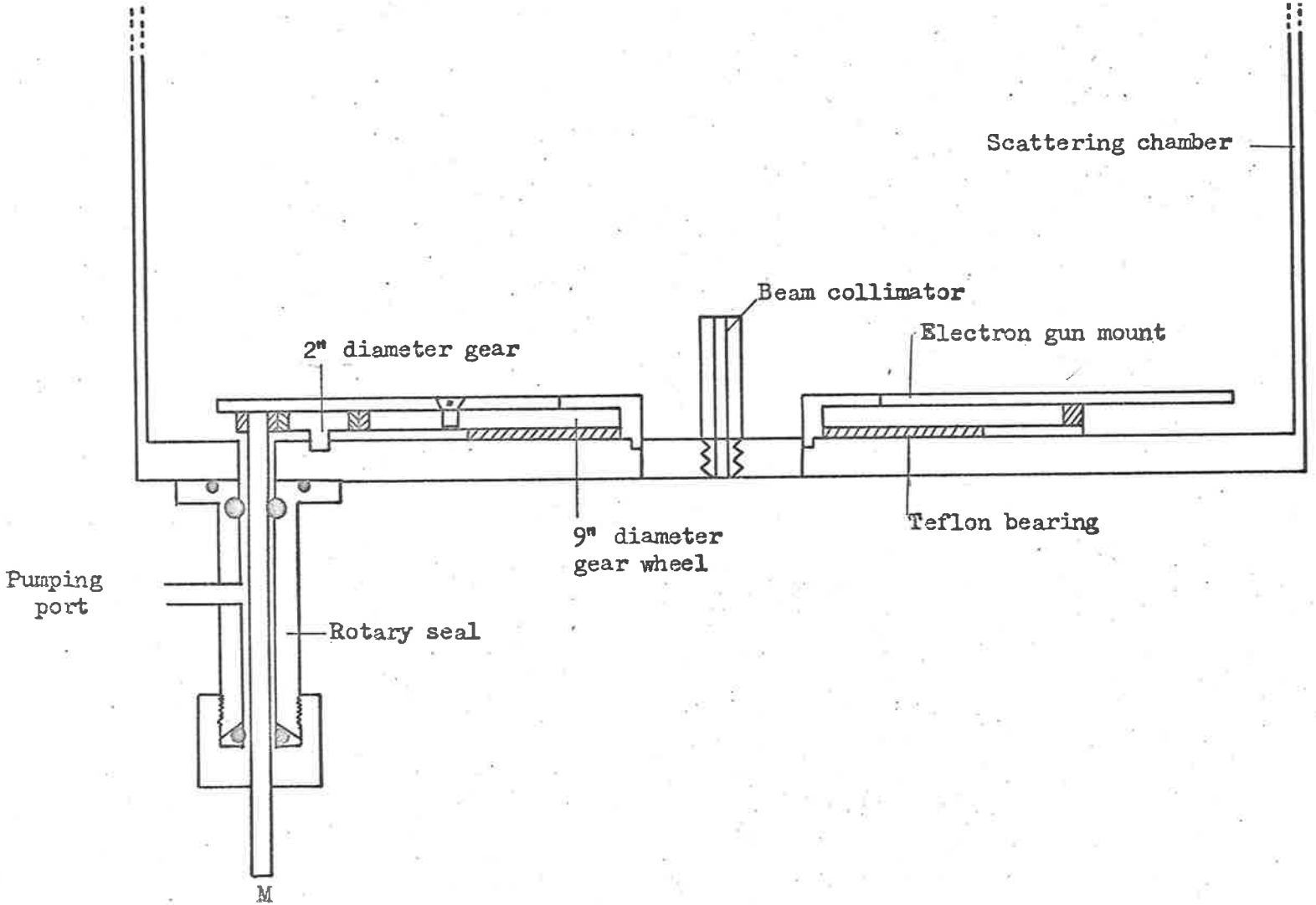

Fig. 3.10: A section through scattering chamber showing the mechanism used to rotate the electron gun.

tungsten reduced the barium oxide to barium.

The temperature of the cathode was held at 1200°C for twenty minutes. The final stage of activation involved reducing the temperature to 1150°C at which stage a potential of -50V was applied to the cathode. After thirty minutes the gun current had stabilised and the potential on the anode could be increased leading to an increase in the beam current.

The time taken to raise the temperature to 1150°C was governed by the pressure in the scattering chamber. As the cathode was heated, the pressure rose due to outgassing from the walls of the scattering chamber and from the gun itself. It was observed that the beam current was more stable if the pressure was less than 1×10^{-5} torr when the initial voltage was supplied to the cathode.

2(a)(ii). Electrical Supplies.

Figure 3.11 shows a schematic diagram of the electrical supplies to the gun.

The heater current was supplied by varying the primary voltage on a step-down transformer. The cathode temperature was made independent of any fluctuations in mains voltage by driving the primary of the transformer from a stabilised mains supply.*

---

* Stabilac.

* L.I.V.S. Low impedence variable supply.

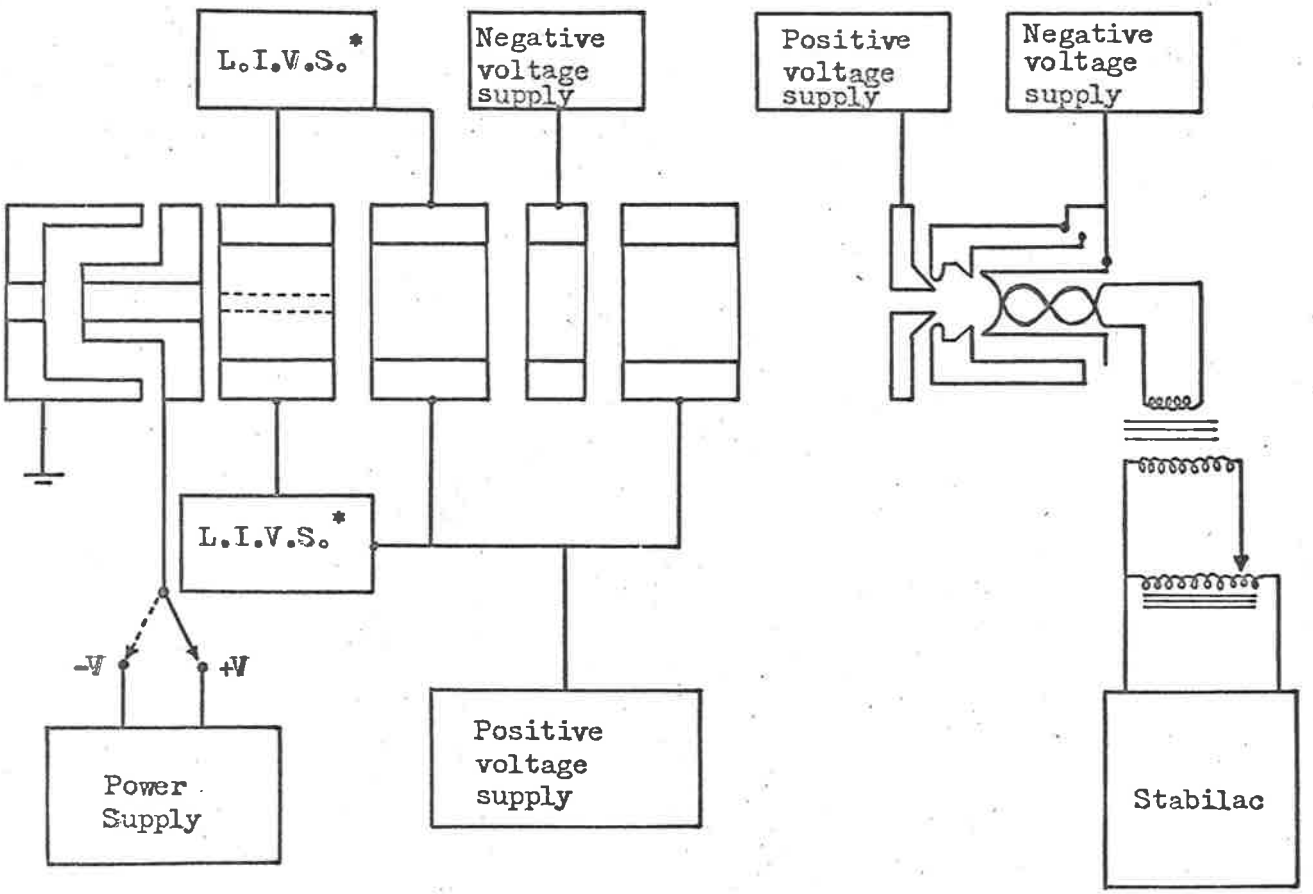

Fig. 3.11: Electrical supplies to the electron gun.

The potentials on the electrodes of the gun were supplied from separate regulated, stabilised power supplies. By the isolation of each electrode in the gun a sufficient number of independently adjustable parameters were available so that optimum focussing conditions and maximum beam current could be determined empirically.

Each power supply was overload protected because of the probability of short circuits to ground occurring when the gun had been heated for some time. Because some electrodes picked up electrons from the beam, it was necessary to use low output impedance supplies. The output impedance of all the supplies was of order 1 or less, thus there was no possibility of the potentials on the electrodes varying as the leakage resistance both between each electrode and between any electrode and ground varied.

2(a)(iii). Focussing.

The optimum focus conditions were determined by adjusting the potentials on the electrodes so that the atomic beam signal was a maximum. This technique was more compatible with the operating conditions than the fluorescent techniques of either Wallmark (1953) or Ausburn (1964).

A quantitative view of the beam shape was provided by moving a diaphragm through the beam. Figure 3.12(a) is a schematic diagram of the diaphragm, electron gun, and collector. When the

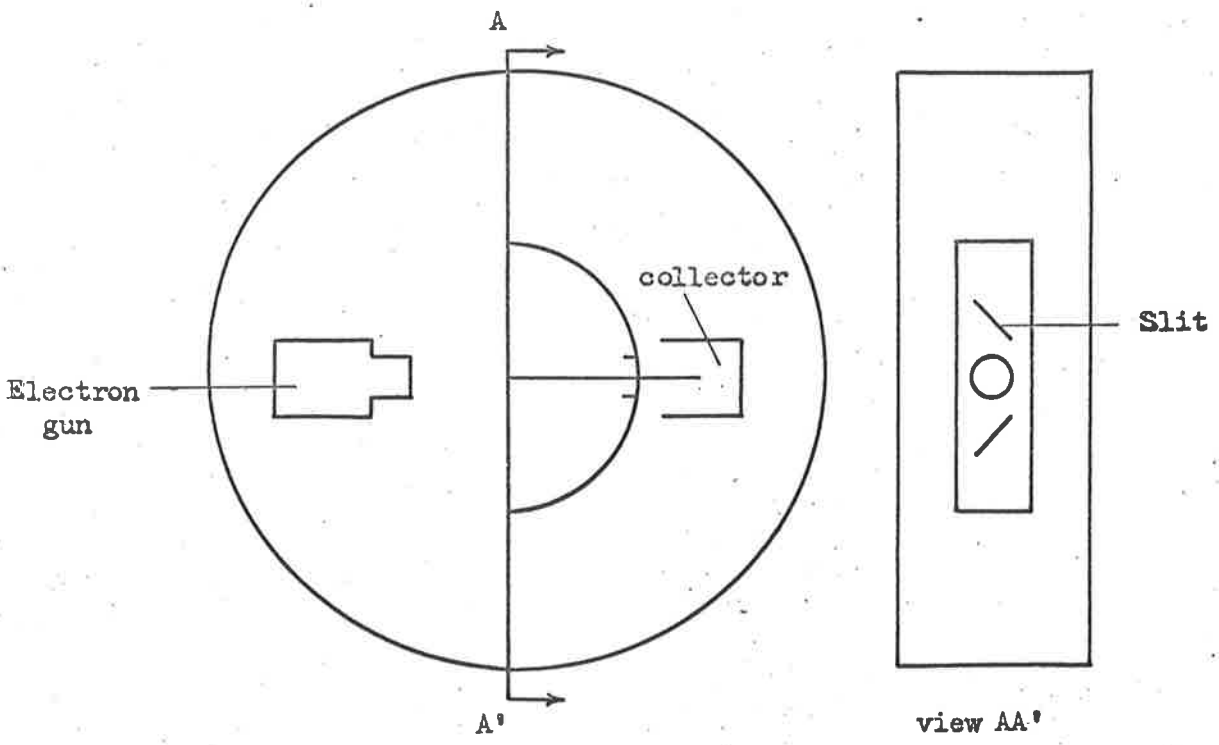

Fig. 3.12(a) : Schematic of Diaphragm used to study the electron beam shape.

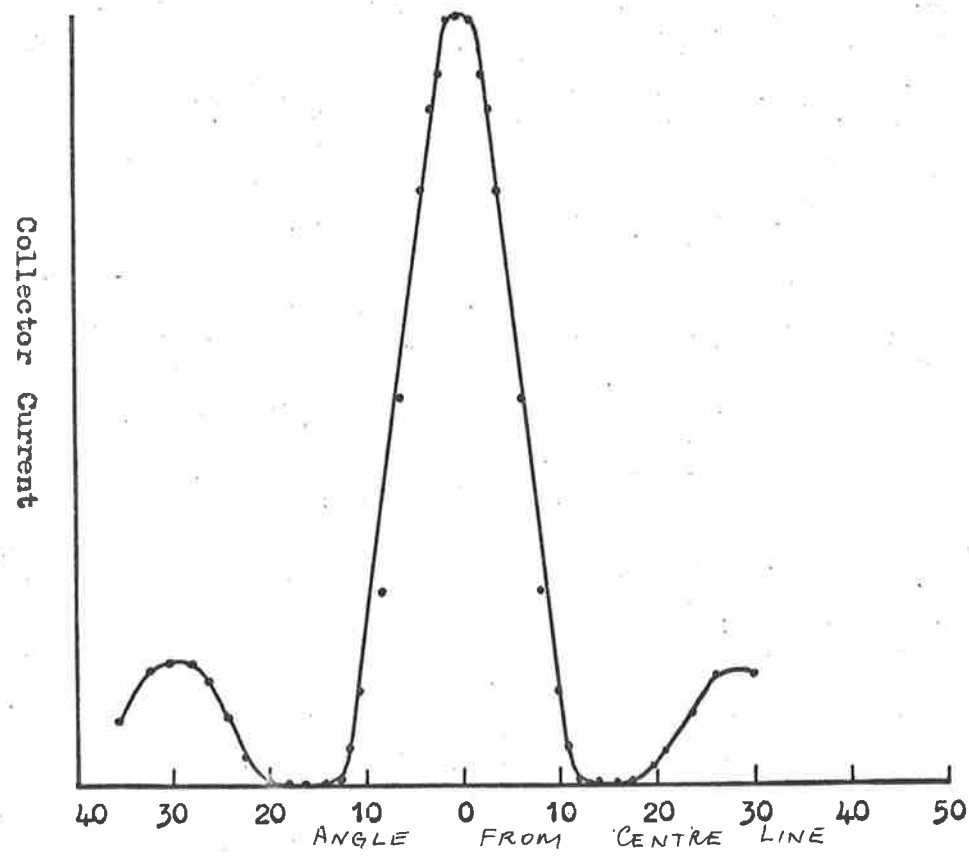

Fig. 3.12(b): The variation in collected current observed when the gun was rotated.

diaphragm was moved through the electron beam, the beam current, collected in the Faraday cup, varied as indicated in figure 3.12(b). The results shown were consistent with a beam of circular cross section and 1.5 cms. in diameter.

2(a)(iv). Electron Beam Monitor.

The major consideration in both the design and positioning of the electron collector was to provide a large aperture so that all of the electrons in the beam could be collected. The entrance aperture of the cup had to be about twice the diameter of the beam in the interaction region because of space charge divergence.

The magnitude of the spread in the beam can be seen from the following example based on the universal beam spread equation (Klemperer (1953)). A 50 electron volt beam from the gun containing a current of 250 microamps which is focussed so that the radius at its minimum diameter is 0.45 cms will spread so that its diameter is 2.5 cms at a distance of 9 cms from the focussing point. After travelling 7 cms from the position of focus, the beam will have spread to a distance of 2 cms.

The collector had an entrance aperture of diameter 2.5 cms and was positioned approximately 6 cms from the interaction region. Because of the large aperture and its proximity to the interaction region, any potentials placed on the collector could penetrate into

the scattering region and influence the paths of the scattered electrons. Although the penetration of the electric field could be removed by placing a grid over the aperture, it was found that insulating layers built up on the grid produced a large background of elastically scattered electrons. The insulating layers were produced by the electron bombardment of oil layers. Thus the grid was removed and the collector run at earth potential.

The potential set up on the collector by the passage of the beam current through the internal resistance of the meter was negligible.

The inside of the cup was painted with colloidal graphite to reduce secondary electron effects.

2(d). Performance.

2(d)(i) Beam Current.

Table 3.1 shows typical beam currents which were used in the modulated beam experiments

Table 3.1.

BEAM ENERGY (e.v.)	BEAM CURRENT (milliamps)
50	0.25
75	0.45
100	0.7
200	3

The beam currents quoted were measured at a pressure of 1.6×10^{-6} torr, and showed the same increase with background pressure as has been observed by Simpson and Wyatt (1963), Spangenburg, Field, and Helm (1942). The increase is caused by the neutralisation of space charge by positive ions associated with the background.

Provided the pressure remained below 5×10^{-6} torr the beam currents given in Table 3.1 were reproducible.

2(d)(ii). Energy Distribution.

The thermal spread in electron energies which is produced by a thermionic source is (Simpson 1964)

$$\Delta E_T = \frac{2.54\,T}{11,600} \qquad (3.1)$$

where T is the temperature of the emitter and ΔE_T the full width at half maximum (F.W.H.M.) in electron volts.

Since in the present case $T = 1400^{\circ}K$, the expected full width at half maximum of the distribution of electrons produced from the gun would be of order 0.3 electron volts.

The electron spectrometer was used to measure this distribution. The resolution of the spectrometer was (Hanrower 1955)

$$\Delta E = CE \qquad (3.2)$$

where E was the incident electron energy and C a constant of the instrument.

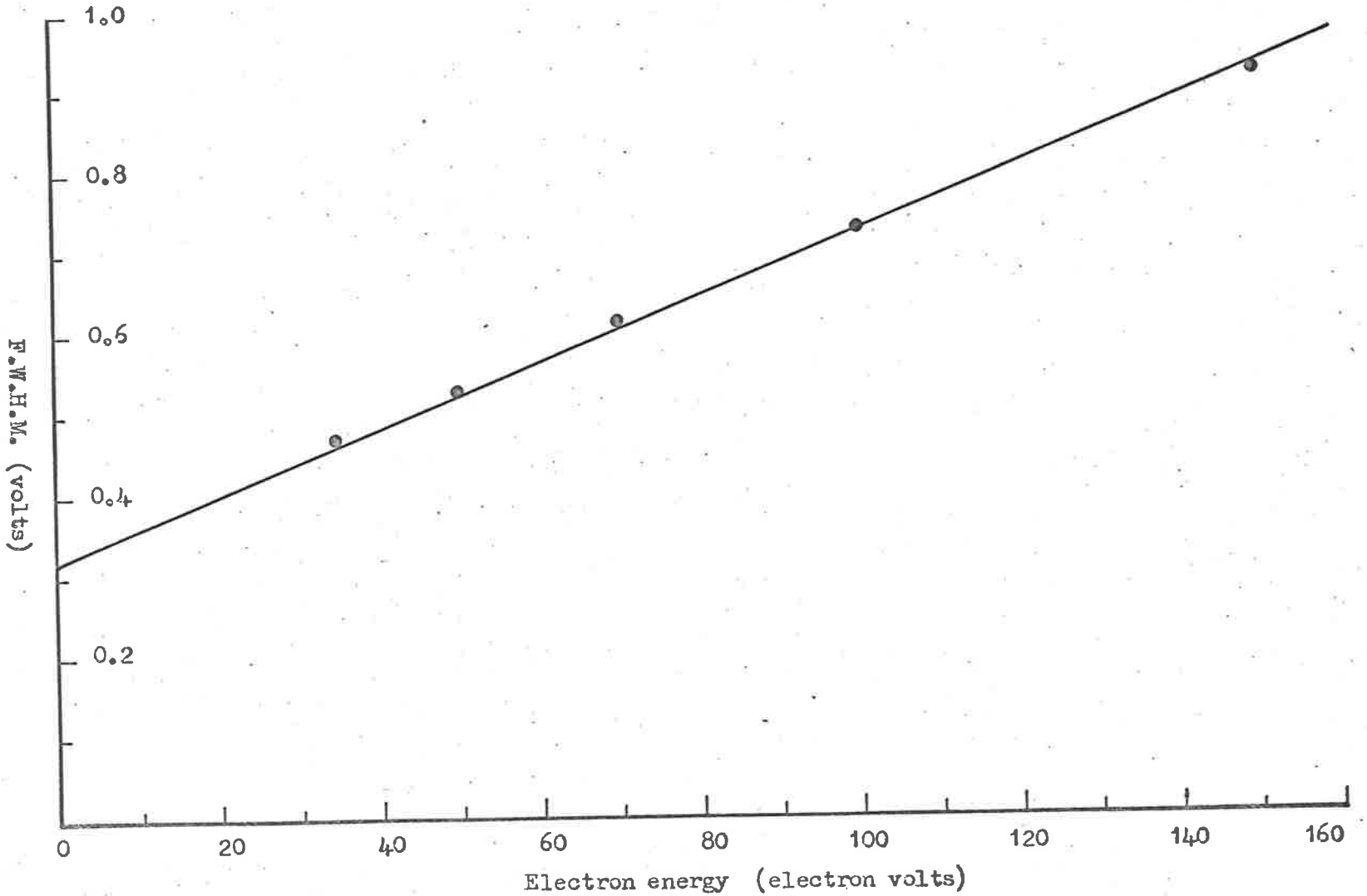

Fig. 3.13: The variation of the full width at half maximum of the elastically scattered electron signal recorded by the electron spectrometer as a function of the incident electron energy.

The F.W.H.M. of a distribution of electrons produced by a thermionic source and measured by spectrometer would be given by the sum of (3.1) and (3.2). That is

$$\Delta E_s = \Delta E_T + CE$$

The value of ΔE_T was determined by measuring ΔE_s as a function of E. Figure 3.13 shows the results of such a determination. The value of ΔE_T given by the intercept of the straight line on the vertical axis was consistent with that predicted by equation 3.1.

An independent measurement of the energy distribution of the electrons produced in the gun was made with the retarding potential difference technique of Fox et al.* The apparatus is illustrated schematically in figure 3.14. A negative potential was applied to the collector in the form of a linear ramp and also to the axis of the X-Y recorder. The current reaching the collector was fed through a microammeter either direct, or through a differentiating network to the Y axis.

Figure 3.15(a) shows the variation of the collector current as a function of the negative potential applied to the collector whilst figure 3.15 (b) shows the differentiated spectrum.

It can be seen that the only electrons produced in the gun were those whose energy corresponded to the difference in potential between the cathode and earth.

* Fox, R.E., Hickam, W.M., Grove, D.J., and Kjeldaas, T. (1955)

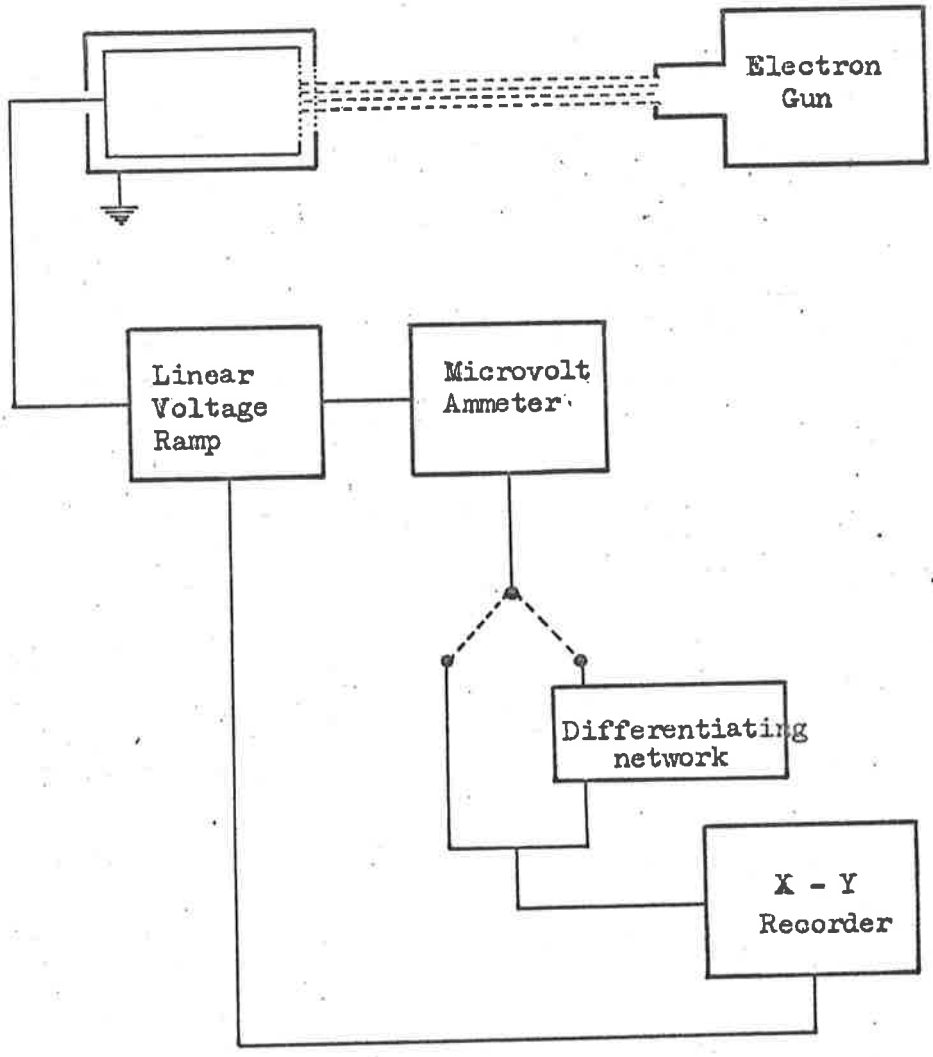

Fig. 3.14: Schematic of the apparatus used in the retarding potential analysis of the electron beam energy.

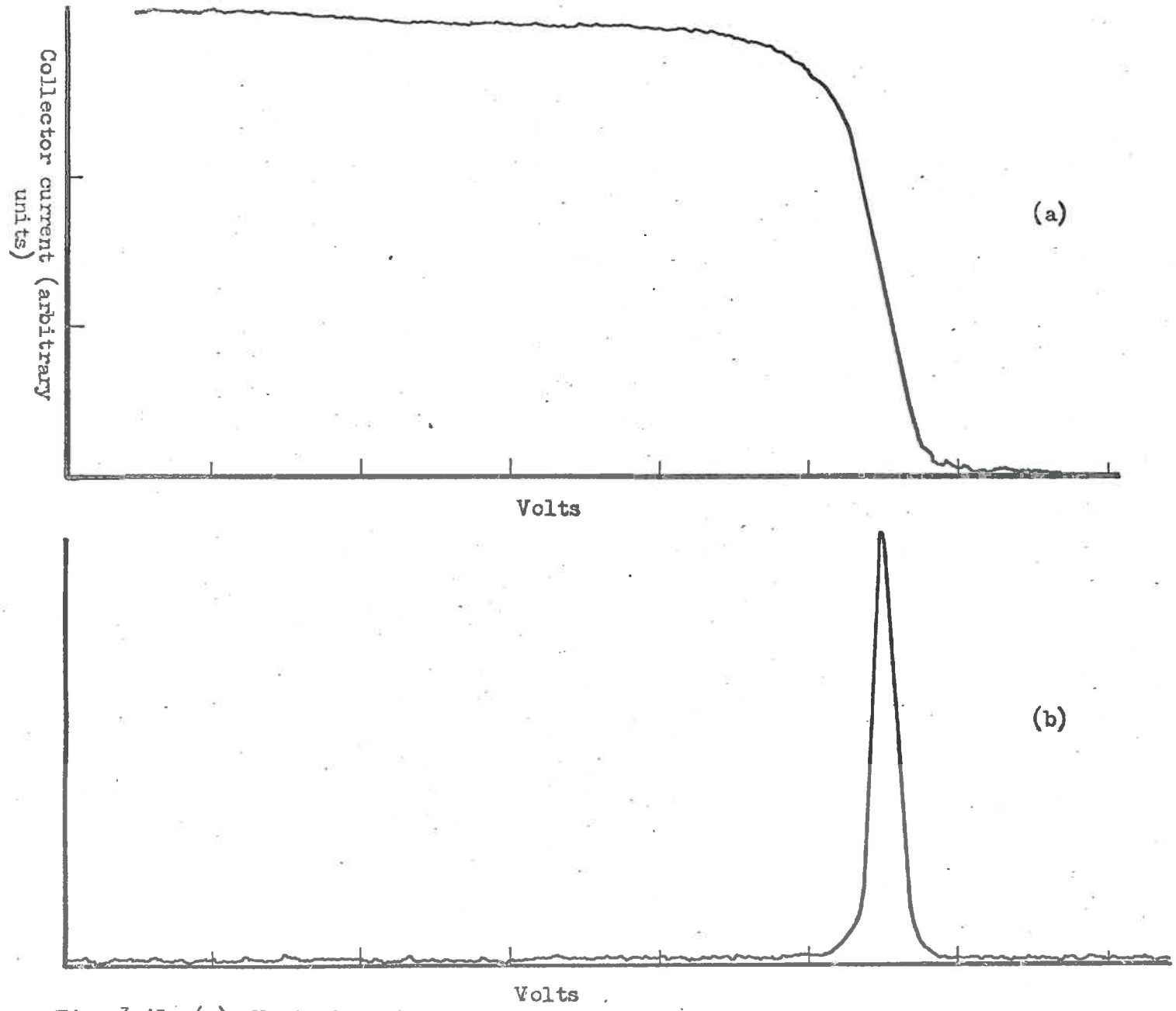

Fig. 3.15. (a) Variation of electron beam signal with negative potential applied to collector.
(b) differentiated spectrum.

The inconsistency of the F.W.H.M. of the distribution measured in this way with that previously described was due to space charge effects in the retarding potential region.

2(d)(iii). Stability.

Dispenser cathodes composed of barium oxide show a marked decrease in emission in the presence of water vapour (Trolden 1959 ; Hughes and Coppola 1957). Therefore to ensure long term stability a high pumping speed liquid air trap was installed in the scattering chamber.

Provided the pressure in the scattering chamber remained below 5×10^{-6} so that the space charge neutralisation mentioned in section III.2(d)(i) did not affect the beam, the beam current was stable to better than 1% for periods of up to six hours continuous running.

CHAPTER IV

Angular Distribution of Elastically Scattered Electrons from Helium and Argon.

Introduction.

In Chapter II it was noted that the modulated crossed beam technique can be used to advantage to measure angular distributions of elastically scattered electrons from helium and argon.

The measurement of the angular distribution of electrons scattered elastically from helium and argon was performed in the energy range from 50 to 200 electron volts and in the angular range from 30° to 130°. The results of the determination are presented in this chapter.

IV.1 Elastic Scattering from Helium.

1(a). Experimental Arrangement.

The experimental arrangement employed during the elastic scattering experiments is illustrated in figure 4.1.

The atomic beam effused through a slit in the wall of a tungsten cylinder and was chopped in a differentially pumped chamber. The chopped beam entered the scattering chamber through a circular aperture in the centre of the chamber. Here it was intersected by an electron beam produced by the gun described in section 3.2. The scattering volume was defined by the intersection of the atomic beam and the electron beam.

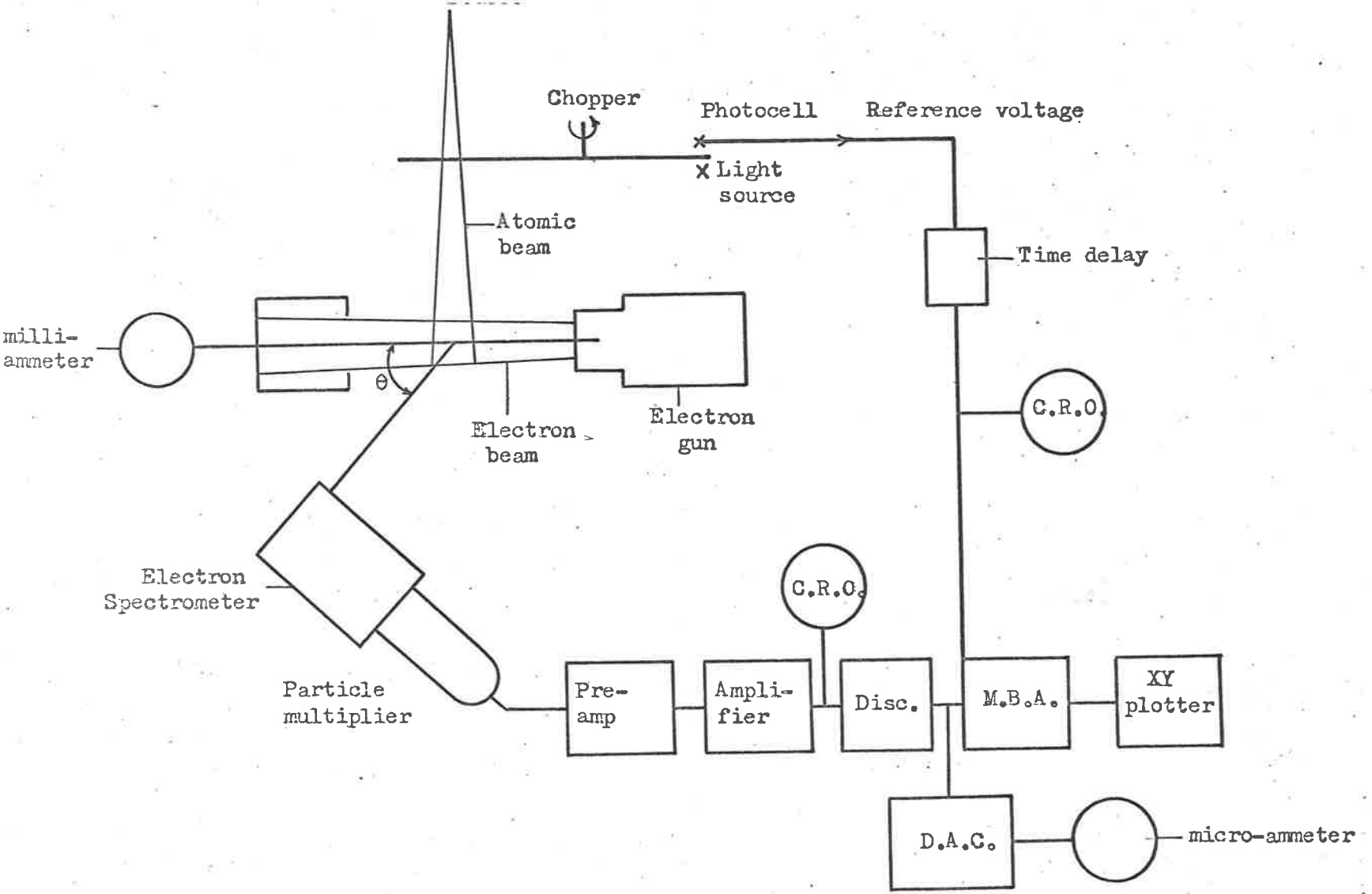

Fig. 4.1: Schematic of modulated beam apparatus used to measure the angular distribution of elastically scattered electrons from helium and argon.

An electron spectrometer was positioned such that its entrance aperture was in the same plane as the electron beam and viewed the interaction region. The scattering angle was defined by the angle between the axis of the electron beam and a line drawn through the centre of the entrance aperture.

The output from the electron gun was monitored in the Faraday cup described on page (47). The cup was mounted on the same table as the gun and rotated with it.

As the primary energies studied were greater than the first excitation threshold for helium, the electrons scattered through a particular angle consisted of elastically and inelastically scattered electrons. A parallel plate electron spectrometer was used to separate the elastically scattered group from the inelastically scattered group. A description of the spectrometer and details of its performance follow.

1(b). The Electron Spectrometer.

1(b)(i). Description.

The spectrometer is illustrated schematically in figure 4.2.

Two parallel plates P_1,P_2 were used to provide an electric field. Plate P_1 was held at earth potential and formed the main

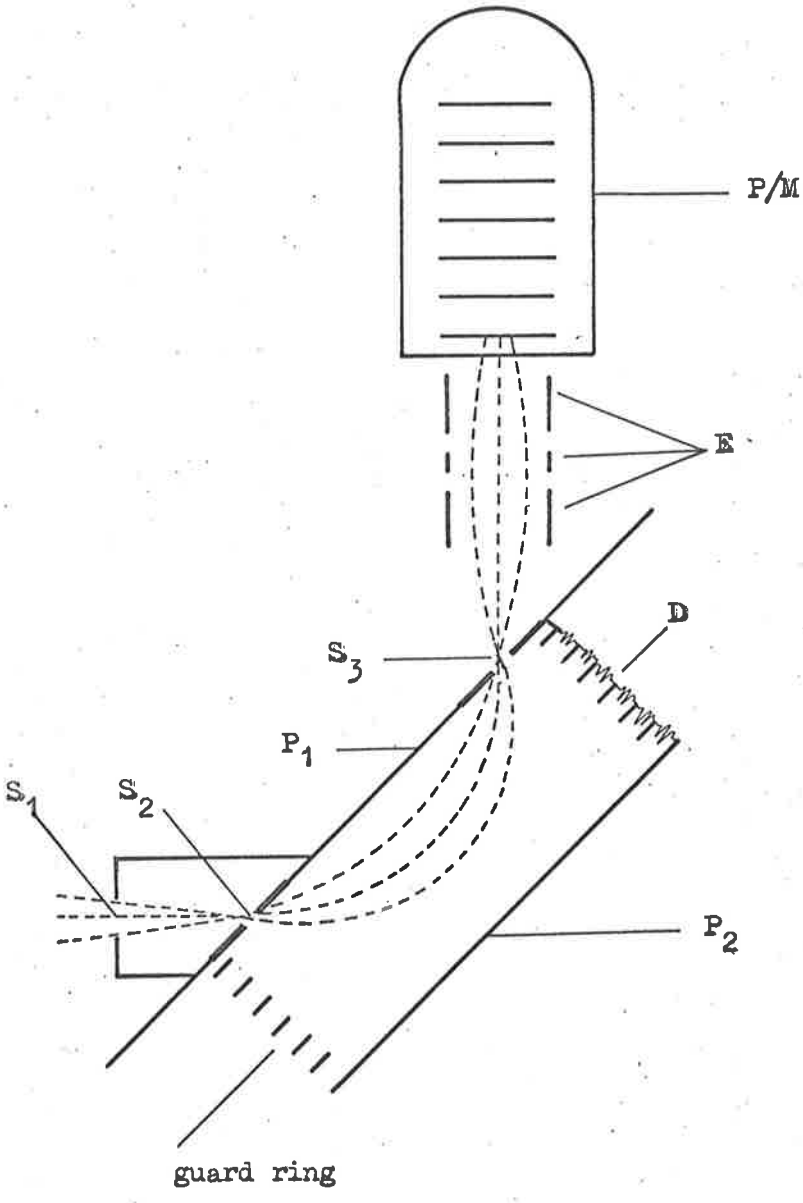

Fig. 4.2: Schematic of parallel plate electron spectrometer.

support of the device. Electrons of equal energy which entered the spectrometer through the slits S_1 and S_2 travelled in parabolic paths to recross at the exit slit S_3. The entrance and exit slits were arranged so that the electrons entered and left the field at 45°.

The electric field was set up between the two plates by applying a voltage to plate P_2. A series of guard rings were placed between P_1 and P_2 to ensure uniformity of the field and to minimise fringe field effects. Guard rings of this type have been used in a parallel plate electron spectrometer by Kuyatt and Simpson (1964). The potentials on the guard ring were set by the divider chain D.

An einzel lens E focussed the analysed electrons onto the first dynode of the particle multiplier tube P/M.

The structure was supported from the lid of the scattering chamber so that slit S_1 was 5 cms from the interaction region.

An earthed metal box surrounded the device to prevent stray electrons from entering the analyser and to preclude the penetration of the electric field from the interaction region.

All surfaces which were exposed to the electrons were coated with colloidal graphite to minimise secondary electron effects.

1(b)(ii). Resolution.

If ΔE is the difference in kinetic energy between two groups of electrons whose images just touch but do not overlap, then the resolving power

$$R = \frac{E}{\Delta E} \qquad (4.1)$$

Yarnold and Bolton (1949) have shown that

$$R = l/w \qquad (4.2)$$

where l is the distance between the slits and w their width.

For the present instrument l = 2" and w = 0.010" hence R was 200.

A spectrometer with R = 2500 has been used by Lassettre et al. (1964) to investigate inelastic scattering of electrons from atoms and molecules at incident energies of order 500 e.v.

With a resolving power of order 200, elastic scattering angular distributions could be measured conveniently and it was possible to resolve the 2^3S, 2^1P and 3^1P states in helium after excitation by 50 e.v. electrons. (Appendix B)

It was possible to measure the resolution of the spectrometer from the slope of the graph in figure 3.13, as described in section III.2(d)(ii). The measured resolution was consistent with that predicted by equation (4.2).

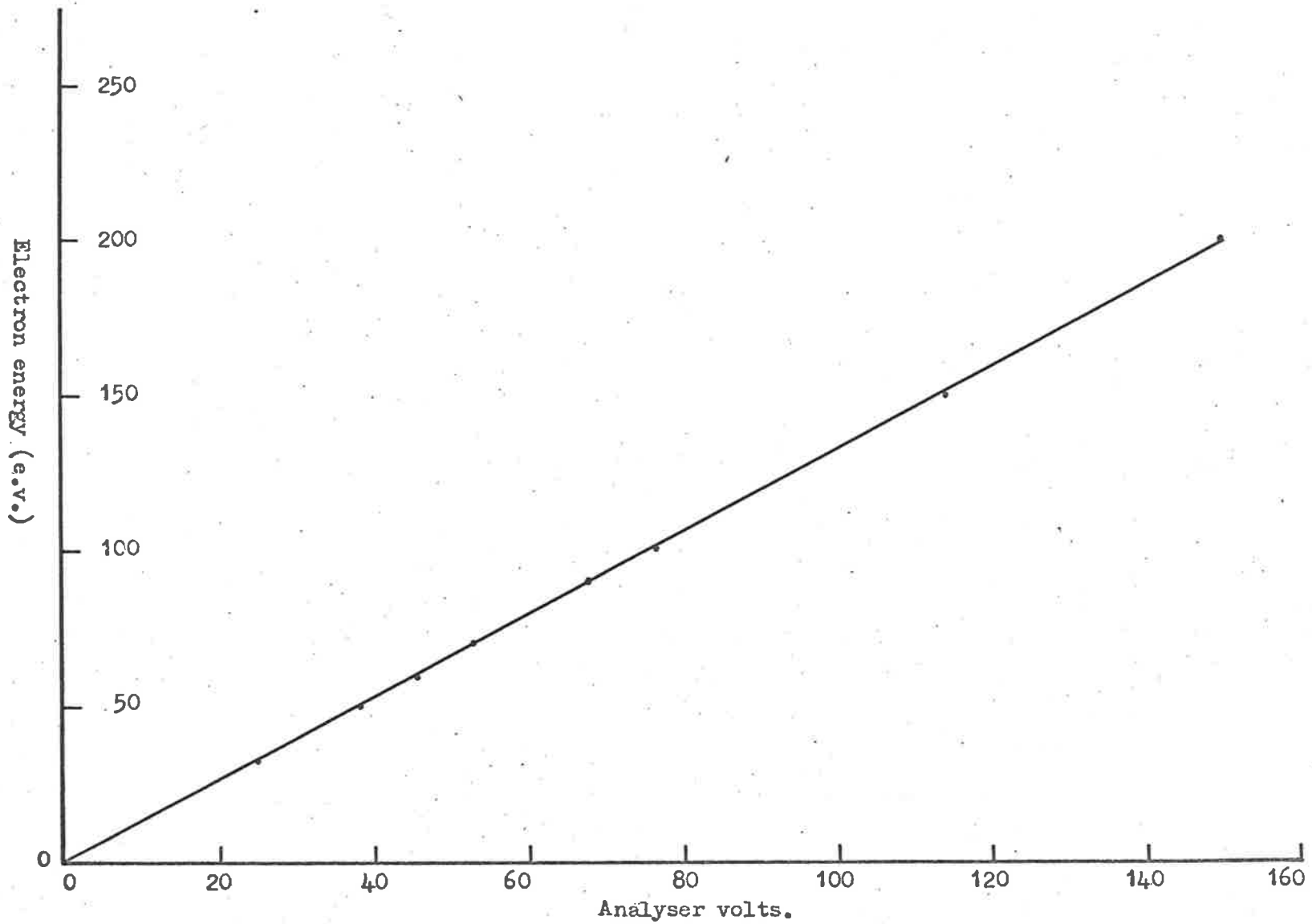

Fig. 4.3. Variation of voltage applied to the Spectrometer with incident electron energy.

1(b)(iii). Calibration.

The potential difference V between the plates P_1 and P_2 which is required to bring the image of slit S_2 onto S_3 is related to the energy E of the incident electrons (Harrower 1955) by

$$E = kV \qquad (4.3)$$

where

$$k = l/2d$$

l has been defined in the preceding section and d is the distance between the two plates.

The most straightforward way of measuring k was to determine the value of V which would produce a maximum in the elastically scattered electron signal of energy E. The voltages V were measured with a high impedance potentiometer* and the value of E was taken to be the potential applied to the cathode of the electron gun.

The results of such a measurement are plotted in figure 4.3. k is given by the slope of the graph. By applying the method of least squares the slope was found to be

$$k = 1.32 \pm 0.003$$

which agreed very well with the value of k = 1.32 predicted from equation 4.3 with l = 2" and d = 0.76".

---

* John Fluke

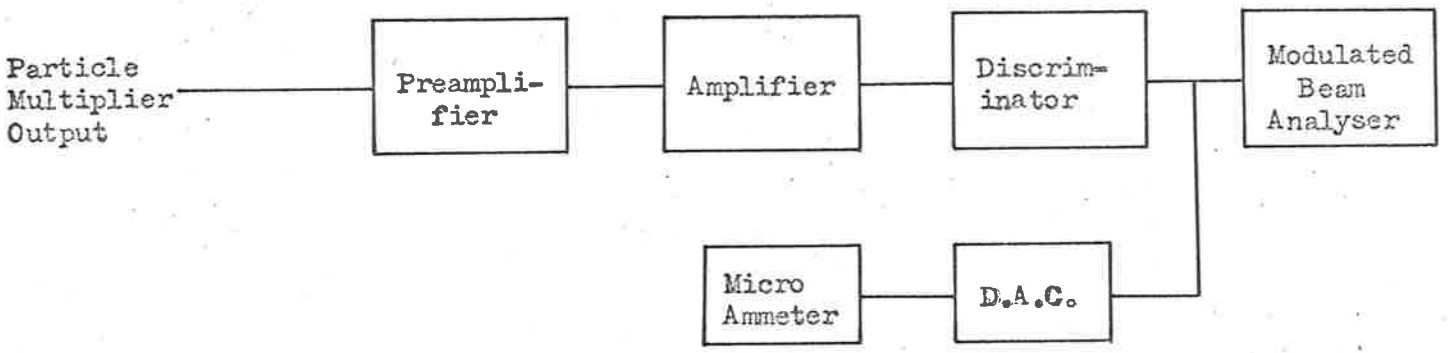

Fig. 4.4: Block diagram of electronics associated with the electron spectrometer.

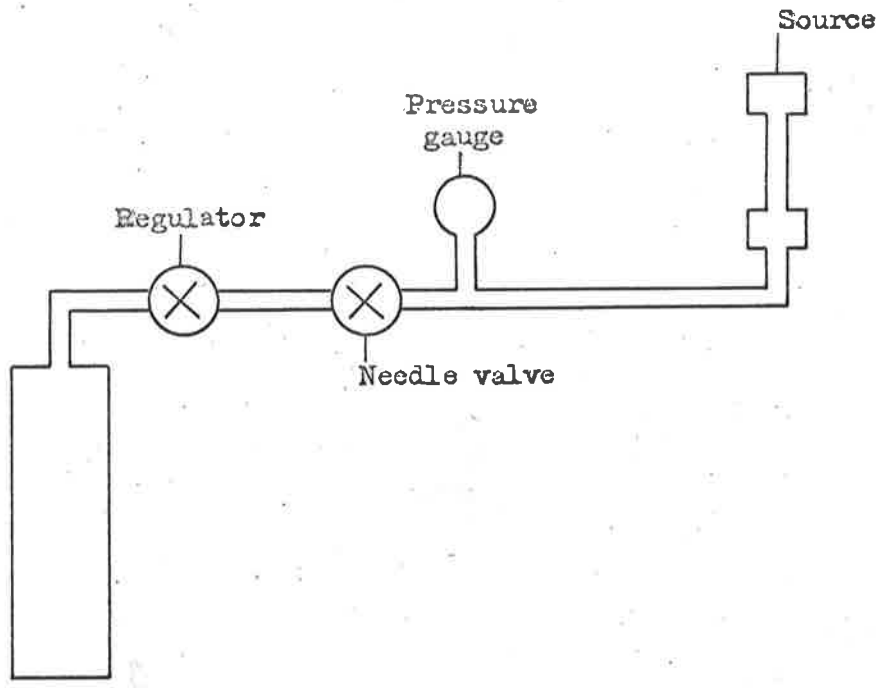

Fig. 4.5: Input to the source.

Figure 4.4. shows a block diagram of the electronics associated with the spectrometer. Pulses from the anode of the particle multiplier tube were passed via a preamplifier** into a linear pulse amplifier** and discriminator**. The output from the discriminator was fed in parallel to a digital to analogue converter and to the modulated beam analyser. The digital to analogue converter was a diode pump, the current from which was fed to a micro-ammeter.

1(e). Procedure.

Figure 4.5 is a schematic diagram of the input to the source. Helium (99.99% pure) was taken from a regulator and flowed into the source along a pipe. The gas flow was controlled by a needle valve.† Variation of the needle valve setting altered the pressure in the source and hence the number of scattering centres in the beam. As the pressure gauge†† was positioned 21 cms from the source, the reading on the gauge represented the source pressure plus the pressure drop along the line.

Figure 4.6 shows the effect of varying the source pressure on the number of 100 e.v. electrons scattered elastically through an

---

** Dynatron.

† Edwards type LB 1A

†† Edwards Speedivac CC 1.

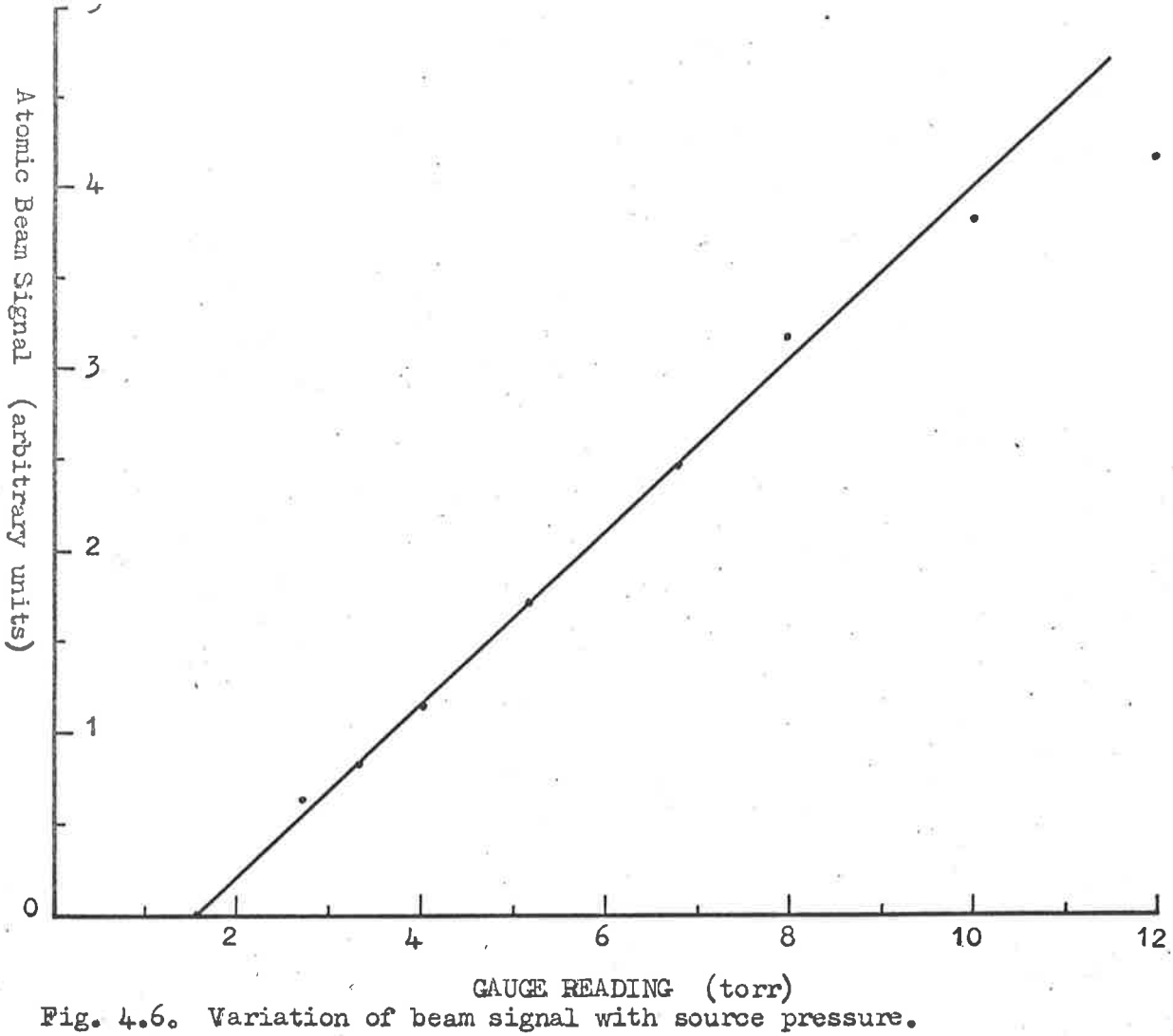

Fig. 4.6. Variation of beam signal with source pressure.

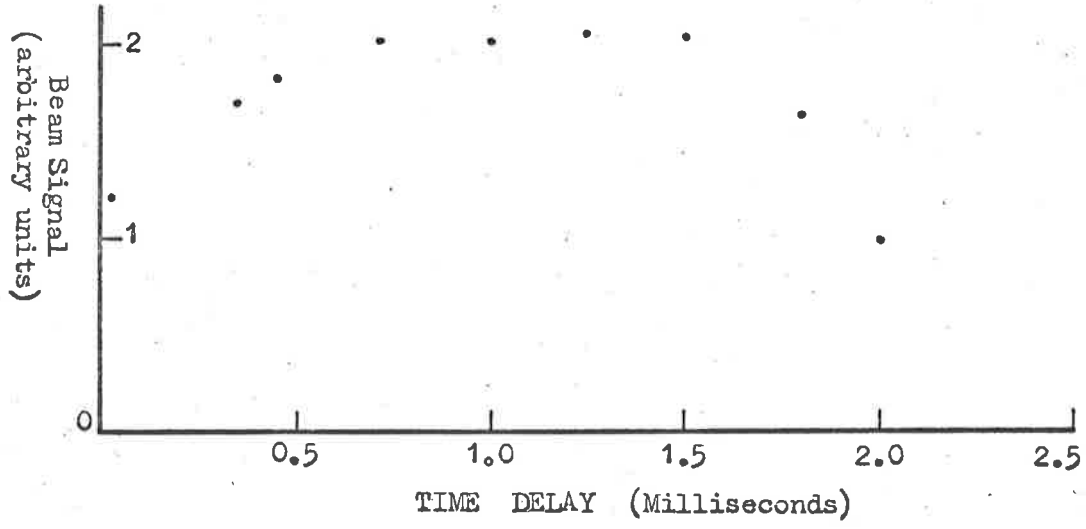

Fig. 4.7. Effect on elastically scattered electron signal by varying phase of the reference voltage.

angle of 50° from the chopped helium beam. It can be seen that there was a linear relationship between chopped beam signal and gauge reading, for readings between 1.5 torr and 10 torr. The 1.5 torr corresponded to the pressure drop along the line. Beyond 10 torr, the mean free path in the source violated the molecular flow criterion (section III.1(a)(ii)) resulting in a cloud formation in front of the slit. The scattering of beam atoms by the cloud gave rise to the breakdown in the linear relationship observed below 10 torr.

The needle valve was adjusted so that the source pressure bore a linear relationship to the beam signal and during the runs was set at 5 torr on the gauge.

The chopping frequency was set at 160 c.p.s. for reasons described in section III.1(b)(iii).

The time delay of the reference signal was adjusted so that the output from the electron spectrometer was in phase with the reference signal. Figure 4.7 shows the effect on the chopped beam signal of varying the time delay. The modulated beam signal shown in figure 4.7 represented the number of 50 e.v. electrons elastically scattered through 40° from helium. The beam shape determined in this fashion was consistent with that described in section II.4(e).

Since the electron spectrometer had a finite energy resolution, the number of elastically scattered electrons was proportional

to the area under the elastic scattering peak. If however the full width at half maximum of the elastic scattering peak remained constant as a function of scattering angle, relative angular distributions could be measured by determining the way in which the peak height varied with angle. The voltage to plate P_2 of the spectrometer was set by the application of a constant fraction (1/k as defined in section IV.1(b)(iii)) of the cathode voltage using a 10 turn helipot. The peak was observed on the digital to analogue converter.

The electron beam was focussed into the interaction region by optimising the modulated beam signal for the reason described in III.2(c)(iii).

The electron beam energy was set by the cathode potential which was measured with a vacuum tube voltmeter.

The electron gun was moved at five degree intervals and the beam signal recorded. As the electron beam current remained constant during each run to better than 1%, the only correction to the recorded signal was that due to dead time effects in the main amplifier.

The dead time of the main amplifier was measured on a cathode ray oscilloscope* and was 1 microsecond. By keeping the

---

* Tektronix 533

maximum counting rate to 100 kcs, the greatest correction involved was 10%. Under these conditions the standard formula (4.4) can be used

$$\dot{N} = \frac{\dot{n}}{1 - \dot{n}\tau} \qquad (4.4)$$

where $\dot{N}$ is the true counting rate, $\dot{n}$ the observed counting rate and τ the dead time of the main amplier.

The counting rate $\dot{n}$ was calculated from the output of the background scaler which has been described in section II.4.

The time spent at any angle was determined by the spread in the data points recorded by the add subtract scaler.

If N_1 was the number of events recorded when the beam was on and N_2 the number when the beam was off then the variance in beam signal was given by

$$\sigma = (N_1 + N_2)^{\frac{1}{2}}$$

Under experimental conditions N_1 was at most 5% greater than N_2, thus to a good approximation

$$\sigma = \sqrt{2N_2}$$

Each data point resulted from an accumulation of events in the add subtract scaler for about 10 seconds. The existence of any other source of fluctuation was checked by recording up to 15 data points. It was verified that the maximum difference between beam

points was within the fluctuation to be expected on statistical grounds.

A mean was taken of the data points and the standard deviation of the mean determined. Counts were collected until a relative error of order 3% was obtained.

1(c). Results and Discussion.

The angular distribution for elastic scattering of 50 electron volt electrons from helium is shown in figure 4.8(a). The present results, which are represented by points, have been normalised to the values of Bullard and Massey (1931) at a scattering angle of 60°. The agreement is very good. The angular distribution shows a shallow minimum at 100°.

The angular distribution for elastic scattering of 75, 100 and 200 electron volt electrons from helium are shown in figures 4.8(b), 4.9(a), and 4.9(b) respectively. The present results have been normalised to the values of Hughes, McMillen, and Webb (1932) at each impact energy. Excellent agreement is obtained in each case thereby confirming the earlier results of Hughes et al. (ibid) which were not measured with the crossed beam configuration.

As indicated in section I.1(c), the energy range was chosen in order to provide new measurements for the several calculations which have appeared recently in the literature. It has been pointed out

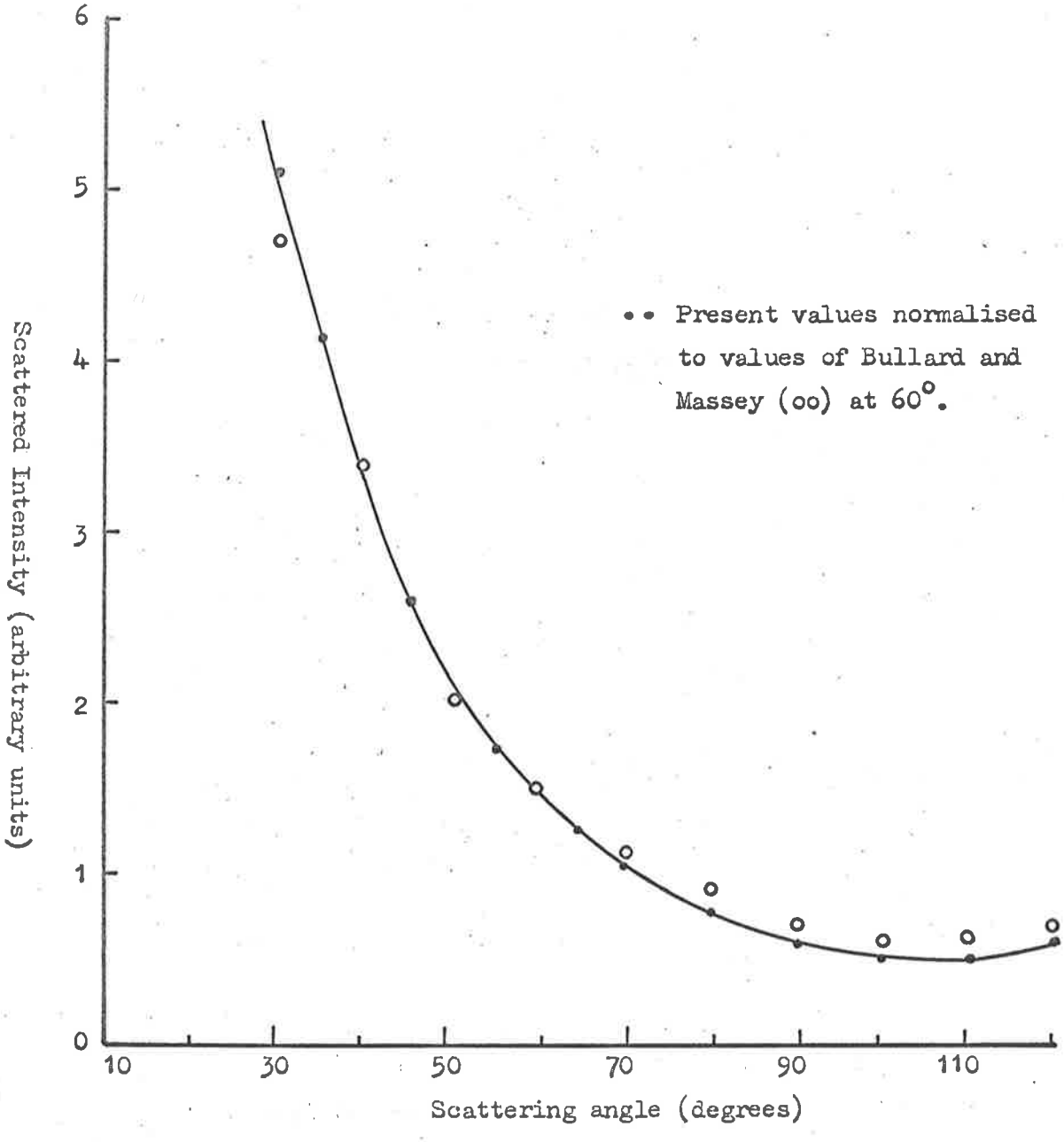

Fig. 4.8(a). Angular distribution of 50 e.v. electrons elastically scattered from helium.

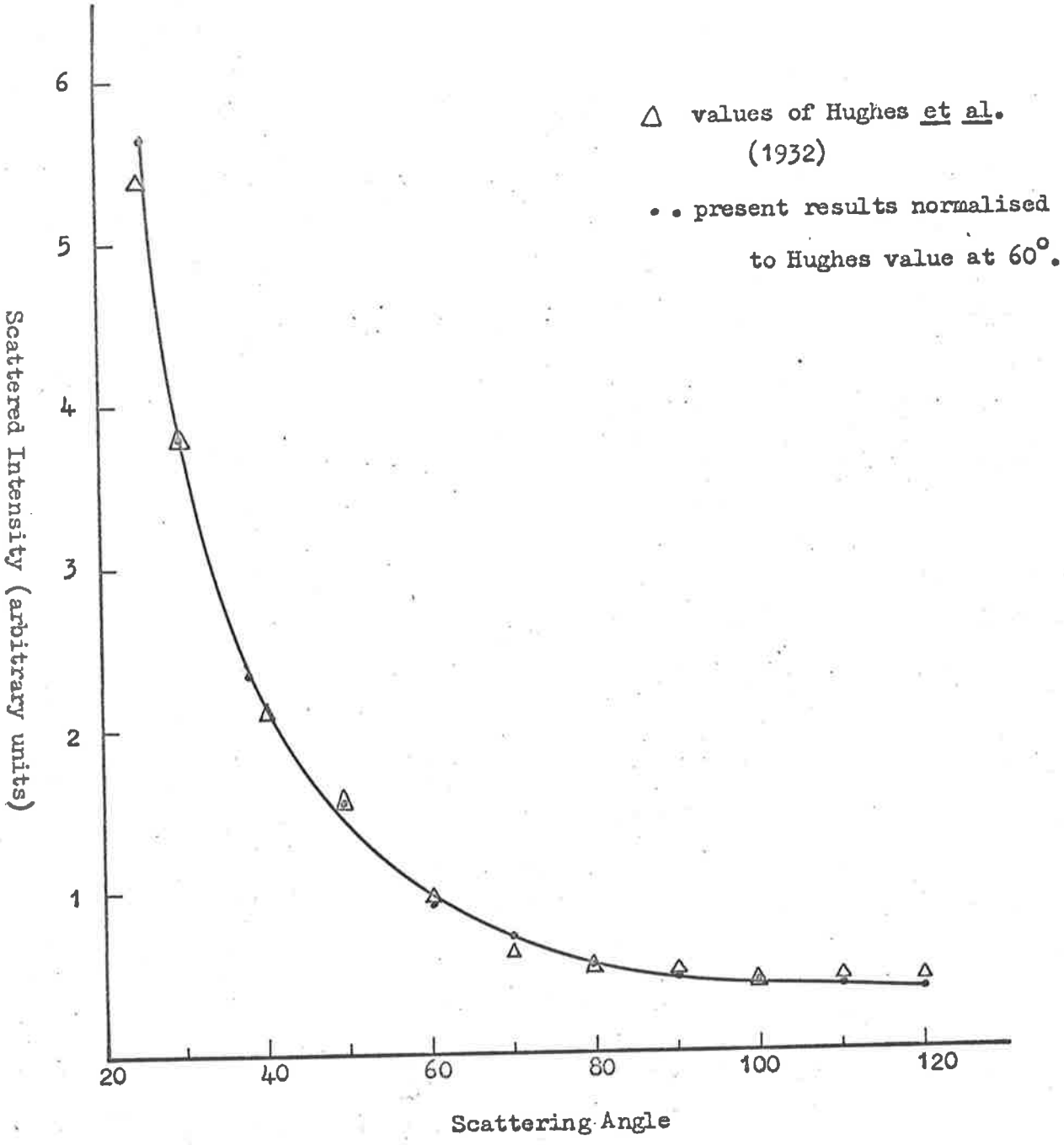

Fig. 4.8(b): Elastic scattering angular distribution from helium. Incident energy 75 e.v.

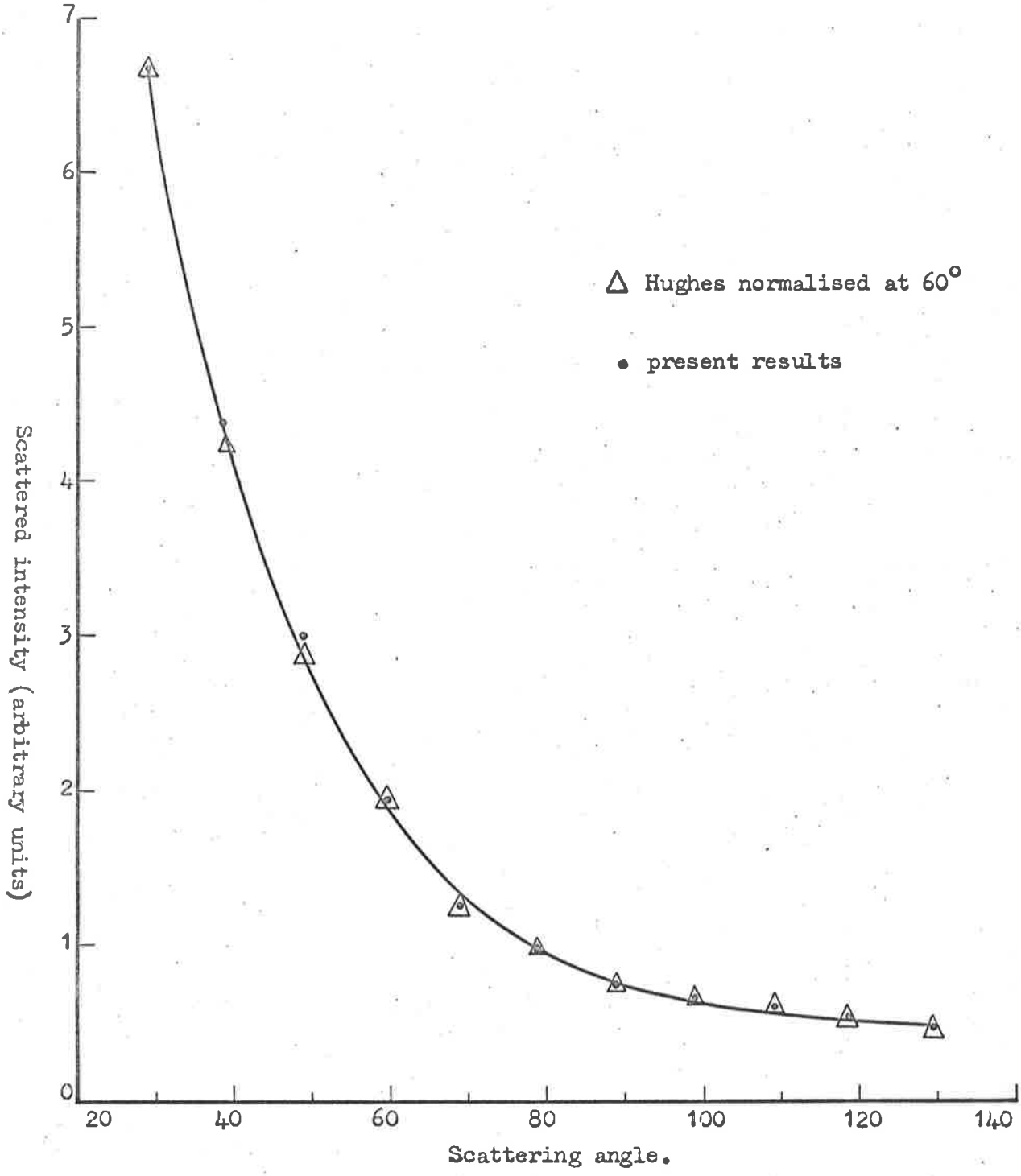

Fig. 4.9(a). Angular Distribution of 100 electron volt electrons elastically scattered from helium.

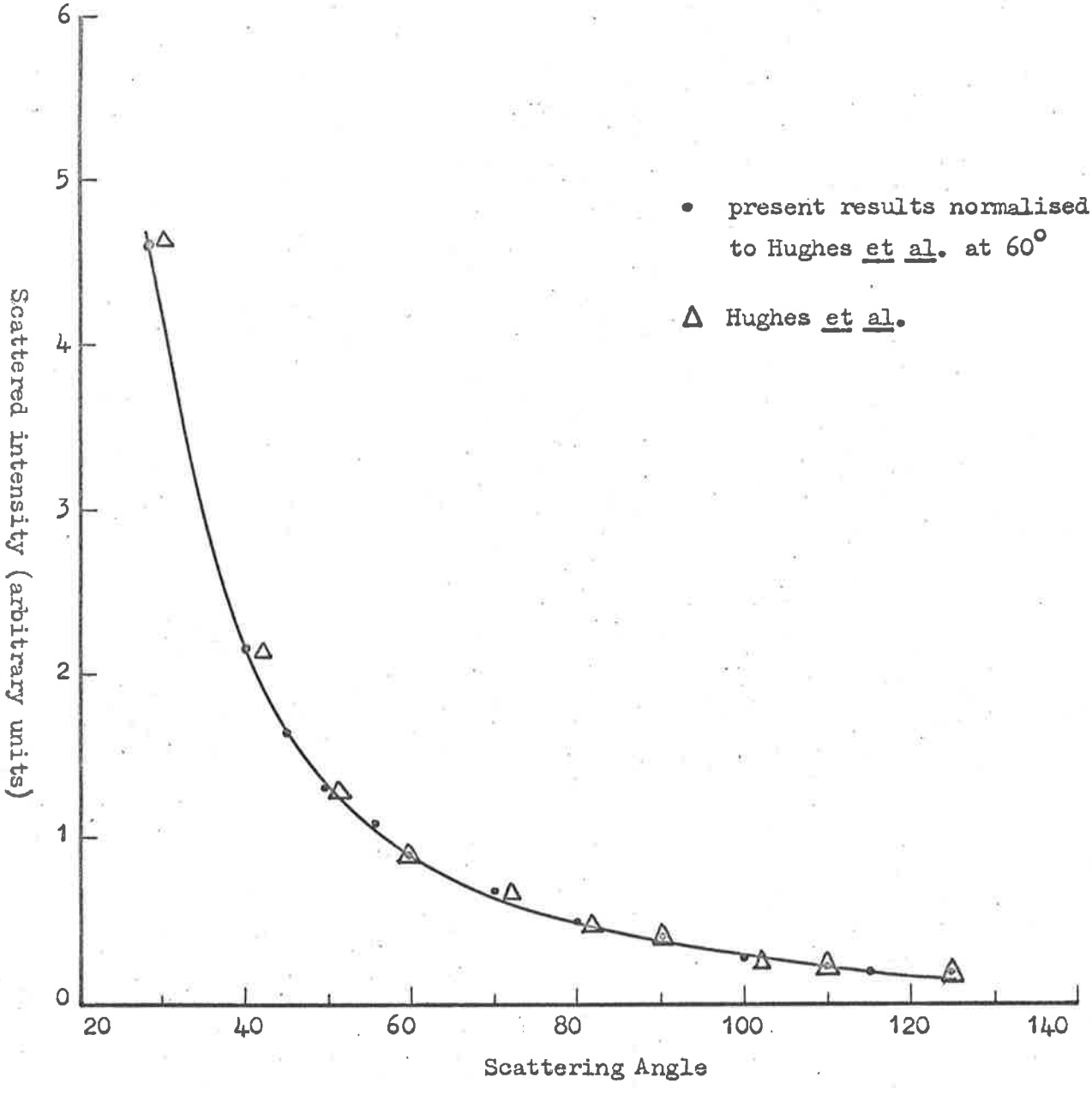

Fig. 4.9(b). Angular distribution for Elastic scattering of 200 e.v. electrons from helium.

in Chapter I that Massey and Mohr (1934) were able to gain satisfactory agreement with the laboratory data of Hughes et al. by using the second Born approximation to allow for polarisation of the atom by the incoming electron. An inconsistency in this method of attack has been pointed out by Kingston, Moiseiwitsch, and Skinner (1960). The rapid increase in scattered intensity at small scattering angles was found by Massey and Mohr (ibid) to arise from the imaginary part of the scattering amplitude which contributes a term of fourth order in the interaction potential. A term of similar order arising from the real part of the scattering amplitude derived from the third Born approximation was omitted. Therefore Khare and Moiseiwitsch (1965) undertook a fresh investigation of the role of polarisation in electron-helium scattering. The basic approximation used by Khare and Moiseiwitsch was the static field approximation. The ground state wave function which they used was the variational wave function of Green et al. (1954). Exchange was included by using the first order exchange approximation. The influence of polarisation was accounted for in the calculation by including an additional potential of the order of r^{-4} in the radial wave equation. The resulting angular distributions were normalised to the Hughes et al. (1932) data and good agreement was obtained to the shape of the distribution.

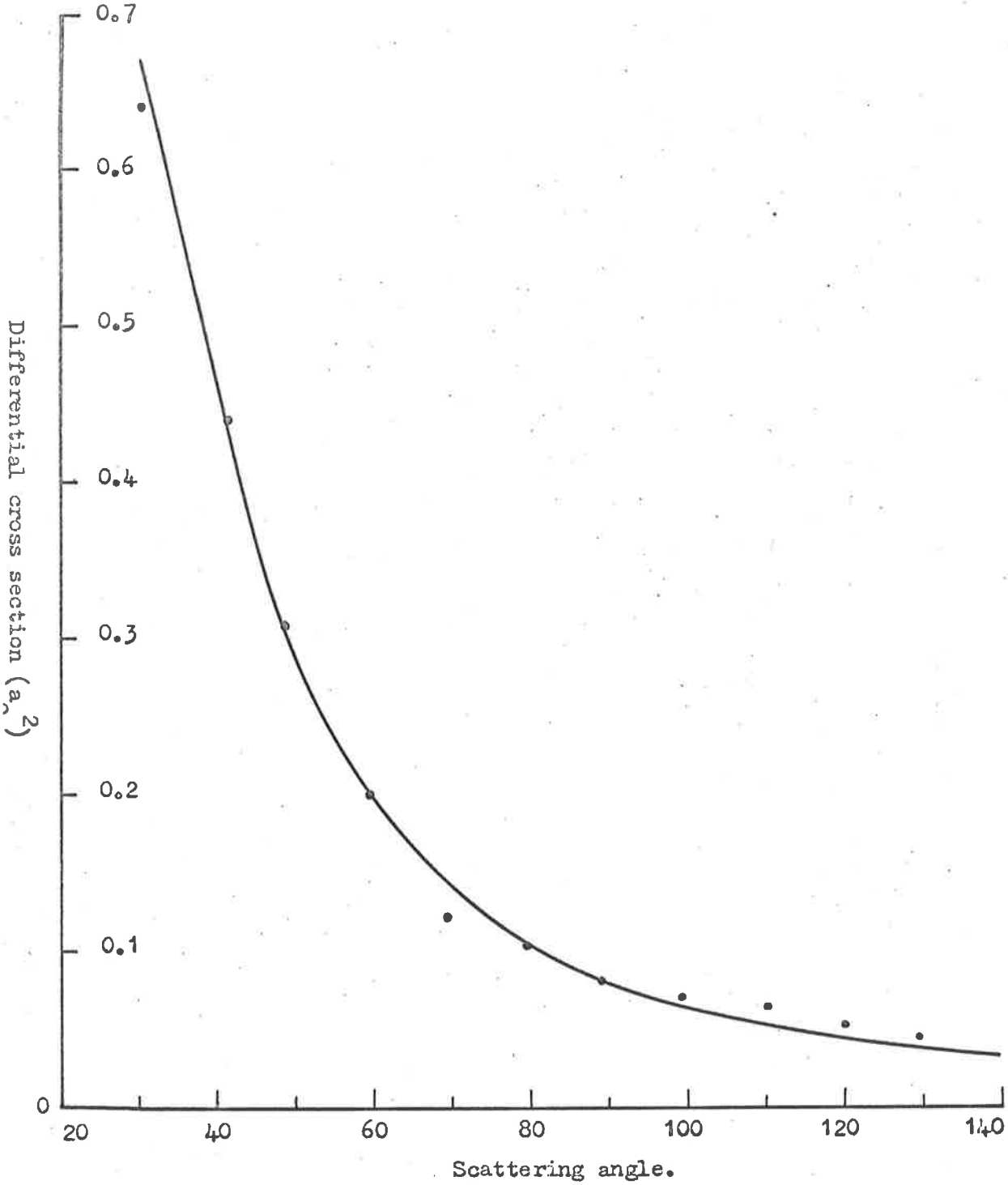

Fig. 4.10: Angular distribution for elastic scattering of 100 electron volt electrons from helium: dots (•) Present results normalised to theoretical at 60°.
curve (——) Theoretical calculations of Khare and Moiseiwitsch.

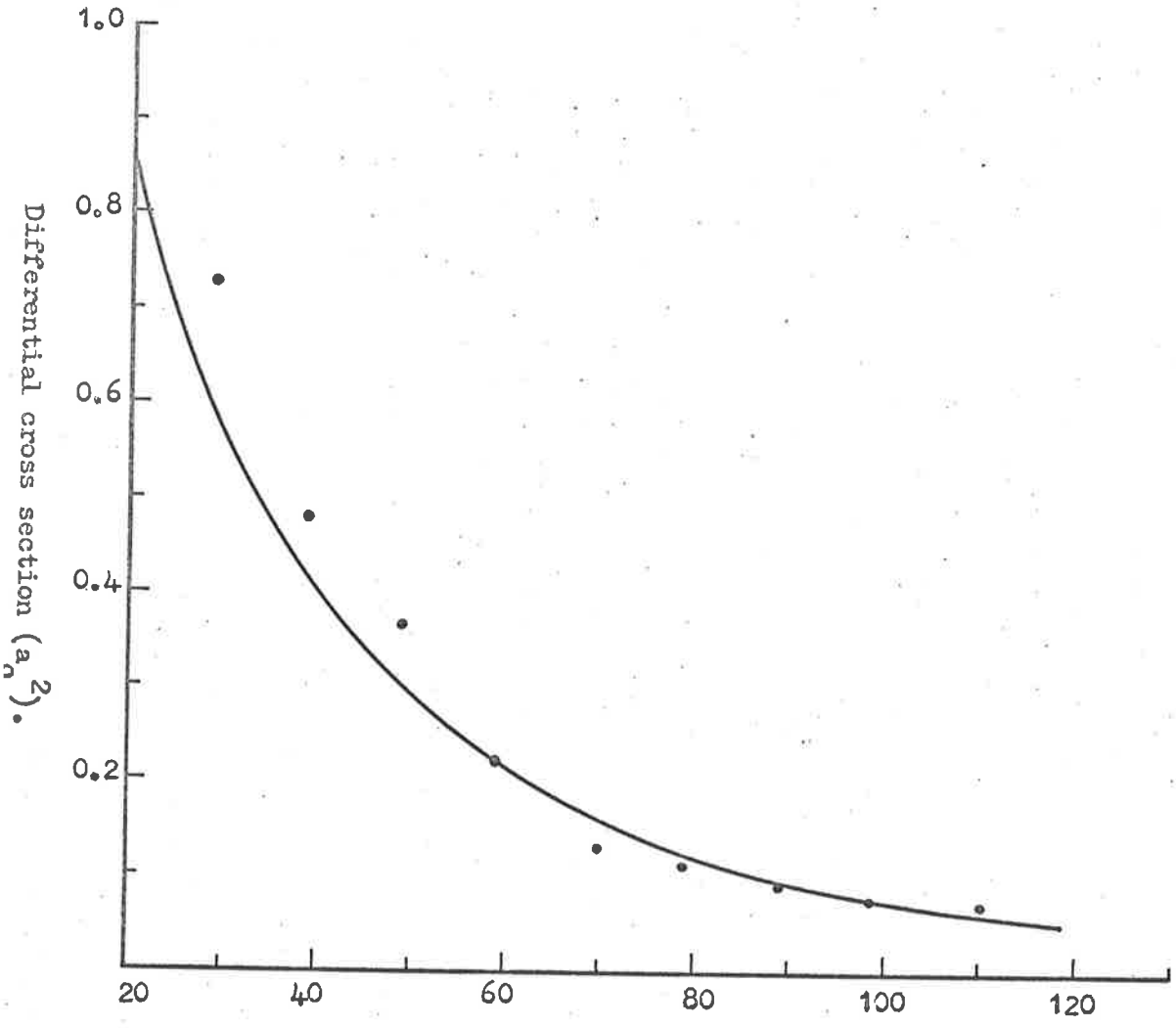

Fig. 4.11: Comparison of present results for angular distribution of elastically scattered 100 e.v. electrons from helium with the Ochkur approximation calculation of Banerjee, Jha, and Sil (1966).

• • present results normalised at 60°.

—— theoretical.

The theoretical predictions for the scattering of 100 e.v. electrons are shown in figure 4.10. The present results have been normalised to the theoretical value at 60°.

Banerjee, Jha, and Sil (1966) have calculated the angular distribution for elastic scattering of 100 electron volt electrons from helium using the Ochkur (1964) approximation. By neglecting higher order terms in the Born-Oppenheimer exchange integral, Ochkur (ibid) has been able to evaluate the total cross section for excitation of the 2^1S state in helium which agrees very well with the experimentally determined total cross section.

Figure 4.11 shows the comparison between the present results at 100 electron volts and the theoretical predictions of Banerjee et al. (ibid) which have been normalised at 60°. The shape of the experimental distribution rises more rapidly at small angles of scattering than the calculations.

Comparison of the two 100 electron volt theoretical curves (figure 4.10 and figure 4.11) shows that the calculations of Khare and Moiseiwitsch represent the shape of the distribution better than do those of Banerjee et al.

IV.2 Elastic Scattering from Argon.

The experimental technique and procedure employed during

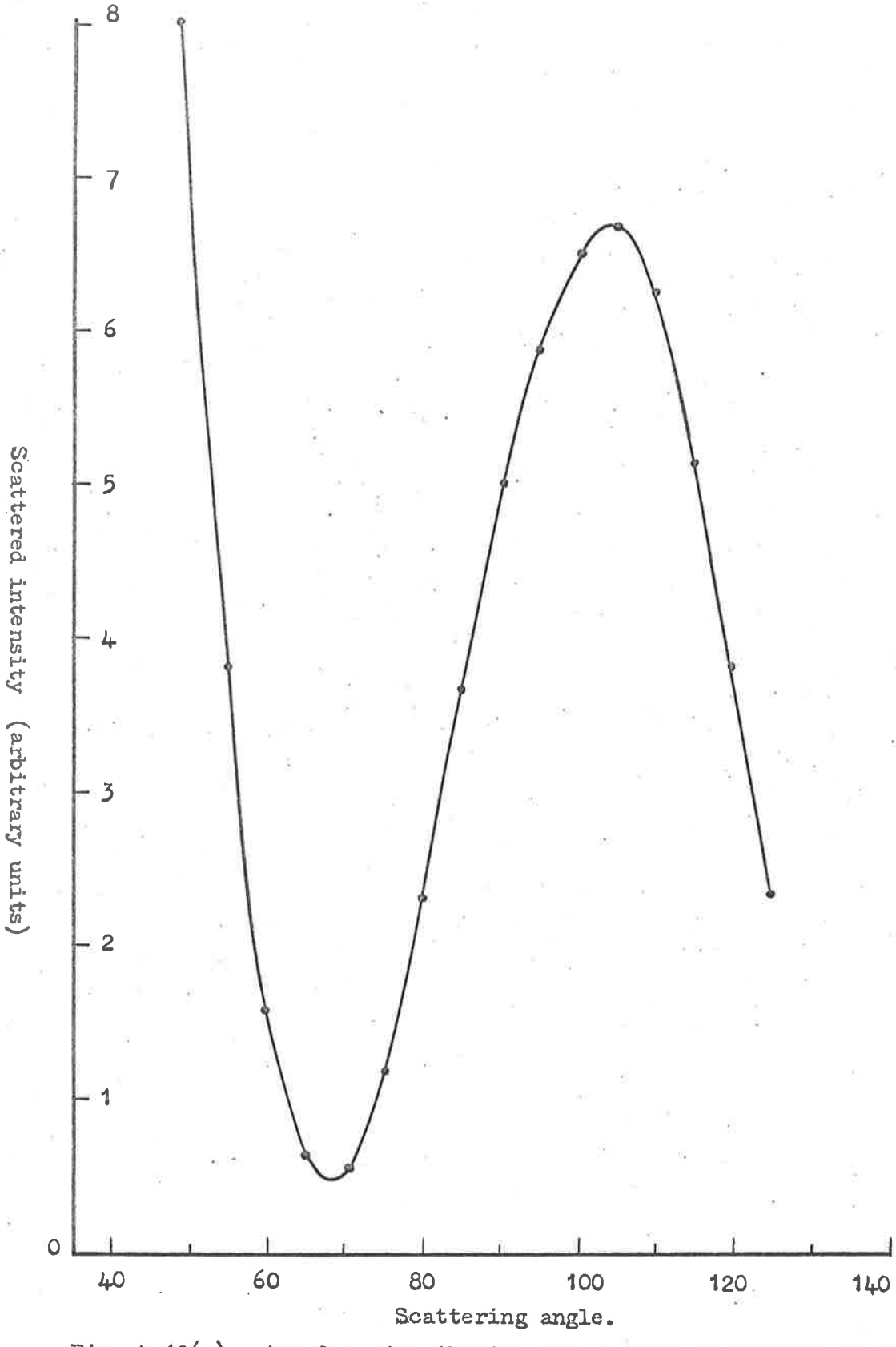

Fig. 4.12(a). Angular distribution for elastic scattering of 50 electron volt electrons from argon.

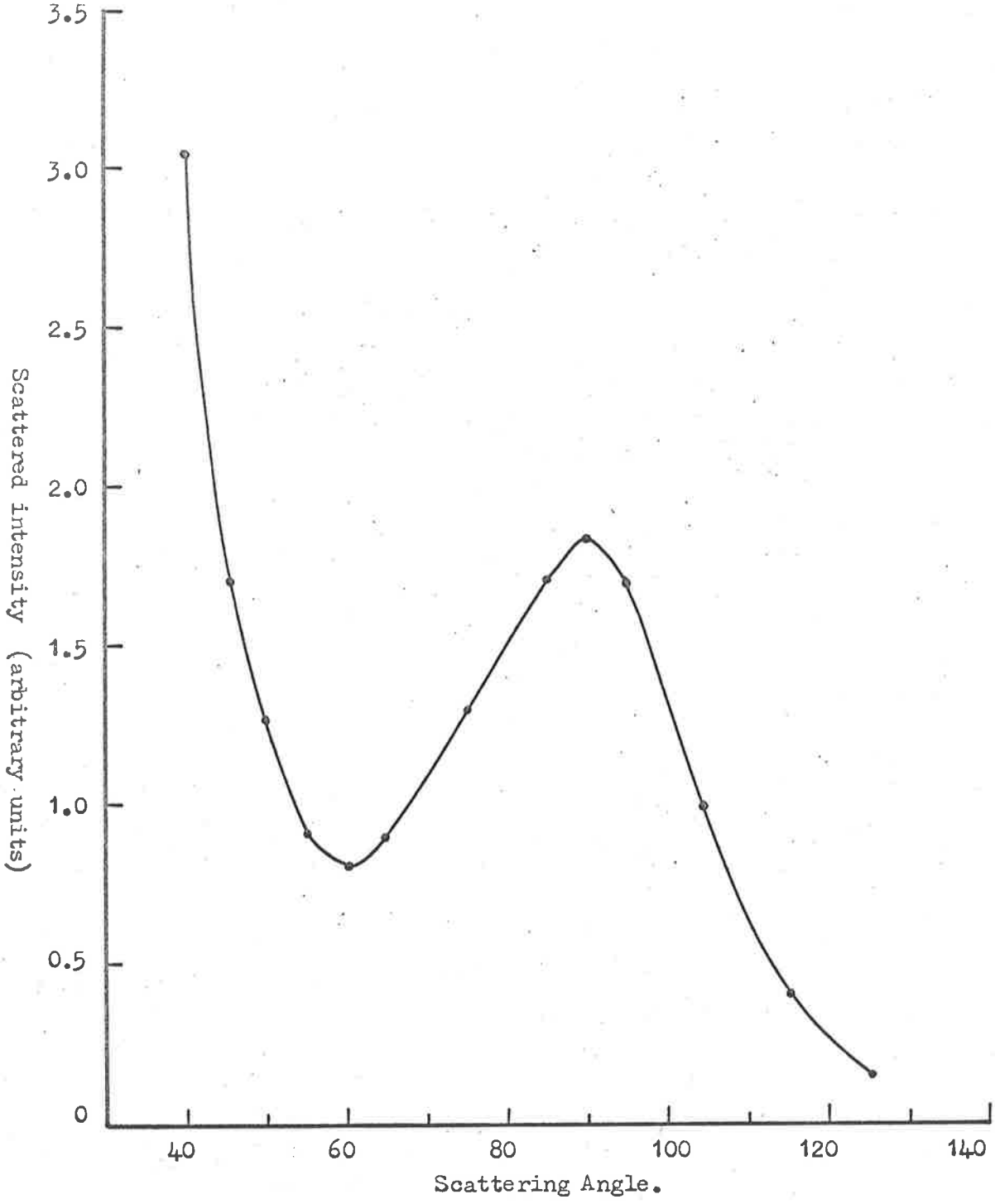

Fig. 4.12(b). Angular distribution for elastic scattering of 100 e.v. electron volt electrons from argon.

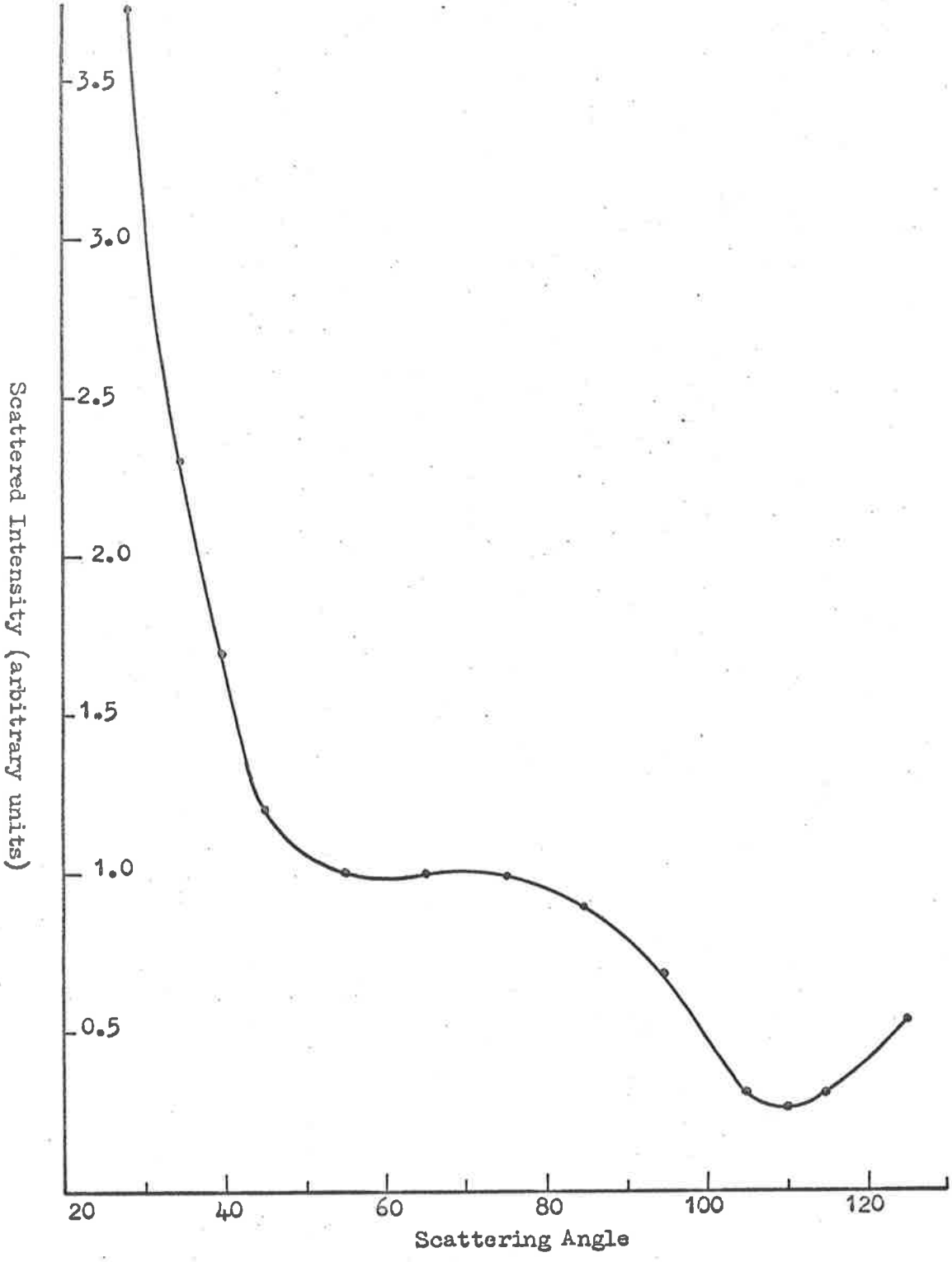

Fig. 4.12(c): Elastic Scattering of 150 electron volt electrons from argon.

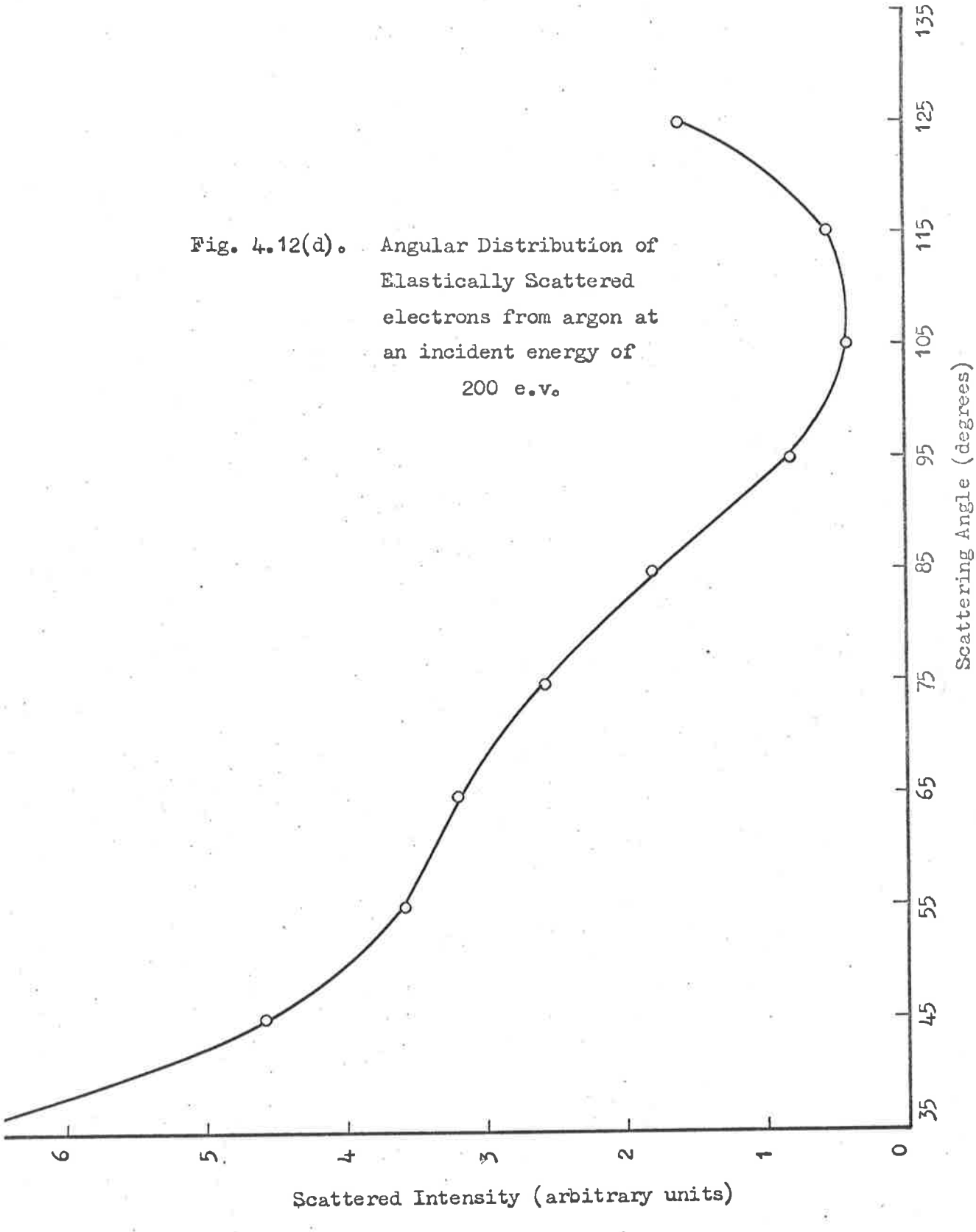

Fig. 4.12(d). Angular Distribution of Elastically Scattered electrons from argon at an incident energy of 200 e.v.

the measurement of the angular distributions for elastic scattering from argon was the same as that used for helium and has been described in sections IV.1(a) and IV.1(c).

The results of the present investigation are shown in figure 4.12.

A characteristic feature of the angular distributions is the strong maximum which appears in the scattered intensity at an angle of about 100° in the 50 electron volt curve and gradually shifts to smaller angles as the energy is raised. At 200 electron volts the peak has been swamped by the strong forward angle scattering and appears as a kink in the distribution.

A qualitative view of the variation of the scattered intensity with angle can be obtained by considering the phase shifts involved in the collision.

The differential cross section is given by

$$I(\theta)\, dw = \frac{1}{4k^2} \left| \sum_{l=0}^{\infty} (2l+1)(e^{2i\eta_l} - 1) P_l(\cos\theta) \right|^2 \qquad (4.5)$$

where k is the wave number expressed in atomic units that is a_0^{-1} where a_0 is the Bohr radius, η_l is the phase shift associated with the l^{th} partial wave, P_l (cos θ) are the Legendre polynomials.

Holtsmark (1929) has calculated the phase shifts for elastic scattering of electrons from argon based on a Hartree field.

He has found that the phase shift associated with the l=2 partial wave tends to $\pi/2$ radians as the energy is increased. At 50 electron volts the differential cross section will be dominated by the η_2 contribution which, from equation 4.5, will closely resemble (Massey and Burhop 1952)

$$I(\theta) = [P_2 (\cos \theta)]^2$$

which shows two minima with a central maximum in approximately the same position as has been observed.

As the incident energy is increased, more partial waves contribute to the differential cross section hence the contribution from η_2 is less significant. Thus the peak in the distribution will not be as apparent at incident energies of 200 electron volts which can be seen in figure 4.11(d).

Figure 4.13 shows the comparison of the present results with those of Webb (1935(a)) for incident energies of 50 electron volts and 100 electron volts. The two sets of measurements have been normalised at a scattering angle of 60°. The present results are represented by the curve and those of Webb by open triangles.

It can be seen that the agreement between the two sets of results is rather poor.

Mehr (1967) has used a high pressure argon beam in the

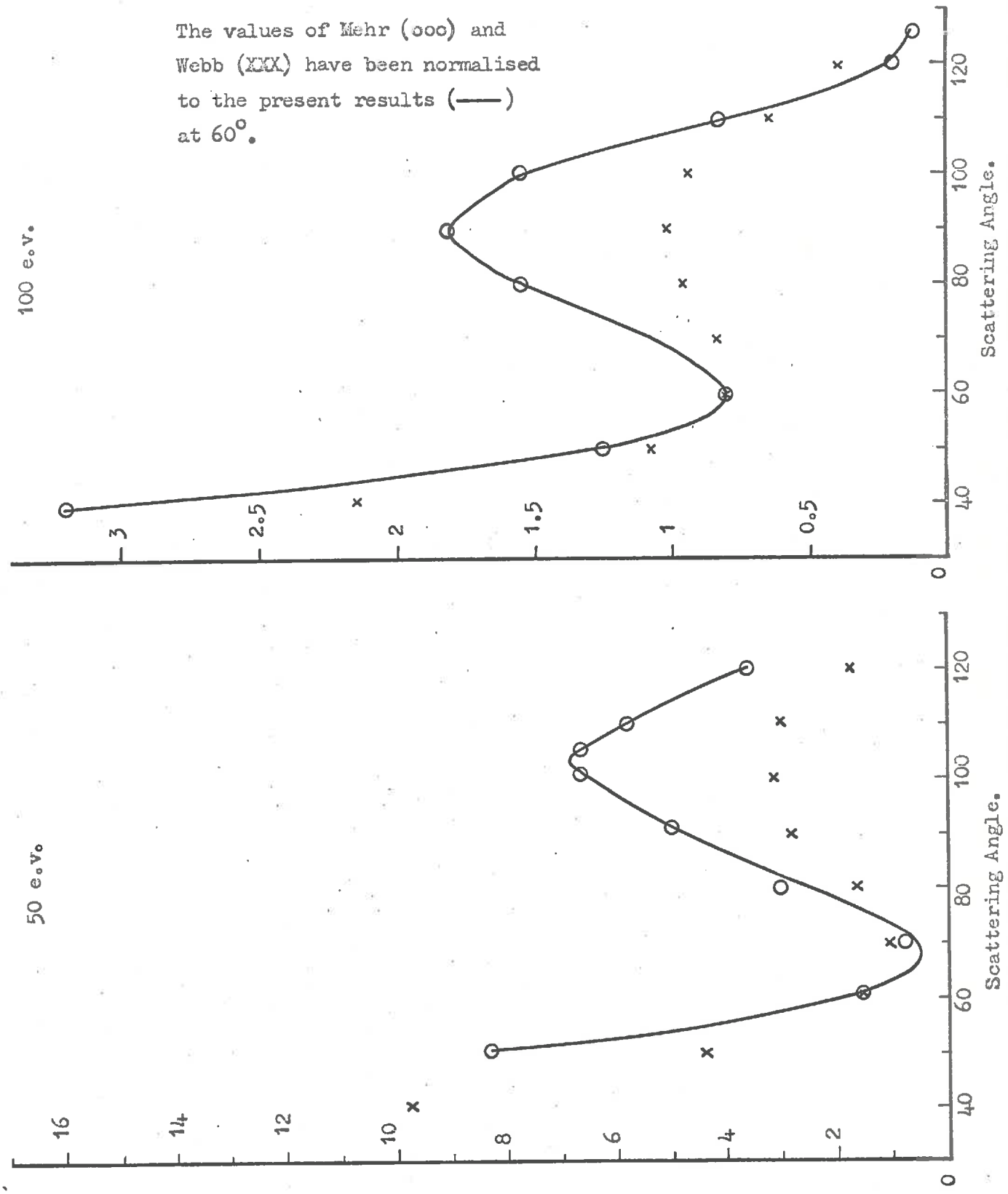

Fig. 4.13. Comparison of present results for elastic scattering of 50 and 100 e.v. electrons from argon with other results.

crossed beam configuration to measure the elastic scattering of electrons from 15 electron volts to 200 electron volts. Mahr's results at 50 electron volts and 100 electron volts are represented in figure 4.12 by open circles and have been normalized at 60^{0}. The agreement between the present results and Mahr is excellent, thereby illustrating that the present results are a better representation of the angular distribution than those of Webb.

CHAPTER V

ANGULAR DISTRIBUTION OF ELASTICALLY SCATTERED ELECTRONS FROM ATOMIC AND MOLECULAR HYDROGEN.

Introduction.

The collision between an electron and a hydrogen atom constitutes the simplest of the many body problems. Consequently much theoretical work has been done on the problem of elastic scattering of electrons from hydrogen atoms. Previous experimental work on electron-hydrogen elastic scattering has been confined to energies below the excitation threshold.

The present investigation has been carried out at incident energies of 50, 75, 100, and 200 electron volts. The relative angular distributions for elastic scattering of electrons from atomic and molecular hydrogen are given in this chapter.

V.1 Experimental Arrangement.

The experimental arrangement used in the present investigation was similar to that which was used by Gilbody, Stebbings, and Fite (1961) in their investigation of the angular distribution of elastically scattered electrons from atomic hydrogen. The major difference between the present arrangement, which is illustrated schematically in figure 5.1, and that used by the above workers was the incorporation of an electron spectrometer which was used in a similar fashion as has been described in section IV.1.

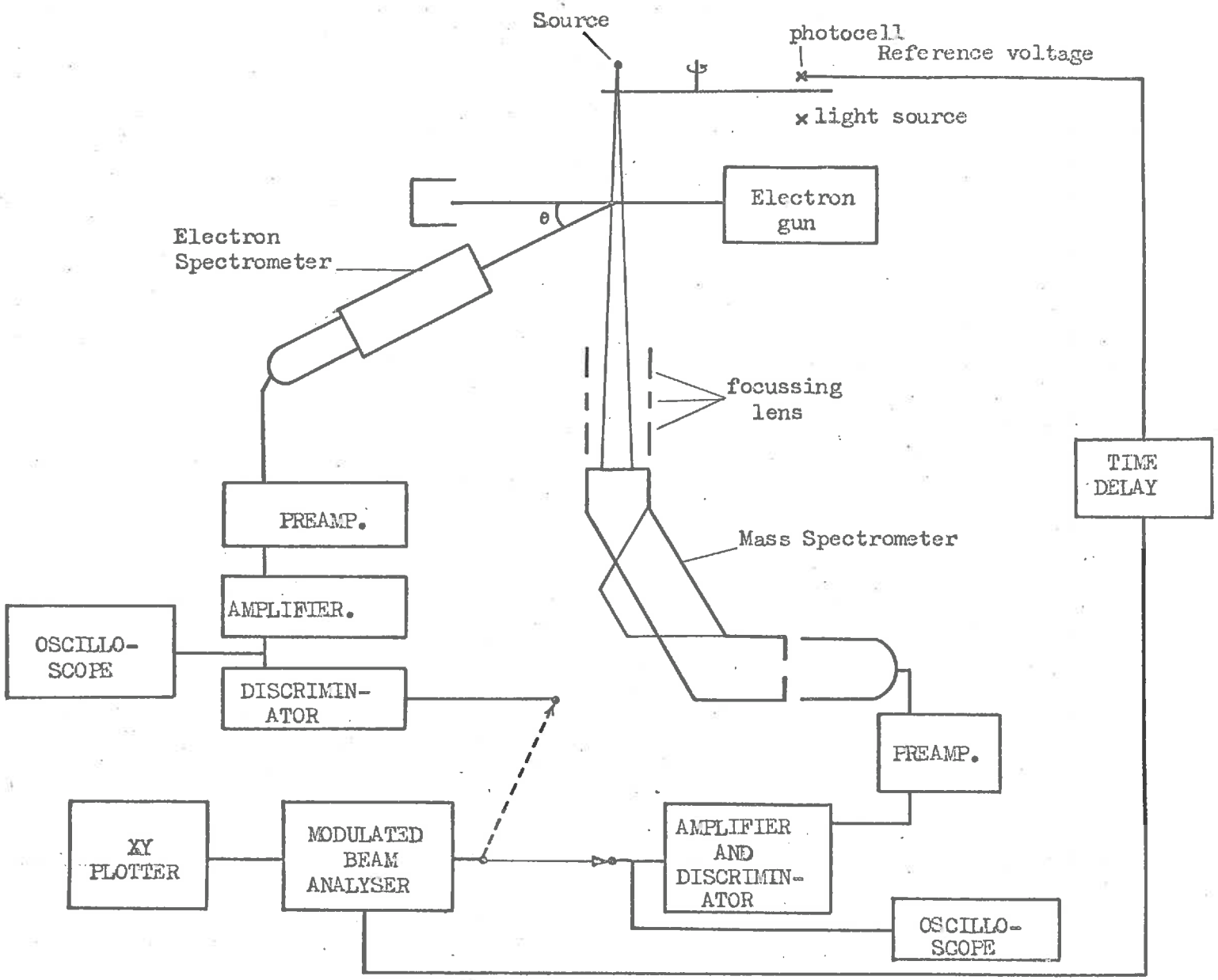

Fig. 5.1. Schematic of apparatus used to measure angular distribution for elastic scattering of electrons from atomic hydrogen.

The experiment consisted of two parts. Firstly the angular distribution for elastic scattering of electrons scattered from the molecule was determined in a similar fashion to that which was used in the electron-helium distributions described in section IV.1. In the second part of the experiment the temperature of the source was increased so that the beam contained a mixture of atomic and molecular hydrogen. By observing the number of elastically scattered electrons from the beam, for which the degree of dissociation was known, the ratio Q_A/Q_M (i.e. atomic to molecular elastic scattering cross section) could be determined. Thus the angular distribution for elastic scattering from the atom could be ascertained by multiplying the scattered electron intensity from the molecule by the ratio Q_A/Q_M measured at a particular angle.

A mass spectrometer was used to determine the degree of dissociation of the beam.

1(a). The Mass Spectrometer.

The mass spectrometer and associated electronics is illustrated schematically in figure 5.2.

Ions formed by the bombardment of electrons with the gas in the interaction region were accelerated and focussed through slit S_1 where mass analysis was performed by the variation of a 60° sector

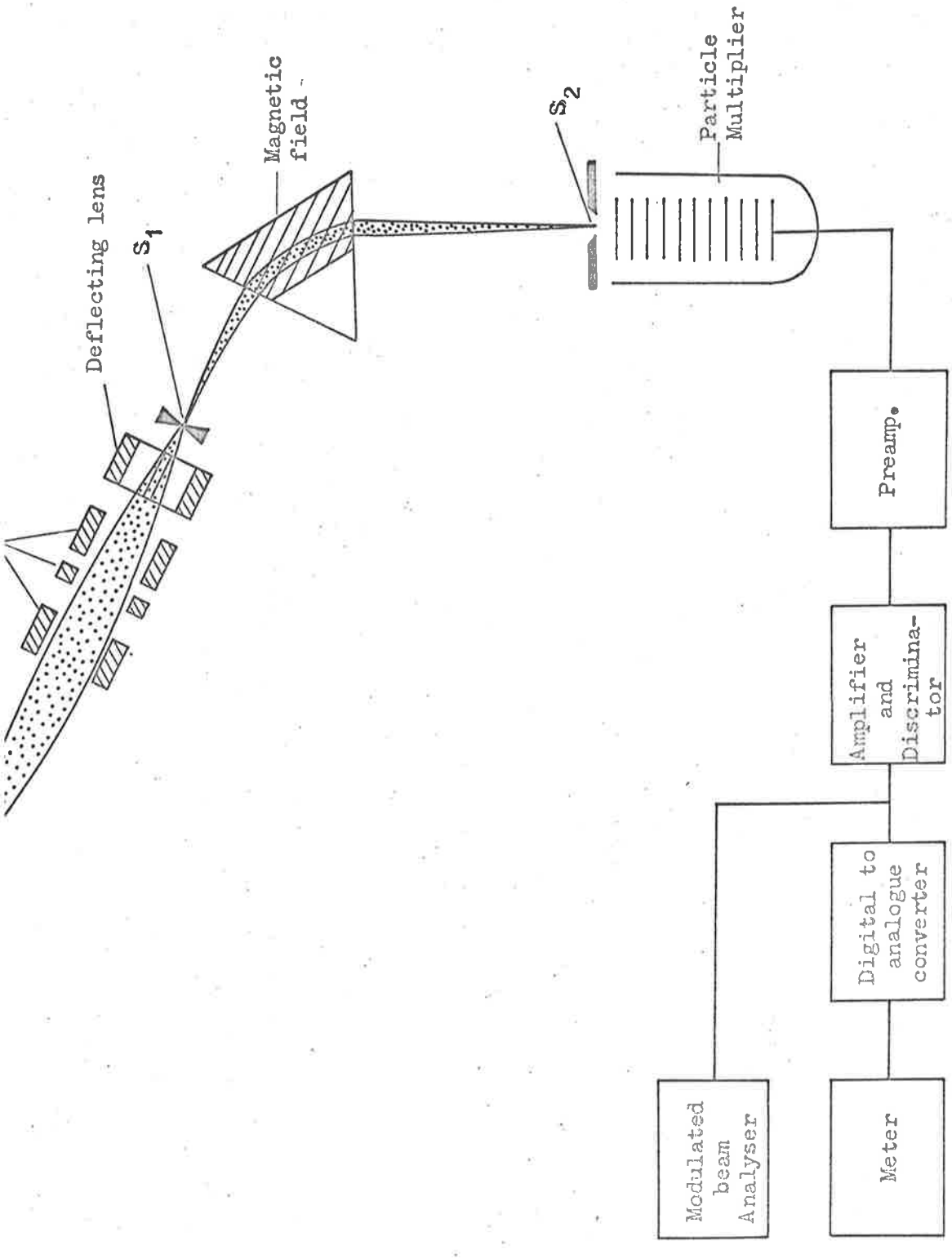

Fig. 5.2. Schematic diagram of the mass spectrometer and associated electronics

magnetic field. The analysed ions passed through slit S_2 and bombarded the first stage of a particle multiplier tube*. The radius of curvature of the ion path was 5.08 cms.

Pulses from the tube were fed via a preamplifier into a pulse amplifier and discriminator**. The output from the discriminator was fed in parallel to the modulated beam analyser and the digital to analogue converter described in section IV.1.

The outer electrodes of the einzel lens was run at -180V, the central electrode was set at a positive potential. By varying the centre electrode potential the ion beam was focussed onto slit S_1.

The pole pieces of the magnet were magnetised by the passage of an electric current through a coil which was linked with the poles by a mild steel armature. The current to the coil was supplied from a regulated, stabilised power supply which is shown in Appendix C.

The peaks in ion current were identified in the following manner.

The radius of curvature R cms of a singly charged ion of

---

* E.M.I. type 9603B.

** Franklin

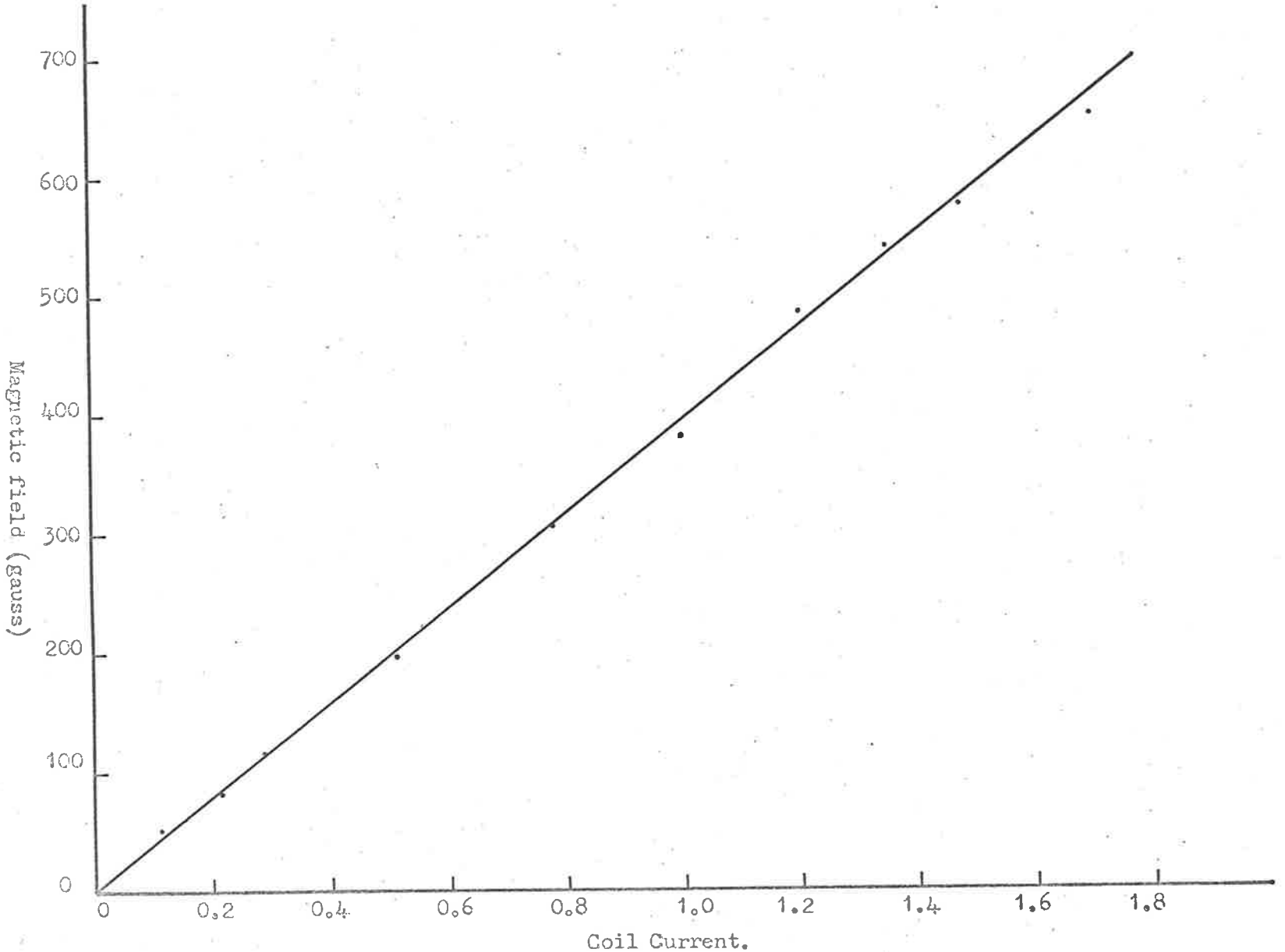

Fig. 5.3(a). Variation of magnetic field with current through the coil.

mass M, accelerated by the application of a potential V volts in a field of B gauss is given by

$$R^2 = \frac{100\,R^2\,q}{2MV \times 10^7} \qquad (5.1)$$

Hence for constant R, q, V

$$M \propto B^2 \qquad (5.2)$$

Figure 5.3a shows the variation of the magnetic field of the electromagnet with the current through the coil. It can be seen that the flux density* was directly proportional to the current through the coil. Thus equation (5.2) becomes

$$M \propto I^2 \qquad (5.3)$$

A spectrum of the background gas is shown in figure 5.4(a). The single peak was attributed to the reaction

$$H_2O + e^- \longrightarrow H^+ + OH^- + e^-$$

which was consistent with the peak at mass 17 in a background gas spectrum taken with a commercial mass spectrometer** and shown in

---

* The flux density was measured with a gaussmeter (R.F.L.)

** A.E.I. model MS.10.

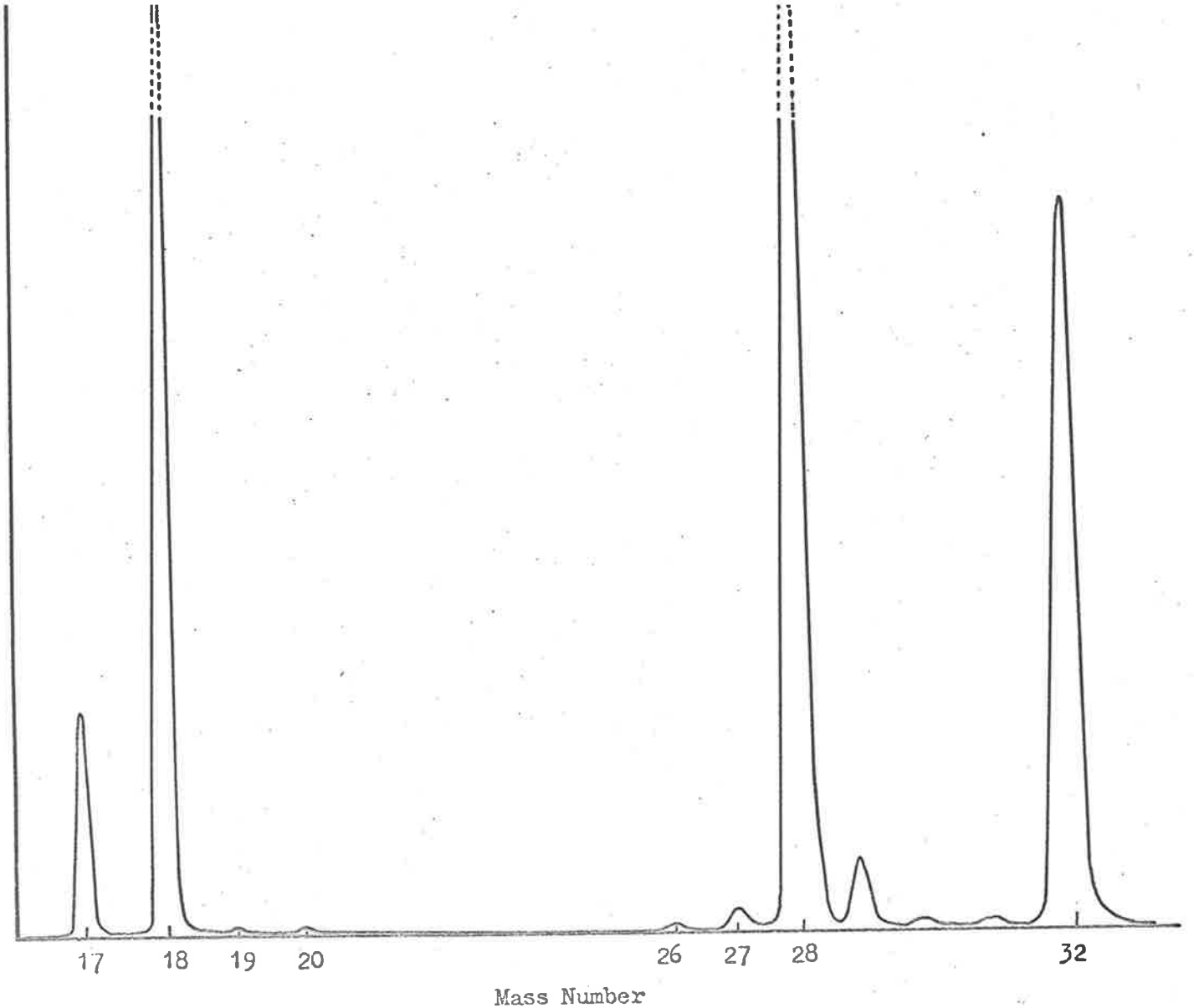

Fig. 5.3b. Spectrum of Background Gas in Scattering Chamber taken with commercial mass spectrometer.

figure 5.3b. It was observed that the height of the mass 1 peak decreased when a liquid air cooled surface was placed in the system.

Figure 5.4(b) shows a spectrum of the background gas which was recorded when molecular hydrogen was admitted to the system. Figure 5.4(c) is a spectrum taken when a mixture of hydrogen and helium was admitted to the chamber. If the peaks were due to H^+, H_2^+, and He^+ then they would have occurred at coil currents which were in the ratio of 1 : 2 : 2.

The values of the currents for the peaks are shown in Table 5.1.

Table 5.1.

Peak	Current (Amps)	Ratio to Peak 1
1	0.68	1
2	0.96	1.4
3	1.36	2

These observations were consistent with the predictions of equation 5.3.

The mass spectra in figure 5.4 were obtained by using the particle multiplier tube as a current amplifier. The current from the anode was fed into a D.C. amplifier*. The output voltage from

---

* Hewlett Packard

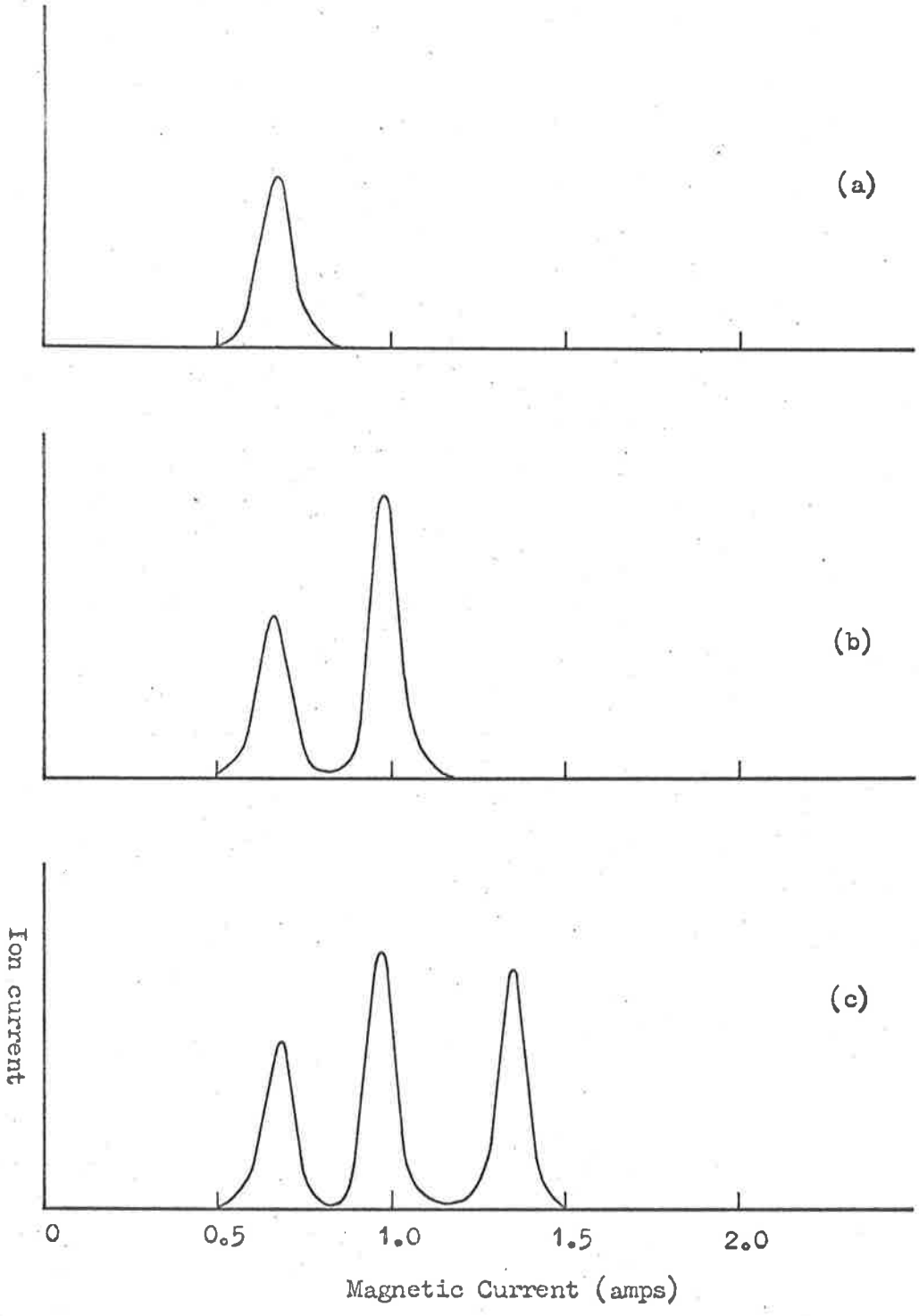

Fig. 5.4. Mass Spectra of background.

(a) showing mass 1 peak

(b) mass spectrum of H_2

(c) mass spectrum when a mixture of H_2 and He was added to the system.

the D.C. amplifier was displayed on the Y axis of the X-Y recorder. The X axis was driven from a sample voltage derived from one side of the differential amplifier in the magnet power supply.

The currents shown in Table 3.1 were taken when zero current corresponded to zero magnetic field. Hysteresis could always be removed from the magnet by cycling the magnet after a spectrum was taken. However the peaks were sufficiently well resolved so that this precaution was only necessary during calibration runs.

The peak positions were found on the modulated beam studies by observing the maximum ion signal as displayed on the digital to analogue converter.

The maximum counting rate of the Franklin amplifier was 500 Kcs. The counting rates during the experimental determination of the degree of dissociation were kept to 25 Kcs. The true counting rate $\dot{N}$ was determined by the formula given in section 4.1, that is

$$\dot{N} = \frac{\dot{n}}{1-\dot{n}\,\tau}$$

where $\dot{n}$ was the observed counting rate and τ the dead time (2 microseconds as explained above).

If the ionisation cross section for electron bombardment of the hydrogen atom and hydrogen molecule were known, the degree of dissociation D could be determined by using the formula [Fite,

Brackmann, and Snow (1958)]

$$D = \frac{1}{\left[1 + \sqrt{2}\,\frac{Q_A^i}{Q_M^i}\,\frac{S_M^i}{S_A^i}\right]} \qquad (5.4)$$

where Q_A^i, Q_M^i are the cross sections for ionization of the atom and molecule respectively. S_M^i, S_A^i are the peak heights of the molecular ion signal and atomic ion signal respectively.

V.2 Contribution of the Molecule to the Scattered Signal.

The number of particles crossing unit area per second at a distance 1 from a source of area A is given by (Ramsey 1956)

$$I = \frac{1}{K}\,\frac{1}{4}\,n\,\bar{v}\,\frac{A}{1^2} \qquad (5.5)$$

where $\frac{1}{K}$ is a factor which takes the finite length of the channel into account and n is the concentration of particles in the source. $\bar{v}$ is the mean velocity of the particles in the source.

As the temperature of the particles increases, the mean velocity $\bar{v}$ will increase as the square root of the absolute temperature. On the other hand n will be inversely proportional to the

absolute temperature. Therefore I in equation (5.5) will be inversely proportional to the square root of the absolute temperature. The number of electrons scattered through an angle θ, S_o, will of course be proportional to I, hence

$$So = CT^{-\frac{1}{2}} \qquad (5.6)$$

Brackmann, Fite, and Maynaber (1958) have illustrated the way in which the contribution of the molecule, in a beam containing molecular and atomic hydrogen, can be determined.

For temperatures greater than the threshold for dissociation the contribution to the signal from those molecules remaining in the beam would be

$$S_2 = (1-D)\,So \qquad (5.7)$$

where D is the degree of dissociation and So is defined in equation (5.6).

The contribution of the atoms in the beam to the total signal is

$$S_1 = \sqrt{2}\,D\,\left(\frac{Q_A}{Q_M}\right)\,So \qquad (5.8)$$

The factor $\sqrt{2}$ arises from the fact that 2 atoms are produced for each molecule which dissociated, but the atoms travel $\sqrt{2}$ times faster than the molecules. Hence each atom scatters $\sqrt{2}$ times less

per unit time than a molecule.

The total elastically scattered electron signal will then be

$$S(T) = S_1 + S_2$$

$$= (1-D + \sqrt{2}\, D \frac{Q_A}{Q_M}) Se \qquad (5.9)$$

But from equation (5.6)

$$Se = S_R (\frac{T_R}{T})^{\frac{1}{2}}$$

where S_R is the signal detected at a reference temperature T_R and T the temperature at which S(T) is measured.

Therefore from equation (5.9) the ratio of the differential cross sections for elastic scattering will be

$$\frac{Q_A}{Q_M} = \frac{1}{\sqrt{2}\, D} \left[\frac{S(T)}{S_R} (\frac{T_R}{T})^{\frac{1}{2}} + D-1 \right] \qquad (5.10)$$

V.3 Experimental Procedure.

Molecular hydrogen was admitted to the source along the input line which has been illustrated schematically in figure 4.5. It was found that there was an optimum pressure of hydrogen in the source. If the pressure was greater than 2.5 torr, thermal equilibrium

in the oven was not reached when the temperature was raised and the $T^{-\frac{1}{2}}$ relationship predicted in equation (5.6) was not followed. At a source pressure of 1.5 torr equation (5.6) was satisfied and as the source temperature was increased from room temperature (290°K) to the temperature required for high dissociation 2750°K, the beam signal dropped by a factor of about three. The background signal on the other hand decreased by at most 5%. Thus in general a larger time had to be spent at the elevated temperature to accumulate data to the required accuracy. If the pressure was below 0.5 torr the relative error in the signal at the elevated temperature S(T) became too large. Therefore the source pressure was set at about 1 torr.

The temperature of the source was increased and measured with an optical pyrometer*. The pyrometer measured brightness temperature which was converted to absolute temperature by the table which appears in the Handbook of Chemistry and Physics (1958).

The number of electrons which were scattered from the beam through a particular angle was recorded in the same way as has been described in section IV.1.

---

* Leeds and Northup. Model 8622C.

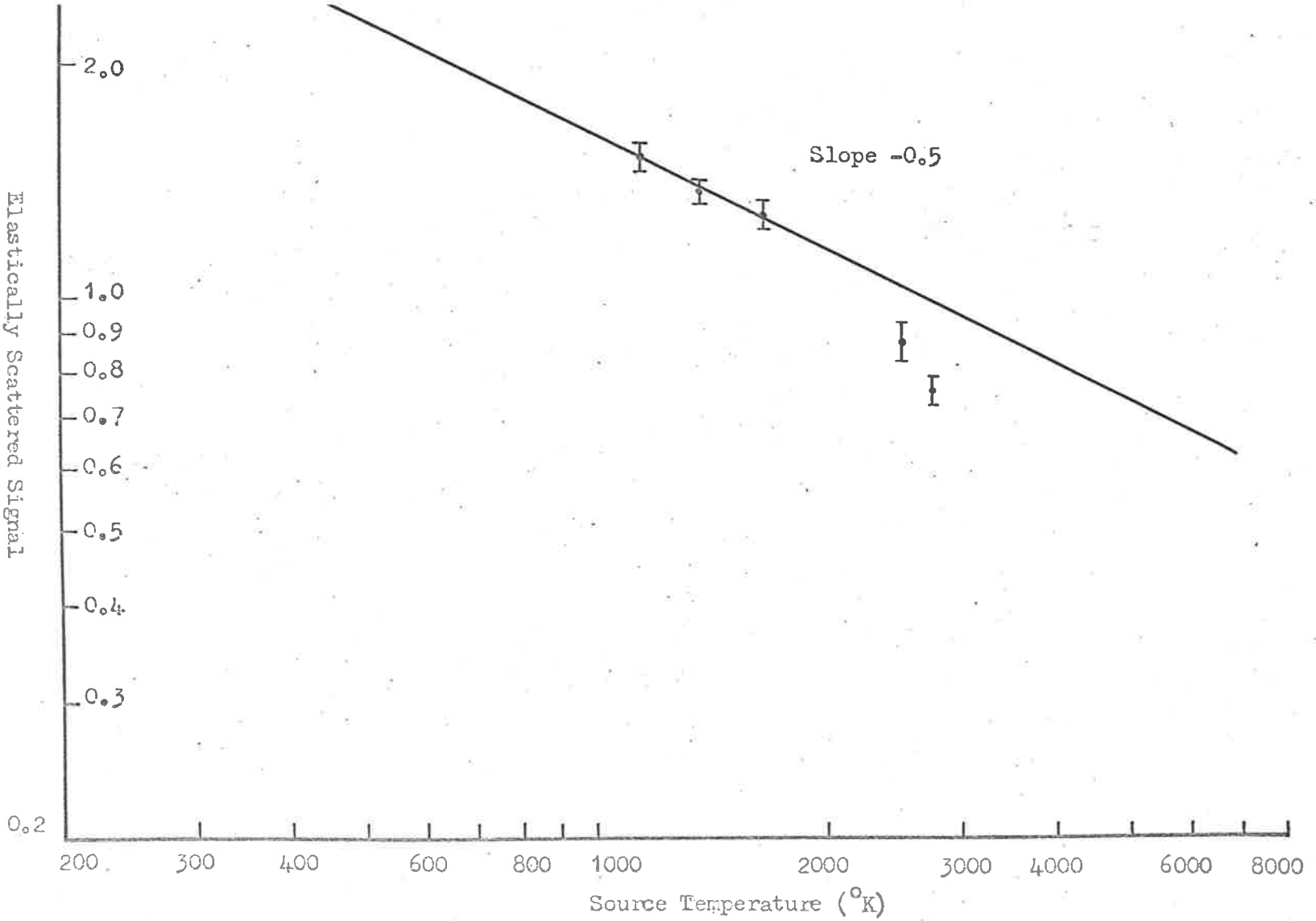

Fig. 5.5. Elastic scattering of 50 e.v. electrons from hydrogen at 40° scattering angle as a function of the temperature. Error bars denote ± one standard deviation of the mean of the values recorded at each temperature.

Figure 5.5 is a sample of data recorded in this fashion. The incident energy was 50 e.v. and the scattering angle was 40°. The logarithm of the elastically scattered signal is plotted as a function of the logarithm of source temperature in degrees kelvin. For temperatures at which there was no dissociation the slope of the straight line was -0.5.

It was found that the magnetic field of the mass spectrometer interfered with the performance of the electron spectrometer. Hence it was not possible to run the two instruments simultaneously. However on each run, for the same source pressure and source temperature, the degree of dissociation D as measured by the mass spectrometer was reproducible.

Two methods were available to determine D. The first was to measure the peak heights of H^+ and H_2^+ in the beam and use equation (5.4). The ionization cross sections were taken as those which were measured by Fite and Brackmann (1958). The second method was to investigate the way in which the H_2^+ peak varied with the source temperature. Equation (5.7) shows that for temperatures at which dissociation occurs the degree of dissociation is given by

$$1 - D = \frac{S_2}{S_0}$$

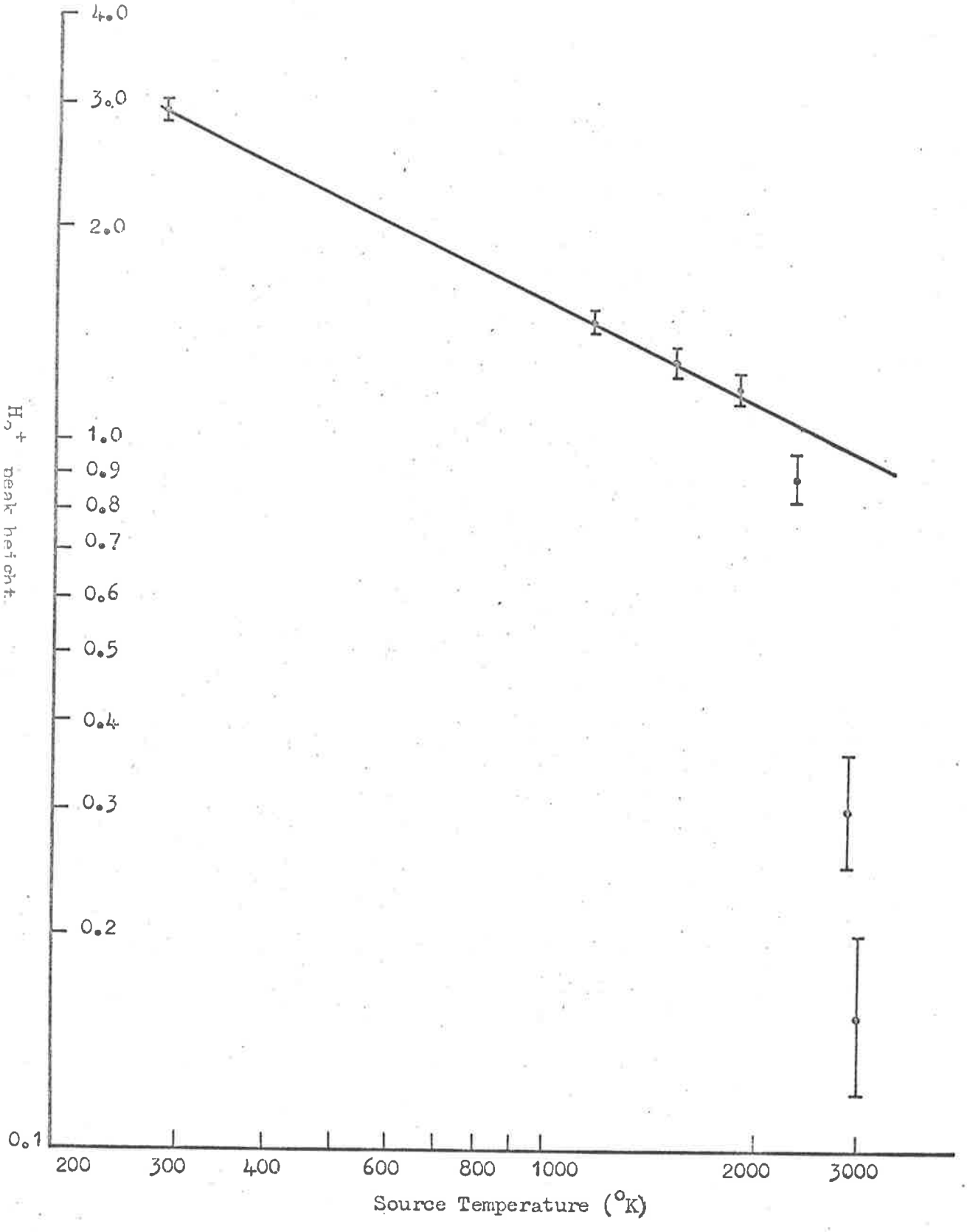

Fig. 5.6. Variation of H_2^+ peak height with source temperature. Error bars denote ± one standard deviation of the mean of the data recorded at each temperature.

Where S_0 is the ion signal which would have been recorded at a temperature T had no dissociation taken place and S_2 is the signal recorded at that temperature.

Figure 5.6 is a log-log plot of variation of the H_2^+ peak height from the beam with temperature. The slope of the line below 2000°K is equal to -0.5 and is therefore consistent with the data from the elastic scattering peak height shown in figure 5.5. Because of the large relative error involved in the measurement of the H_2^+ peak height at elevated temperatures, the value of D obtained from figure 5.6 was not as accurate as that which could be obtained from equation (5.4). Therefore equation (5.4) was used to determine D; however the values obtained by the two methods agreed within the error as is shown in Table 5.2.

Table 5.2.

Temperature °K	D From Figure 5.6	D From Equation (5.4) and Fite and Brackmann ionisation x sections.
2670	0.70 ± 0.10	0.59 ± 0.03
2740	0.83 ± 0.06	0.75 ± 0.03

The ratio of the elastic differential cross sections at each angle

and for each energy could therefore be calculated from equation (5.10) from the measured values of D, S(T), S_R, T_R, and T.

The angular distribution for the elastic scattering of electrons from molecular hydrogen could in principle be determined from the room temperature measurements S_R. [illegible]. However it was necessary to change the gain of the electron recording system several times during a particular run because of the way in which the beam signal varied with angle and with temperature. Hence separate angular distributions were taken for elastic scattering from molecular hydrogen and were measured using the same technique as that which was used for the electron-helium elastic scattering angular distributions described in section IV.1.

V.4 Results and Discussion.

4(a). Molecular Hydrogen.

The angular distribution for the elastic scattering of 50 electron volt electrons from molecular hydrogen is shown in figure 5.7. The present results are represented by points and the curve has been drawn through these points. The results of Webb (1935b) for the scattering of 50 e.v. electrons from molecular hydrogen have been normalised at a scattering angle of 60° and are shown as open triangles. Agreement is very good.

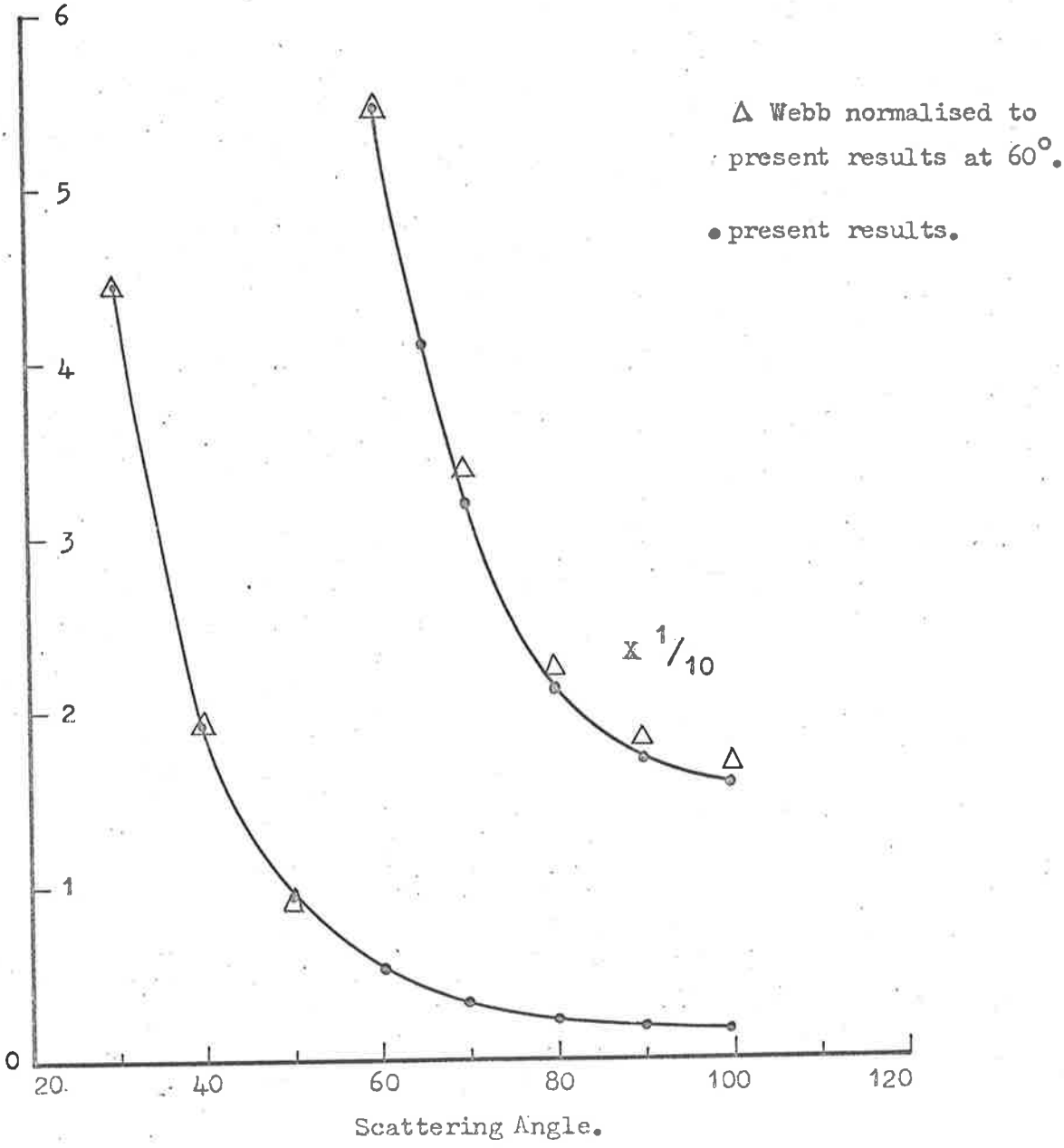

Fig. 5.7. Angular Distribution of elastically scattered electrons from molecular hydrogen at an incident energy of 50 e.v.

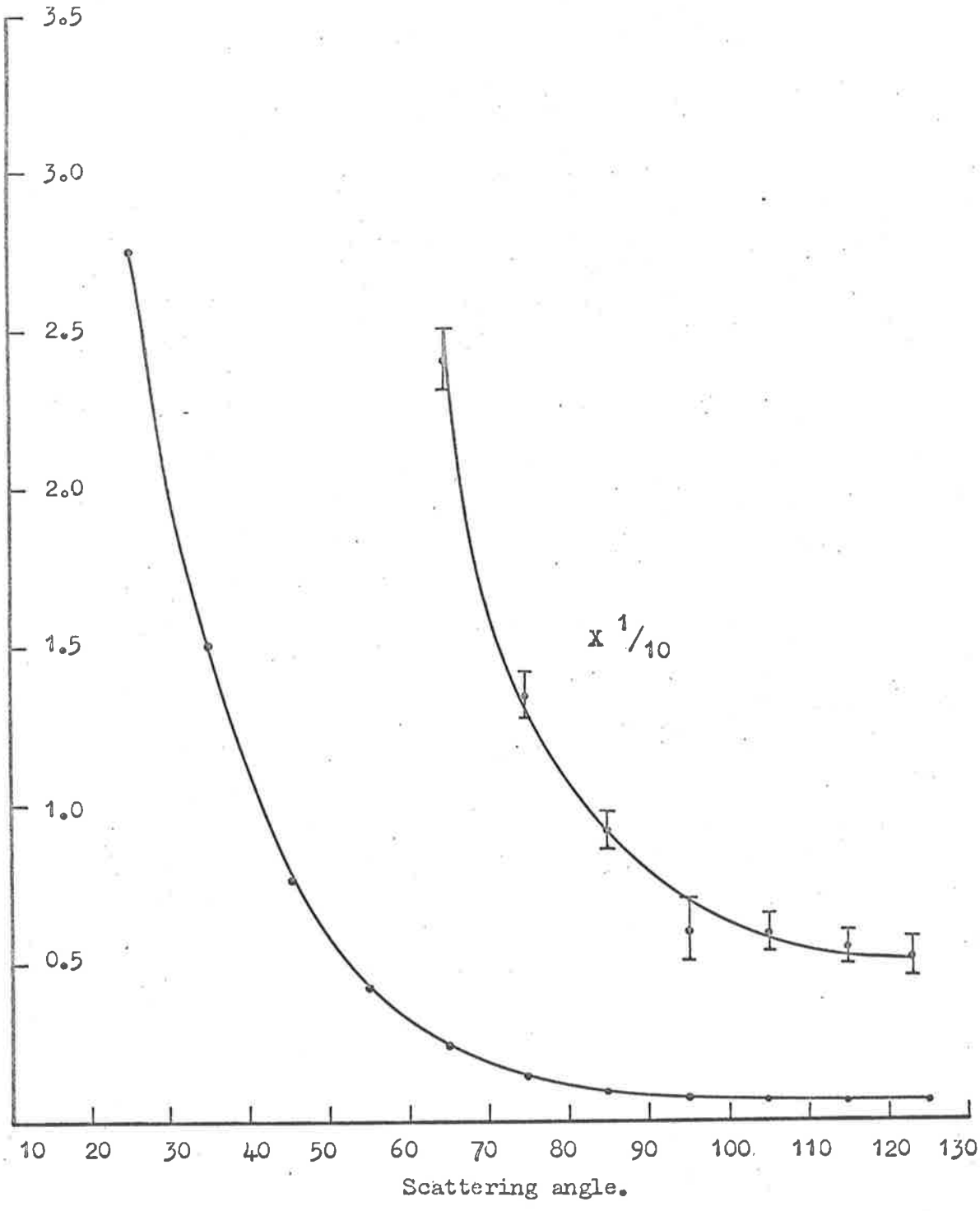

Fig. 5.8. Angular distribution of elastically scattered electrons from molecular hydrogen at an incident energy of 75 e.v. Error bars denote ± one standard deviation in the mean of data recorded at each angle.

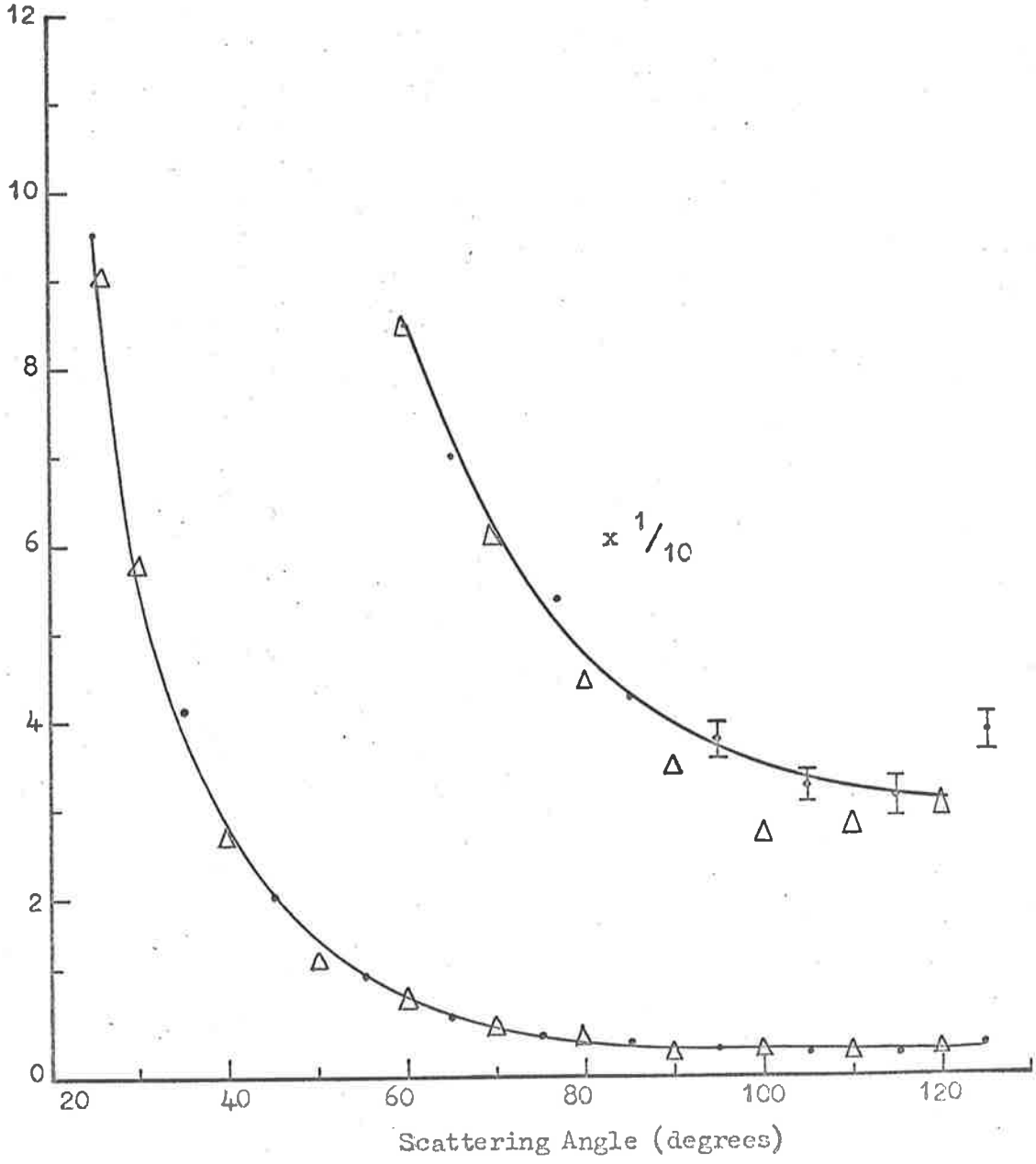

Fig. 5.9. 100 e.v. elastic scattering from molecular hydrogen.

• : present results; Δ : Webb.

Error bars denote ± one standard deviation of the mean of the data recorded at each angle.

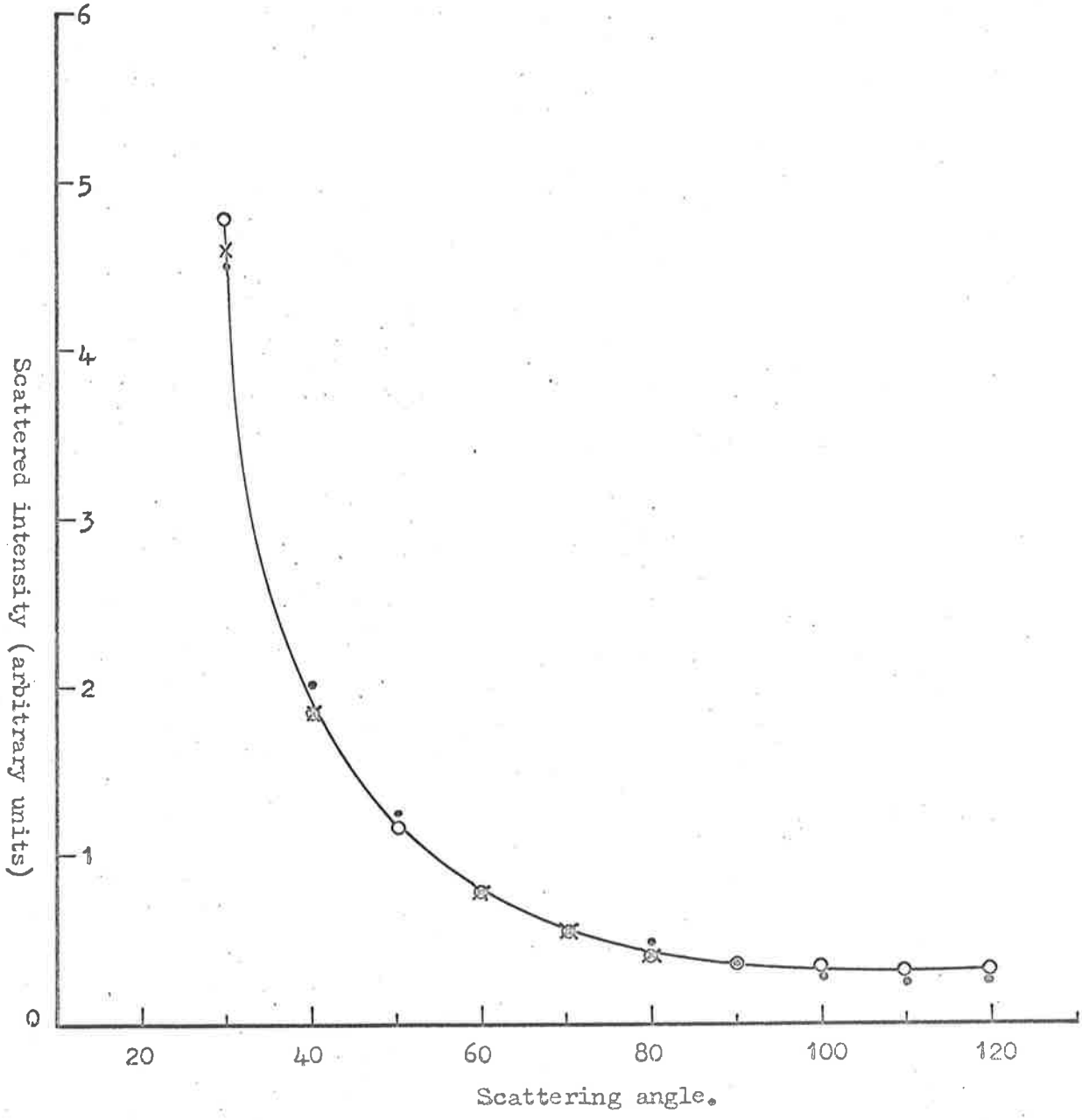

Fig. 5.10. Angular Distribution for elastic scattering of 200 e.v. electrons from molecular hydrogen.

The present values (•••) and those of Arnot (XXX) have been normalised to Webb's (ooo) value at 60°

Figure 5.8 shows the angular distribution for the elastic scattering of 75 electron volt electrons from molecular hydrogen. There have been no previous measurements of this distribution.

The 100 electron volt angular distribution is shown in figure 5.9. Good agreement is found with the results of Webb (ibid).

Figure 5.10 is a comparison between the present angular distribution for the elastic scattering of 200 electron volt electrons and the measurements of Webb (ibid) and Arnot (1931). Arnot's results are represented by crosses. All angular distributions have been normalised at 60°. The agreement between the present measurements and the previous results is very good.

Since the hydrogen molecule is a two-electron system and since its ground state can be described by a symmetric space wave function, the angular distribution for elastic scattering of electrons from molecular hydrogen should behave in a similar fashion to the angular distribution observed from helium. Comparison of figure 4.9 with the above angular distributions shows that the variation of scattered intensity with angle is similar, however the distributions from molecular hydrogen rise more rapidly at small angles of scattering than is the case for the helium distributions.

The fact which makes scattering from the hydrogen molecule different from atomic scattering is the possibility of interference

effects being set up by the scattered electrons from the two atoms which comprise the molecule.

The theory of elastic scattering from molecular hydrogen is more complicated than that from the atom. The problem is twofold; first the Schrödinger equation for an axially symmetric field is, in general, insoluble and secondly there is less certainty about the molecular field than the atomic field. Khare and Moiseiwitsch (1965) have used the separated atom approximation and have determined the direct scattering amplitude for the elastic scattering of electrons from atomic hydrogen in the Born approximation. The influence of exchange has been determined using the first order exchange approximation.

The present results are compared with the theoretical calculations in figure 5.11 for incident energies of 50 electron volts and 100 electron volts. The logarithm of the scattered intensity has been plotted as a function of the scattering angle and the two sets of results have been normalised at 60°.

It can be seen that the agreement between theory and experiment is rather good between 30° and 90° but at angles of scattering greater than 90° the experimental points lie above the theoretical. The minimum in the scattered intensity at 100° and an incident energy of 100 electron volts is not predicted by the calculations.

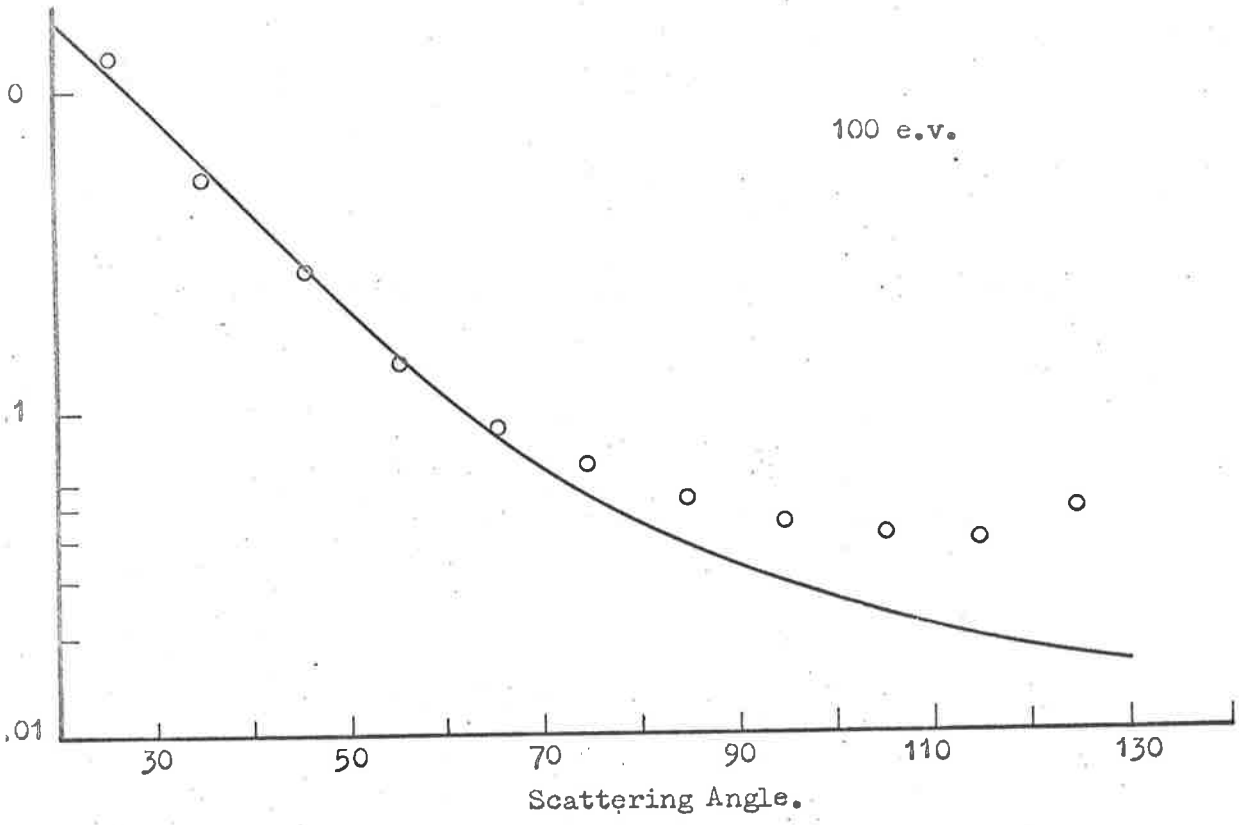

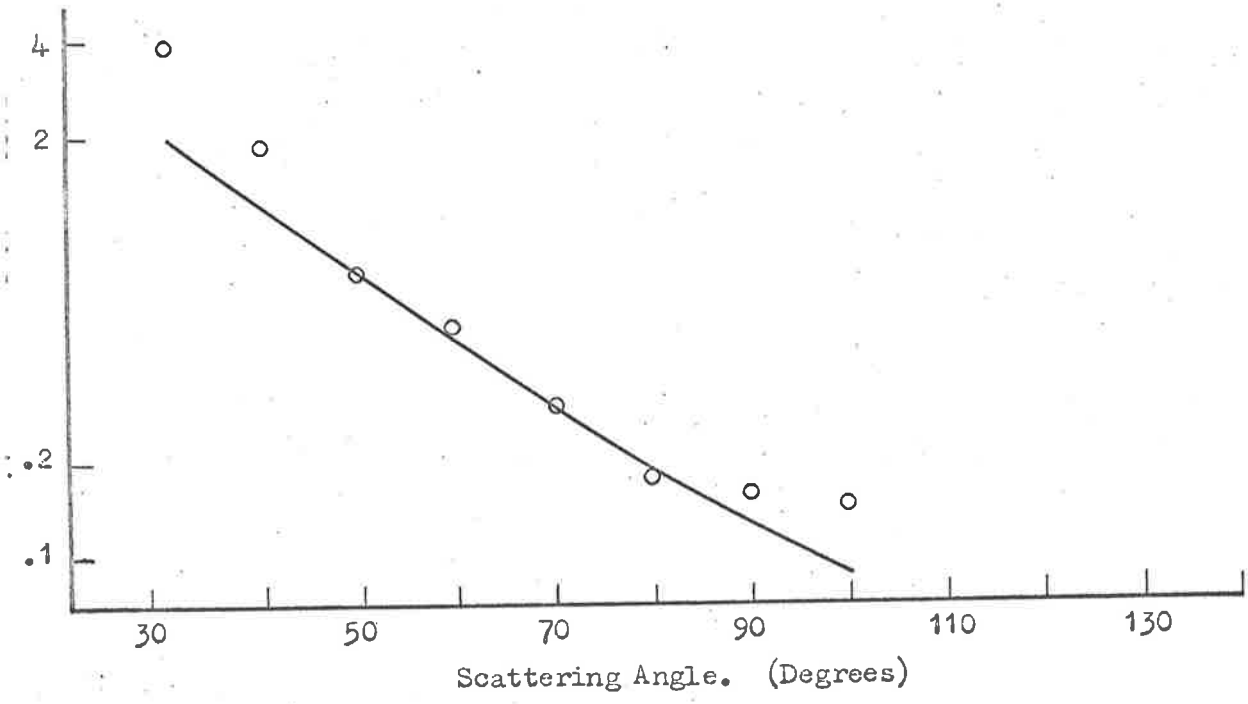

Fig. 5.11. Angular Distribution of elastically scattered electrons from molecular hydrogen. (ooo) present results normalised to theoretical value of Khare and Moiseiwitsch (——) at 60° for each impact energy.

Khare and Meiseiwitsch have not included polarization in their calculation and were unable to explain the fact that the effect of polarization was not very great except at low energies, despite the fact that the dipole polarizability of H_2 is greater than that for helium.

Clearly there is a need for more theoretical work to be undertaken on the elastic scattering of electrons from molecular hydrogen. The agreement of the present results with the earlier measurements provides a firm basis of experimental values with which the calculations can be compared.

4(b). Atomic Hydrogen.

(i). 50 electron volts.

The ratios of the differential cross sections for the elastic scattering of electrons from atomic hydrogen and molecular hydrogen were obtained from equation (5.10) at scattering angles from 25° to 90° for an incident energy of 50 electron volts and have been tabulated in Appendix A.5.

The intensity of elastically scattered electrons from atomic hydrogen at each angle was found by multiplying the ratio of the cross sections at each angle by the scattered intensity from the molecule at that angle. The relative angular distribution which was obtained is shown in figure 5.12. The experimental values have been normalised to the theoretical curve of Scott (1965) at a

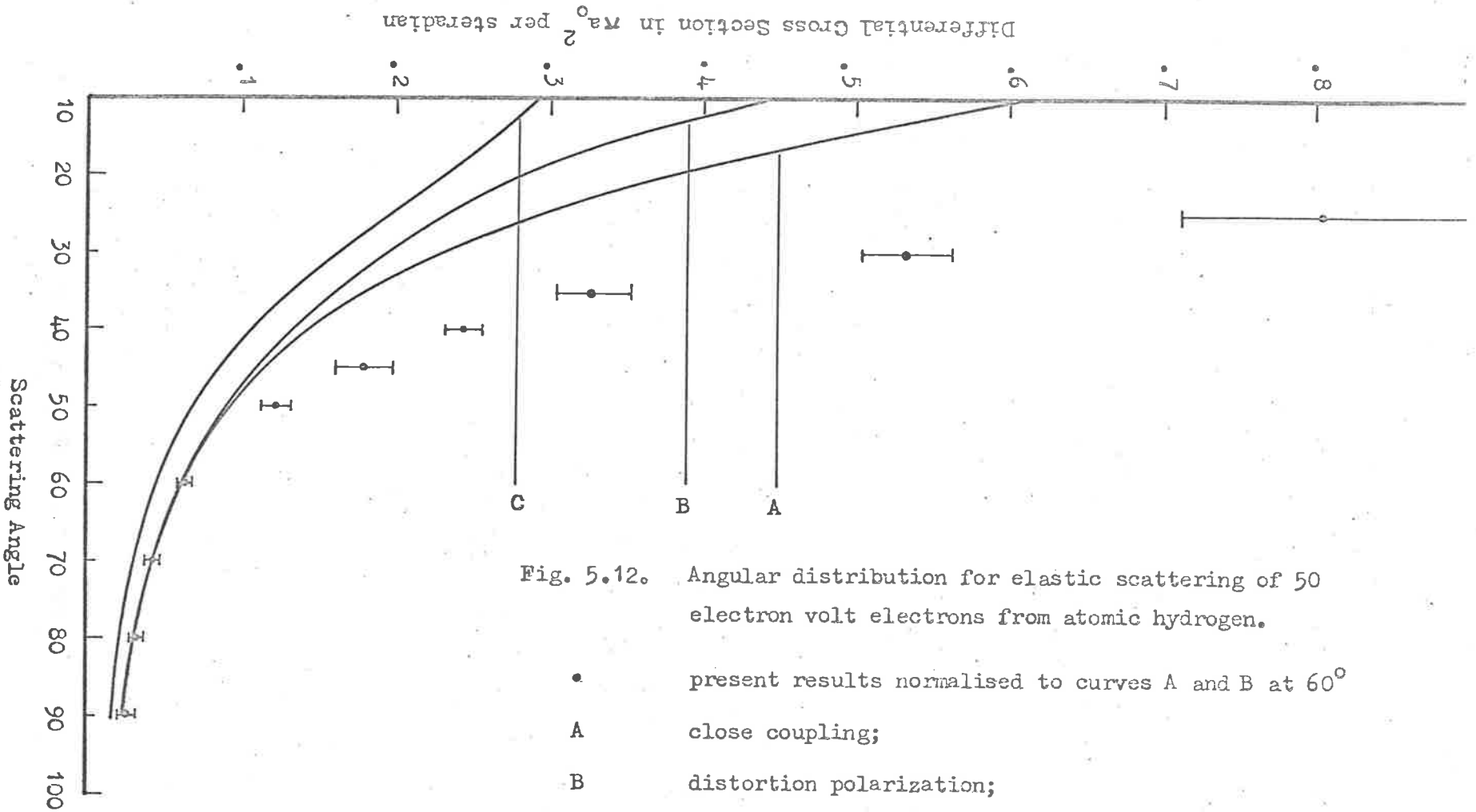

Fig. 5.12. Angular distribution for elastic scattering of 50 electron volt electrons from atomic hydrogen.

- • present results normalised to curves A and B at 60°
- A close coupling;
- B distortion polarization;
- C first Born approximation.

The error bars represent $\pm$ one standard deviation in the values of Q_A/Q_M

scattering angle of 60°. The differential cross section is given in units of πa_o^2 per steradian where a_o is the first Bohr radius ($a_o = 5.29 \times 10^{-9}$ cm).

Scott (1965) has calculated the differential cross section for the elastic scattering of $k^2 = 4a_o^{-2}$ electrons from atomic hydrogen using the 1S-2S - 2P close coupling approximation. The resulting differential cross section has been drawn as curve A in figure 5.12. It can be seen that the present results rise more rapidly at small angles of scattering than is predicted by the close coupling expansion.

Scott (1967) has pointed out that the failure of the calculation could be due to the slow convergence of the series in the equation

$$\frac{d\sigma^S}{d\Omega}(nl_H - n'l'_H) = \frac{2S+1}{4(2l_H+1)k_n^2\pi} \sum_{L=0}^{\infty} B_L^S(nl_H - n'l'_H) P_L(\cos\theta)$$

Even though values of the orbital angular momentum L of the incident electron up to L = 13 were included in the calculation, the convergence of the series is poor at small angles of scattering.

Kingston and Skinner (1961) have calculated the differential cross section for the elastic scattering of $k^2 = 4a_o^{-2}$ electrons using the second Born approximation. Terms to the third order in the

interaction energy were included. Allowance was made for both distortion and polarisation by evaluating the terms which corresponded to transitions from the 1S to the 2S and 2P intermediate states. The resulting differential cross section is shown as curve B in figure 5.12.

It can be seen that the distortion-polarisation approximation of Kingston and Skinner underestimates the differential cross section at small angles even more than the close coupling expansion.

Curve C is the differential cross section which is predicted by the first Born approximation and is due to Kingston and Skinner* (ibid).

---

* The units of the differential cross sections given by Kingston and Skinner have been taken as a_o^2 (instead of πa_o^2 as published) to make their Born approximation values consistent with Moiseiwitsch and Williams (1959), Mott and Massey (1965).

(ii). 75 electron volts.

The ratio of the atomic to the molecular differential cross section for elastic scattering was measured for scattering angles from 25° to 120° and an incident energy of 75 electron volts; the results are tabulated in Appendix A.

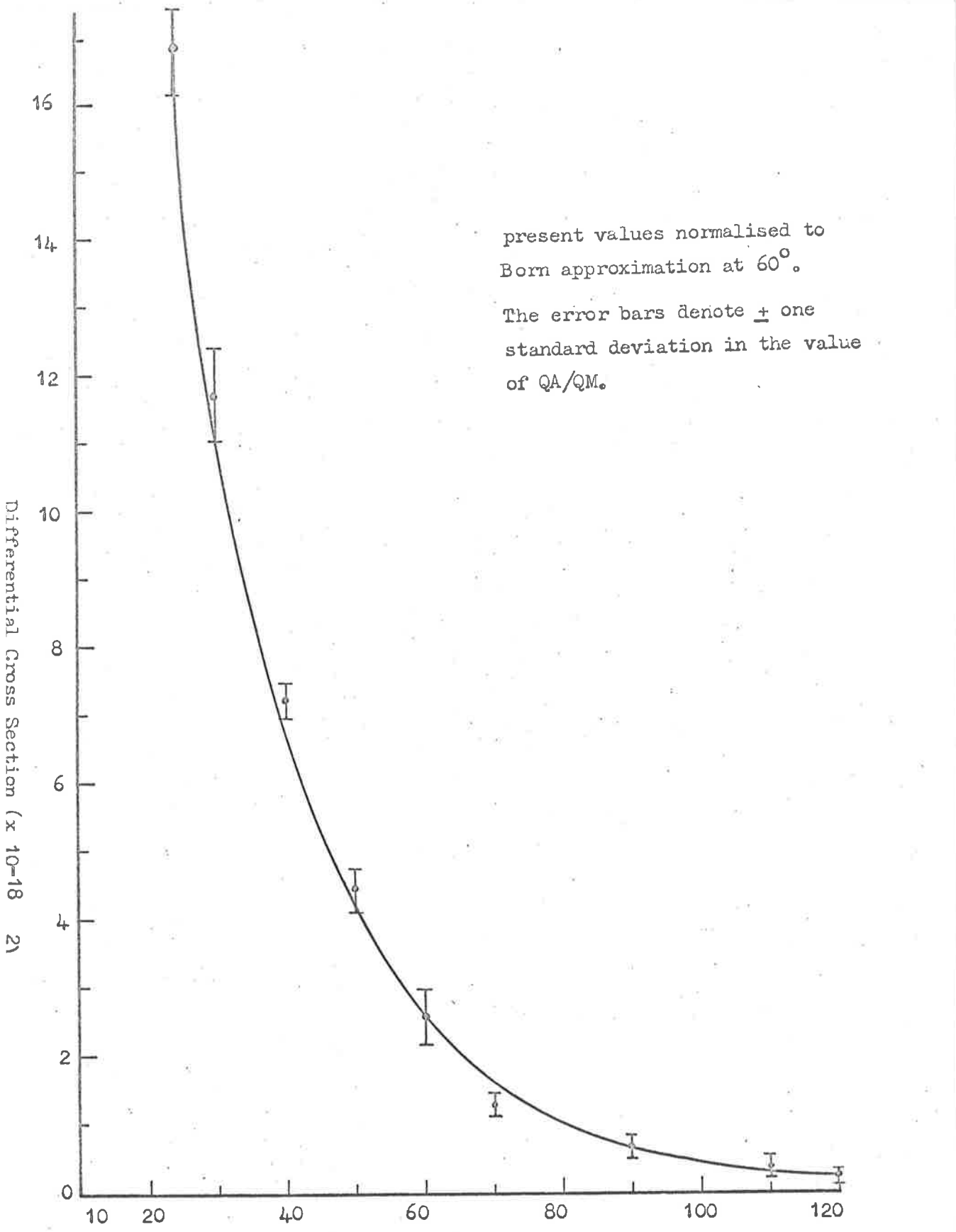

Fig. 5.13: Angular distribution for elastic scattering of 75 e.v. electrons from atomic hydrogen.

• present values. —— Born approximation.

The relative angular distribution for the elastic scattering of 75 electron volt electrons from atomic hydrogen was found by multiplying the scattered intensity from the molecule at each angle by the ratio of the atomic to molecular cross sections at that angle. The experimental values were normalised at a scattering angle of 60° to the theoretical curve which is shown in figure 5.13.

The theoretical differential cross section for the elastic scattering of 75 electron volt electrons from atomic hydrogen was calculated from the table of values given by Mott and Massey (1965). Mott and Massey have tabulated the differential cross section for elastic scattering of electrons from hydrogen atoms which is predicted by the Born approximation as a function of $k_o \sin \theta/2$ where k_o is the wave number of the incident electron and θ the scattering angle.

By comparing the exact phase shifts for the $l = o$ partial wave as calculated by McDougall (1932) with that predicted by the Born approximation, Mott and Massey (ibid) have deduced that the Born approximation for elastic scattering of electrons from atomic hydrogen should be fairly accurate at an incident energy of 75 electron volts. The present results support this conclusion since good agreement is obtained between the theoretical values and the experimental results in figure 5.13.

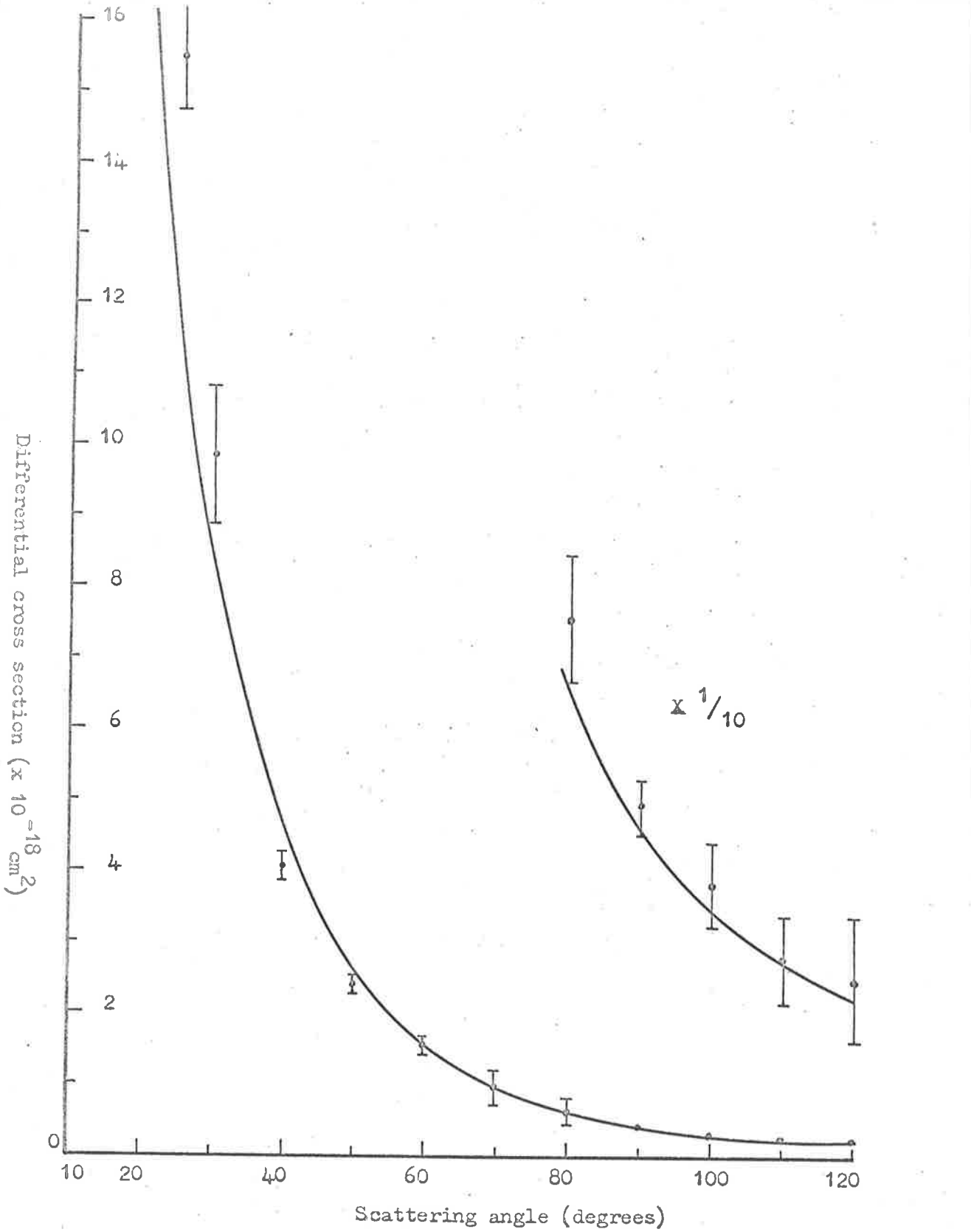

Fig. 5.14: Angular distribution for elastically scattered electrons from atomic hydrogen at 100 e.v. dots (•) present experimental values normalised at 60°.

curve (——) Born approximation. Error bars denote ± one standard deviation in the value of the ratio QA/QM.

(iii). 100 electron volts.

Figure 5.14 shows the angular distribution for elastic scattering of electrons from atomic hydrogen at an incident energy of 100 electron volts. The ratios of the atomic to the molecular cross section at angles of scattering from 25° to 130° are tabulated in Appendix A.

The curve was calculated from the tabulated values of Mott and Massey (ibid) and is that which is predicted by the Born approximation.

The experimental values have been normalised to the curve at a scattering angle of 60°.

It can be seen that the first Born approximation accurately predicts the shape of the differential cross section for the elastic scattering of 100 electron volt electrons from atomic hydrogen over the angular range from 40° to 130°. However the experimental values are greater than the theoretical at scattering angles less than 40°.

(iv). 200 electron volts.

The ratios of the differential cross section for elastic scattering of 200 electron volt electrons from atomic and molecular hydrogen are shown in Appendix A.

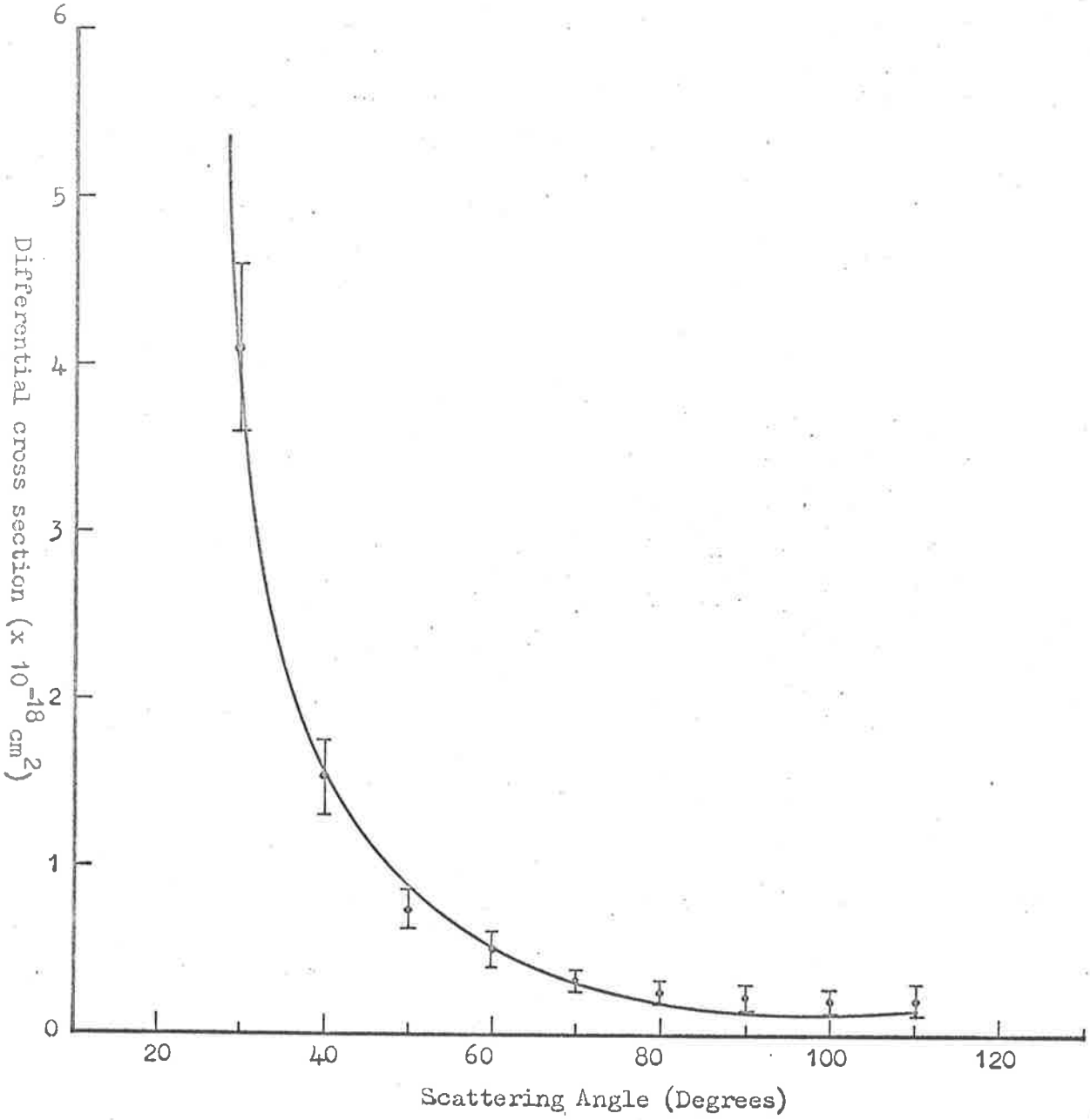

Fig. 5.15. Elastic scattering of 200 e.v. electrons from atomic hydrogen.
Present values (• •) normalised to Born approximation (——) at 60°.
Error bars denote ± one standard deviation in the value of Q_A/Q_M.

The angular distribution for elastic scattering of 200 electron volt electrons from atomic hydrogen was obtained by multiplying the ratio at each angle by the scattered intensity from the molecule at that angle.

The experimental points obtained in this way are shown in figure 5.15 and have been normalised to the theoretical curve at a scattering angle of 60°.

The theoretical differential cross section was obtained from the values of Mott and Massey in the same way as the curve for an incident energy of 75 electron volts.

It can be seen from figure 5.15 that the agreement between the theoretical values and the present results is very good for scattering angles between 30° and 90°. The values at 100° and 110° which lie above the curve reflect the accuracy of the measurement rather than any failure in the Born approximation.

V.5. Discussion of Errors.

The major contribution to the error in the ratio of the differential cross sections, Q_A/Q_M, came from the statistical error in $S(T)$ and S_B which were used in equation 5.10. It has been noted in section IV.1(c) that the variance of the beam signal was caused

by the statistical fluctuation in the number of electrons scattered from the background. In order to determine $S(T)$, up to 20 points were taken at 2750°K for a particular angle and a particular energy. $S(T)$ was obtained by taking the mean of these points and the standard deviation of the mean was calculated from the relation

$$\sigma_{mean} = \sqrt{\frac{\Sigma S(T)_i - \bar{S}(T)}{N(N-1)}}$$

The relative error in $\bar{S}(T)$, the mean value of $S(T)$, was then

$$\frac{\sigma_{mean}}{\bar{S}(T)}$$

S_R, and the error in S_R, was calculated in a similar fashion.

The error in Q_A/Q_M arose from the combination of the errors in $S(T)$ and S_R. The error bars in figures 5.13 to 5.17 represent $\pm$ one standard deviation in the value of Q_A/Q_M.

In order to check for possible sources of systematic error in the atomic hydrogen studies, an angular distribution of 100 e.v. electrons from argon was measured with 300 amps flowing through the oven. If the magnetic field associated with this large current influenced the paths of the scattered electrons in the scattering chamber, the influence would have been apparent in the distribution.

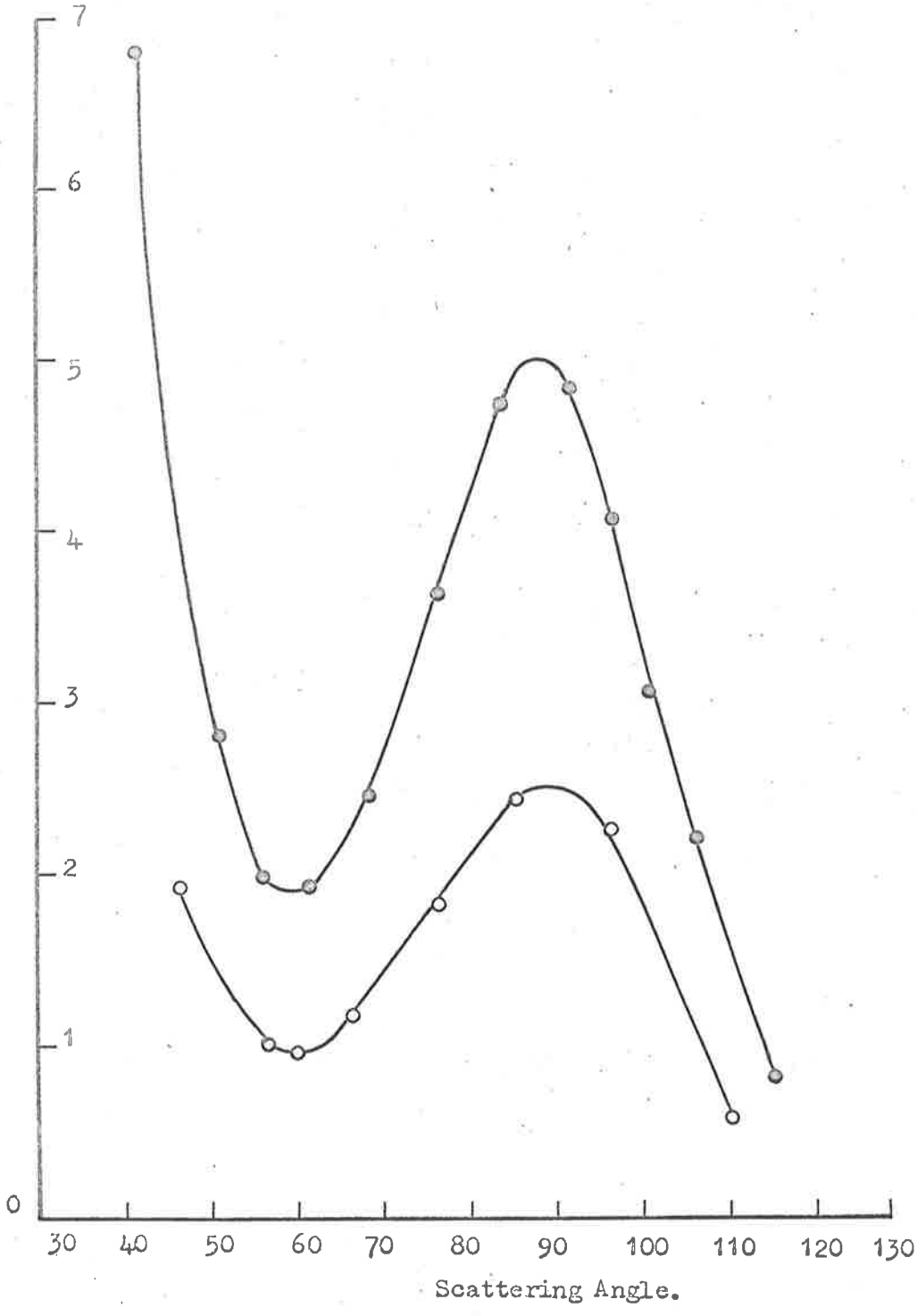

Fig. 5.16. Angular distribution of 100 e.v. electrons from argon taken at room temperature (•••) and with 300 amps flowing through the source (ooo)

Figure 5.16 shows the measured distributions with the beam at room temperature and with the beam at 1700°K. Since the shapes of the distributions were identical it can be assumed that no systematic error was introduced by the magnetic field of the oven.

Since the molecular hydrogen dissociated at temperatures in excess of 1700°K it was not possible to check the inverse root T relationship up to temperatures where the ratio of the elastic scattering cross sections was measured using hydrogen. Therefore argon was used to test the relationship predicted by equation 5.6. at temperatures greater than the threshold for the dissociation of the hydrogen molecule.

Figure 5.17 is a log-log plot of the elastically scattered electron signal from argon as a function of the source temperature. The incident energy was 200 electron volts and the scattering angle was 50°. The slope of the line is -0.49 ± 0.02 from room temperature to 2500°K.

The fact that the line has a slope of -0.5 offers evidence that there was negligible contribution to the atomic beam signal from gas entering the interaction region from the chopping chamber which was not in the beam. If such an effect was present it would have been more noticable with argon than with hydrogen because the

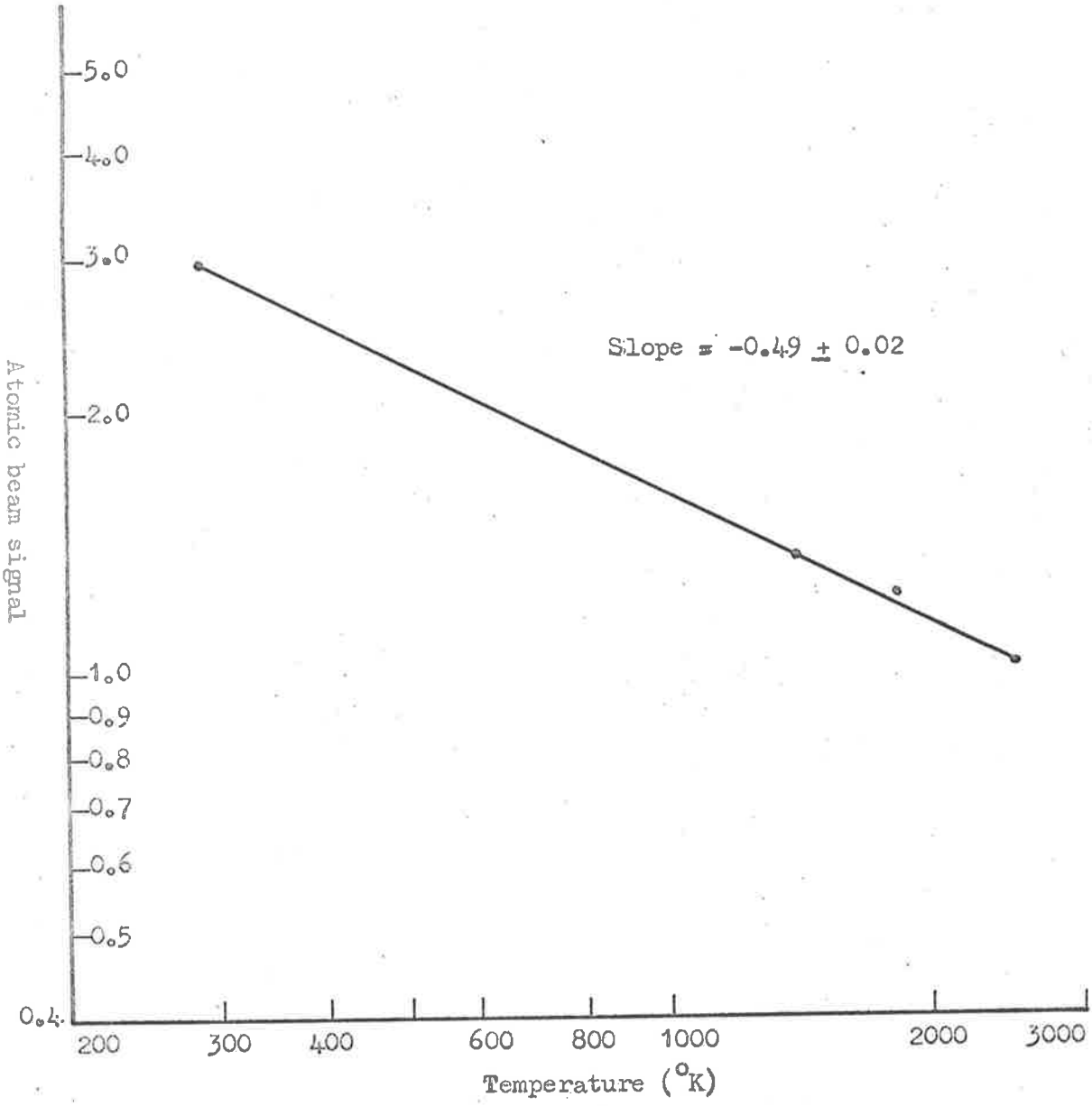

Fig. 5.17. Variation of elastically scattered signal from argon with source temperature. Electron beam energy 200 e.v.; scattering angle 50°.

pumping speed of the chopping chamber pump was much less for argon than for hydrogen. Since gas streaming through from the chopping chamber would not have been at the temperature of the beam any errors caused by this streaming would have been apparent in figure 5.17.

There have been two determinations of the absolute ionisation cross section for atomic hydrogen; the one already mentioned by Fite and Brackmann (1958) and a measurement by Rothe et al. (1962). The lower limit of the Rothe et al. data is 100 e.v. and at 100 e.v. the cross sections differ by about 25%. The effect of this discrepancy on the value of D calculated from equation 5.4 was only 5% in the value of D when D = 0.75. However, there is good agreement between the Fite and Brackmann data and a relative angular distribution measurement of Boyd and Boksenberg (1959). Also good agreement was obtained in the present work between values of D calculated from equation 5.4 using incident energies of 75 electron volts and 100 electron volts and the ionisation cross sections of Fite and Brackmann.

V.6
Conclusions.

The present measurement of the angular distribution for elastic scattering of 50 electron volt electrons from atomic hydrogen has shown that the close-coupling expansion does not describe the

small angle scattering very accurately. Because of the finite number of l values which have been used in the calculation it is not possible to say whether the lack of agreement between theory and experiment is due to a breakdown in the close coupling expansion or whether insufficient terms have been used in the series for the differential cross section. In view of the large number of terms which must be used it is clear that the close coupling expansion has rather limited usefulness at an incident energy of 50 electron volts.

Since the distortion polarisation approximation also underestimates the small angle scattering at 50 electron volts other approximations must be tried. The present results at 50 electron volts will provide a basis for testing the results of the calculations.

As the incident energy is increased, it has been found that the first Born approximation becomes more accurate in the prediction of small angle scattering of electrons from atomic hydrogen. These results support the deduction of Mott and Massey (1965) that the first Born approximation should be fairly accurate in the description of the angular distribution of elastic scattering of electrons from atomic hydrogen for incident energies greater than 75 electron volts.

APPENDIX A.

The ratios of the differential cross section for elastic scattering of atomic to molecular hydrogen measured at several scattering angles for incident energies of 50, 75, 100, and 200 e.v.

Scattering Angle.	Q_A/Q_M	
	50 e.v.	75 e.v.
25	0.61 ± 0.071	0.67 ± 0.03
30	0.60 ± 0.03	0.61 ± 0.04
35	0.54 ± 0.04	
40	0.60 ± 0.03	.71 ± .03
45	0.64 ± 0.07	
50	0.64 ± .05	.65 ± .05
60	0.58 ± .04	.93 ± .15
70	0.63 ± .07	.82 ± .1
80	0.74 ± .07	
90	0.73 ± .14	0.95 ± 0.25
100		1.00 ± 0.25
110		0.79 ± .19
120		0.43 ± .13

Scattering Angle	Q_A/Q_M	
	100 e.v.	200 e.v.
25	0.79 ± 0.04	
30	0.78 ± 0.08	0.85 ± .11
40	0.70 ± 0.04	0.82 ± .12
50	0.79 ± 0.04	0.65 ± 0.08
60	0.83 ± 0.08	0.6 ± 0.15
70	0.8 ± 0.20	0.59 ± 0.06
80	.79 ± 0.10	0.65 ± 0.1
90	0.68 ± 0.04	0.55 ± 0.09
100	0.64 ± 0.11	0.75 ± 0.2
110	.45 ± .097	0.71 ± .25
120	.39 ± 0.14	

APPENDIX B.

(Inelastic Scattering of Electrons from Atoms).

INTRODUCTION.

The experiments which have been described in Chapter IV and V were concerned with the elastic scattering of electrons from atomic systems. The techniques which were used in these experiments can also be applied to the determination of angular distributions of inelastically scattered electrons from atoms. Several experiments were undertaken to determine whether the apparatus, which has been described in the preceding sections, could be used to measure the angular distribution of electrons which had suffered a loss in energy after exciting the atoms. The results of these experiments are given in this Appendix.

1. INELASTIC SCATTERING FROM ATOMIC HYDROGEN.

In view of the discrepancy which exists between the laboratory measurements of the total cross section for the excitation of Lyman-α photons from the 2P-1S transition in atomic hydrogen and the theoretical predictions (Smith 1965), a measurement of the differential cross section for electrons which have lost 10.17 e.v. in a collision with hydrogen atoms would be very useful.

Such a measurement has an advantage over the elastic scattering process because of the fact that an electron scattered from the atom is uniquely specified over that scattered from the molecule in a mixed beam.

However the absolute value of the differential cross section for the inelastic scattering process varies so rapidly that for scattering angles greater than 30°, the differential cross section is at least an order of magnitude less than the cross section for the elastic scattering process. Mott and Massey (1965) have tabulated the differential cross section for 1S-2P transition from 0° to 40° at energies of 100, 200, 400 electron volts. At 0° and 100 e.v. the predicted value is 99.8 a_o^2 per steradian whereas at 30° the value has dropped to 0.024 a_o^2. For the elastic scattering case at 30° and 100 e.v., the differential cross section is 0.31 a_o^2 per steradian. At 40° the ratio of inelastic scattering to elastic scattering has decreased to 1:50. Thus the scattered electron flux through angles greater than 30° would be expected to be very small.

It has been possible to measure an energy loss spectrum from atomic hydrogen using the modulated crossed beam technique and the apparatus which has been described in the preceding section.

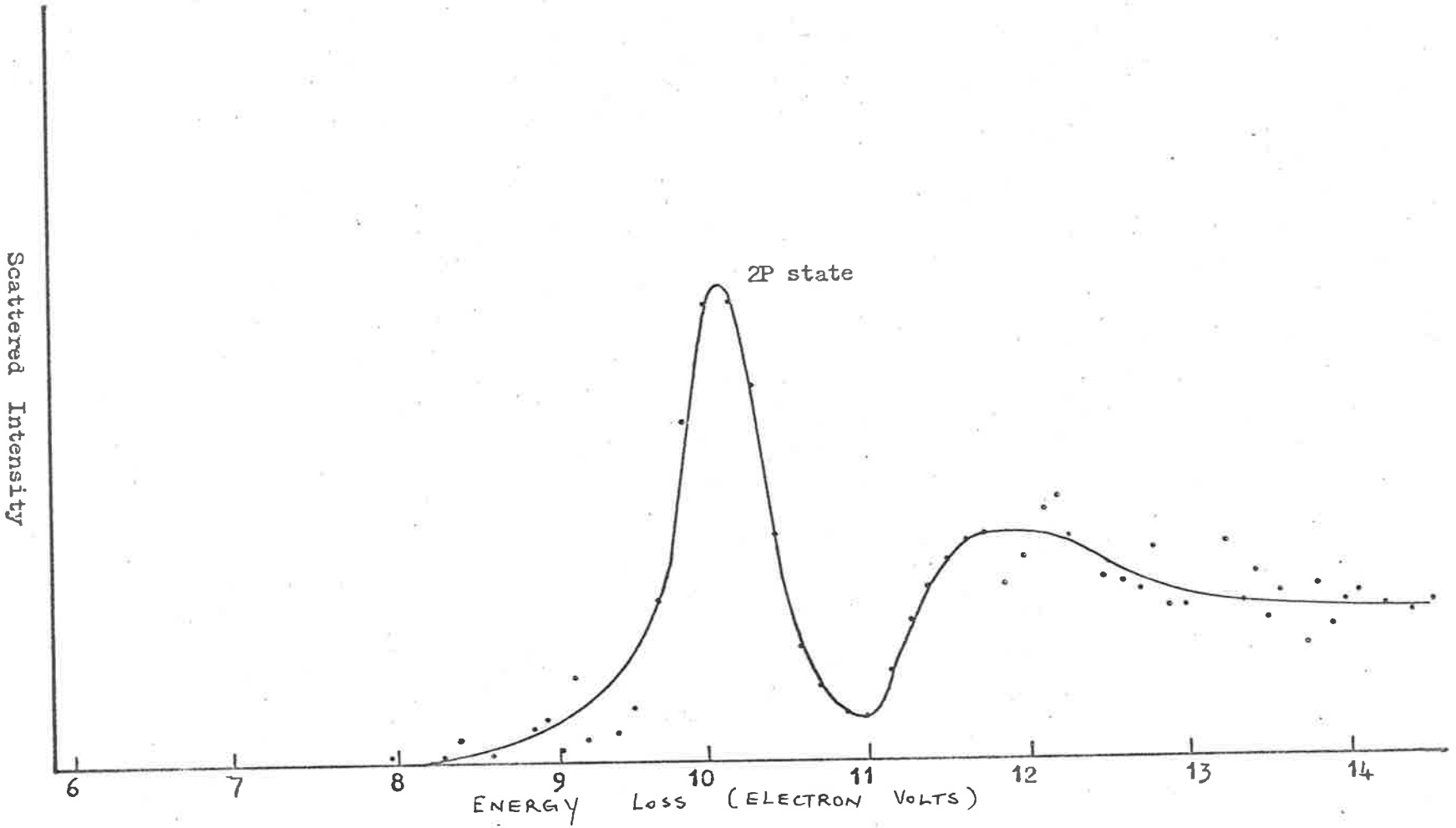

Fig. B.1: Energy loss spectrum of electrons from atomic hydrogen showing 2P state; incident energy 100 e.v.; scattering angle 25°

The spectrum is shown in figure B.1. The incident energy was 100 electron volts and the scattering angle was 25°.

The source pressure was 3 torr and the source temperature was 3000°K. Each point shown in the spectrum resulted from an integrating time of 400 seconds.

The peak was centred at 10.15 ± 0.05 electron volts from the elastic scattering peak which is not shown in the figure. The contribution of molecular hydrogen at the peak position was negligible. The ratio of the elastic scattering peak height to the inelastic scattering peak height was approximately 10:1. Because of the high source pressure which was used it was not possible to define the ratio more precisely because of the breakdown in the $T^{\frac{3}{2}}$ relationship which has been indicated in section V.3.

Figure B.1 shows that it is possible to use the apparatus to determine the differential cross section for the excitation of a composite of the 1S-2S and 2P states.

B.2. Inelastic Scattering from Helium.

Mohr and Nicoll (1932) have measured the differential cross section for electrons which have excited the 2¹P state in helium in the energy range from 20 to 100 electron volts.

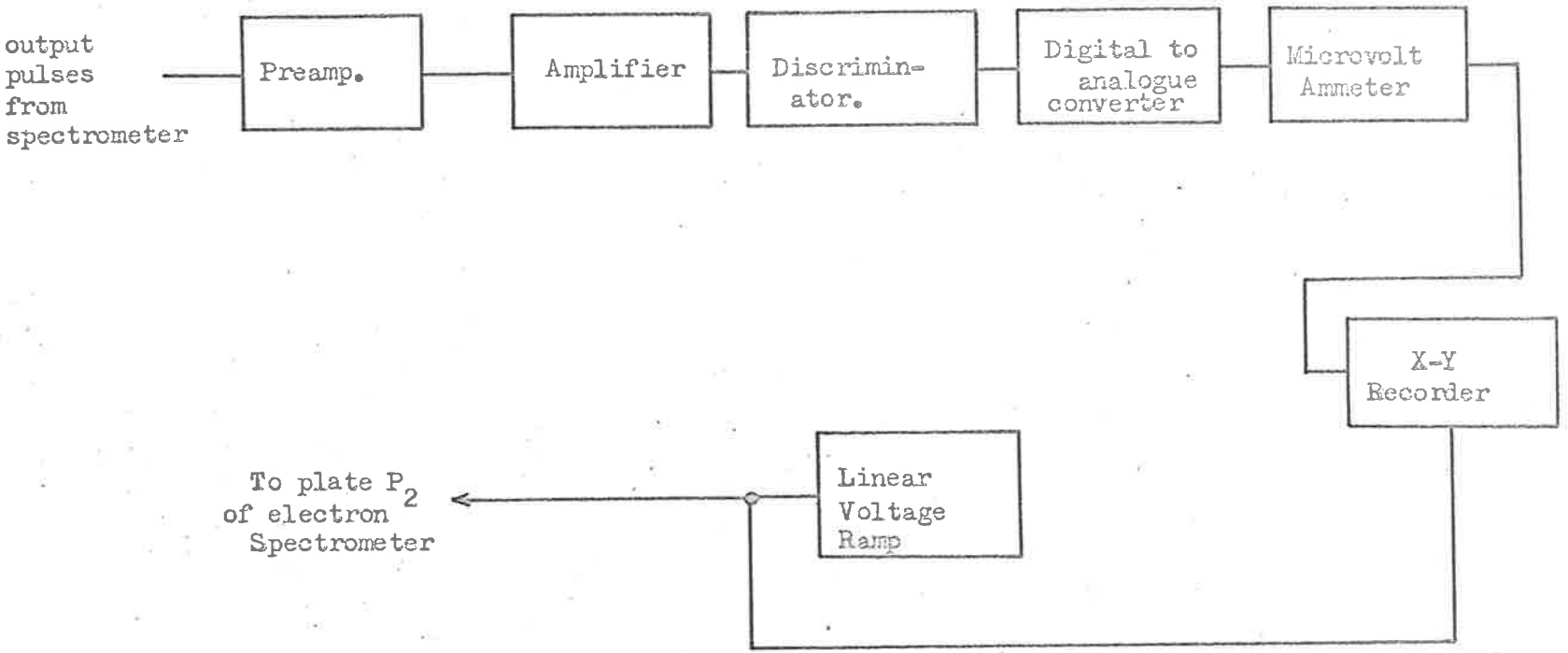

Fig. B.2. Block diagram of electronics used to record energy loss spectra of electrons from helium.

A study has been made of the angular distribution of inelastically scattered electrons from 25° to 35° for an incident energy of 50 electron volts. D.C. techniques were used.

The procedure was to evacuate the scattering chamber to a base pressure of approximately 1.6×10^{-6} torr. Helium was admitted to the system to a pressure of 7×10^{-6} torr. A negative potential was placed on plate P_2 of the spectrometer in the form of a linear ramp and was fed in parallel to the X axis of the X-Y recorder. The output pulses from the particle multiplier tube were fed through the amplifier network shown in figure B.2 into the digital to analogue converter which has been described in section IV.1. The output from the digital to analogue converter was fed via a microvolt ammeter to the Y axis of the X-Y recorder.

Figure B.3 is an energy loss spectrum of electrons scattered from helium. The incident energy was 50 electron volts and the scattering angle was 25°.

The difference in energy ΔE between the elastic scattering peak and a peak corresponding to an excited state as measured on the spectrum, is from equation 4.3

$$\Delta E = k \Delta \nu \qquad (6.1)$$

where k was defined in section IV.1.

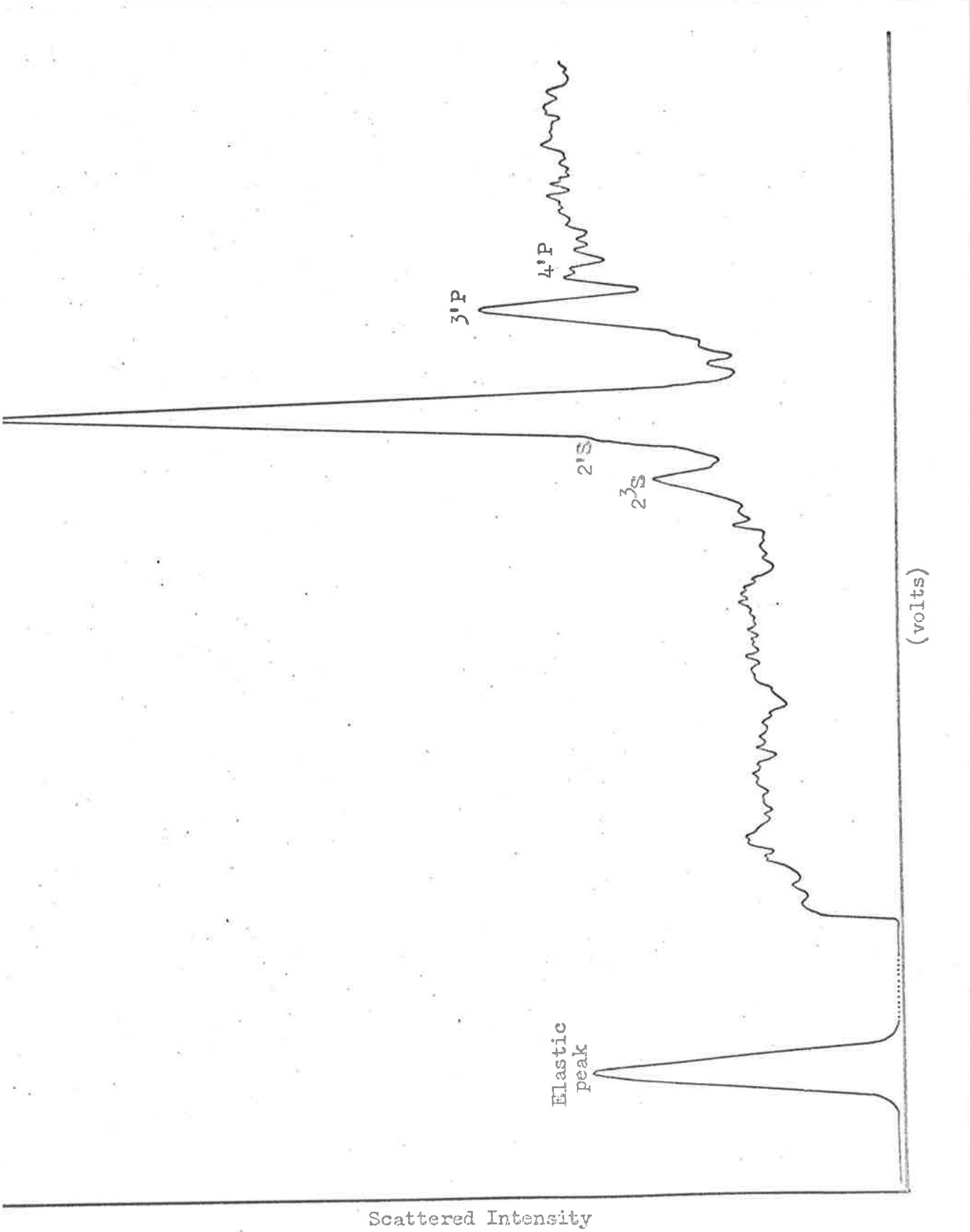

Fig. B.3. Energy loss Spectrum of electrons from helium. Incident energy 50 e.v. Scattering angle 25°.

Table B.1 shows the values Δ v measured from the elastic scattering peak to the various excited states shown in the spectrum. The absolute energy difference Δ E between the ground state and the various excited states are also shown in Table B.1 and were found by putting k = 1.32 in equation 6.1.

Table B.1.

State	Δ v (volts)	Δ E (e.v.)	Δ E (optical) from Moore
2^3S	15.1	19.9	19.8
2^1S	15.65	20.6	20.6
2^1P	16.1	21.2	21.2
3^1P	17.5	23.1	23.07
A^1	18.0	23.7	23.73

The energy loss from the optical measurements were taken from the table of energy levels of Moore (1949) and it can be seen that the present electron excited states agree favourably with the optical values from Moore (1949).

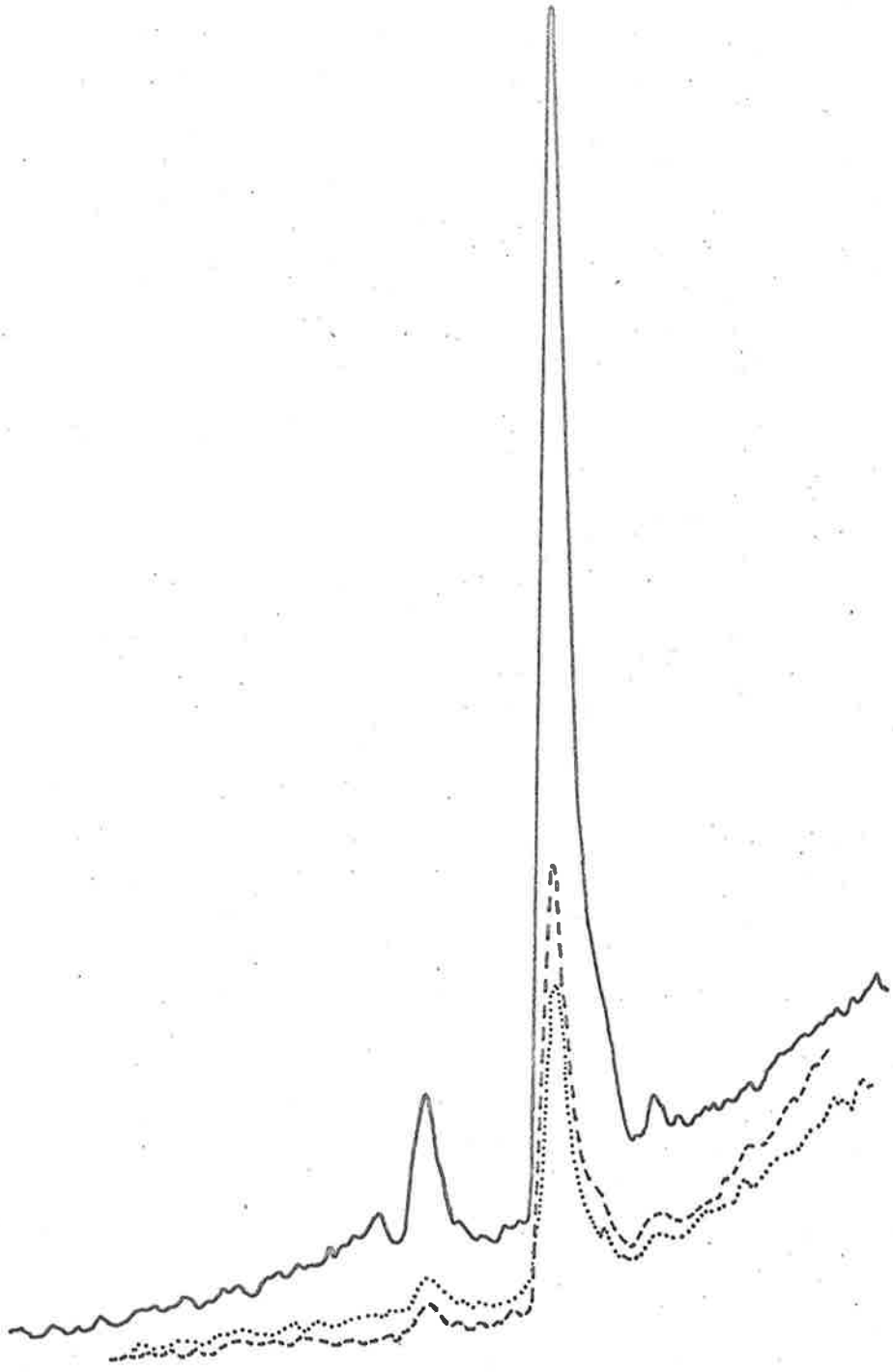

Fig. B.4. Energy loss spectra of electrons from helium which are observed at 25° (——); 30° (- - -) and 35° (·····).

The 2^3S, 2^1P, 3^1P, and 4^1P states are clearly resolved. The asymmetry on the left-hand side of the 2^1P peak is due to the contribution of the 2^1S state. The peak due to excitation of 2^1S state could be determined by subtracting the signal on the right-hand side of the 2^1P peak from that on the left. The resulting peak was centred at 20.6 electron volts which agrees with the value from the optical measurements.

The spectrum shown in figure B.3 is of much higher resolution than that given by Mohr and Nicoll (1932) of inelastic scattering from helium. However even better spectra have been reported by Chamberlain, Heideman, Simpson, and Huyatt (1965) for 0° scattering in helium, using the hemispherical spectrometer of Simpson (1964). Nevertheless the present apparatus has sufficient resolution at 50 electron volts for it to be used in angular distribution studies of the n = 2 excited states in helium.

To measure the angular distribution of these states the gun was rotated and the spectrometer was kept fixed.

The energy loss spectra shown in figure B.4 were recorded.

The peak heights of the various states have been plotted in figure B.5 as a function of angle.

Several features are apparent from figure B.5. Firstly the rapid fall in the peak height of the 2^1P state. Such a rapid drop is characteristic of a state due to an electric dipole transition and

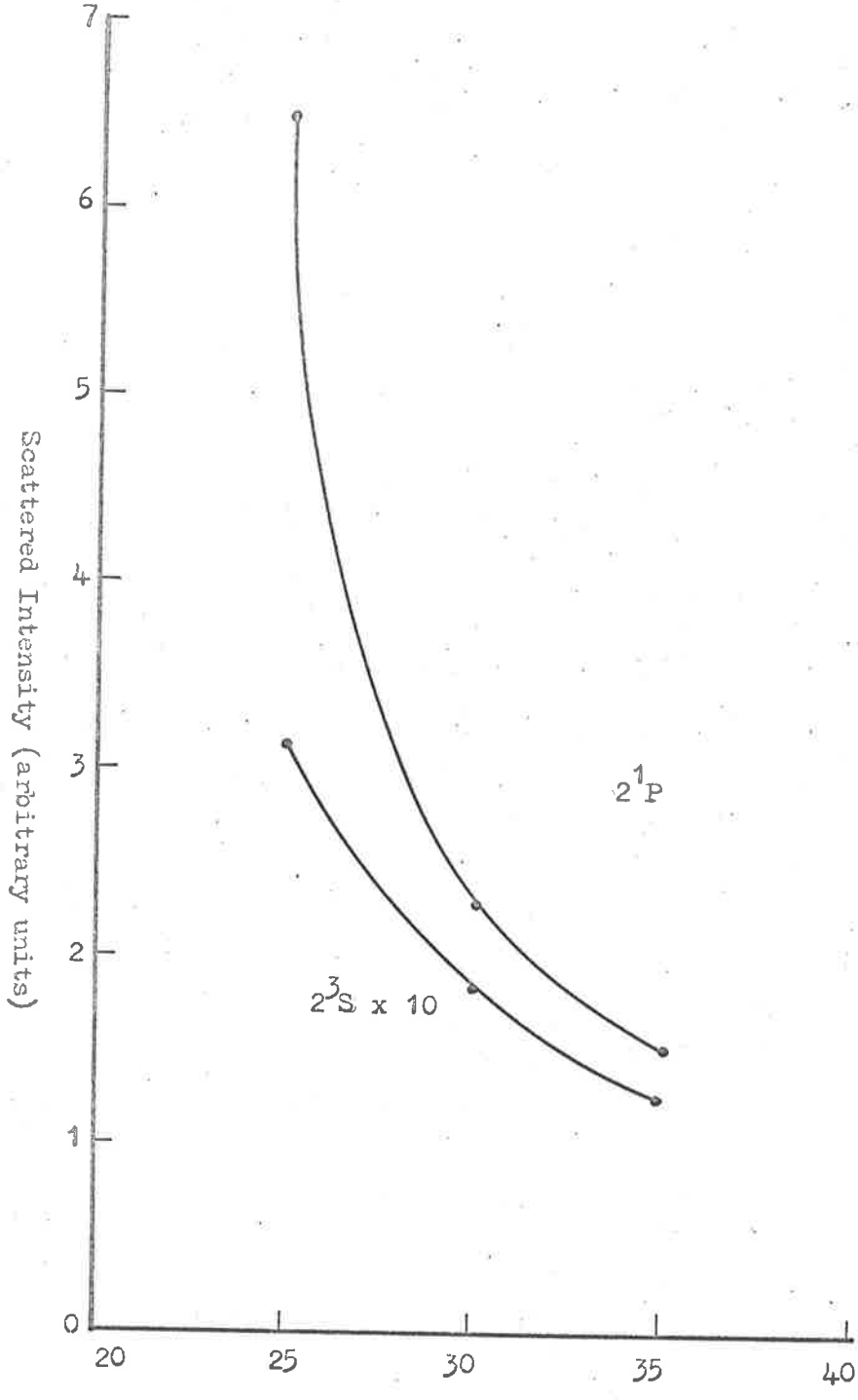

Fig. B.5. Variation of peak heights of 2^1P and 2^3S states with angle.

is caused by the large number of phase shifts which are used to describe the transition.

The second feature is the small variation in scattered intensity of electrons which have excited the 2^3S state. Such an excitation involving a change in multiplicity is strongly forbidden under photon bombardment. In the case of electron bombardment however the total spin of the atom and incident electron must be conserved. Therefore the change in multiplicity of the atom can only arise from the exchange of the incident with the atomic electron. Thus only a few partial waves will contribute to the cross section and the variation of scattered intensity with angle will not be as marked as is the case for the 2P state.

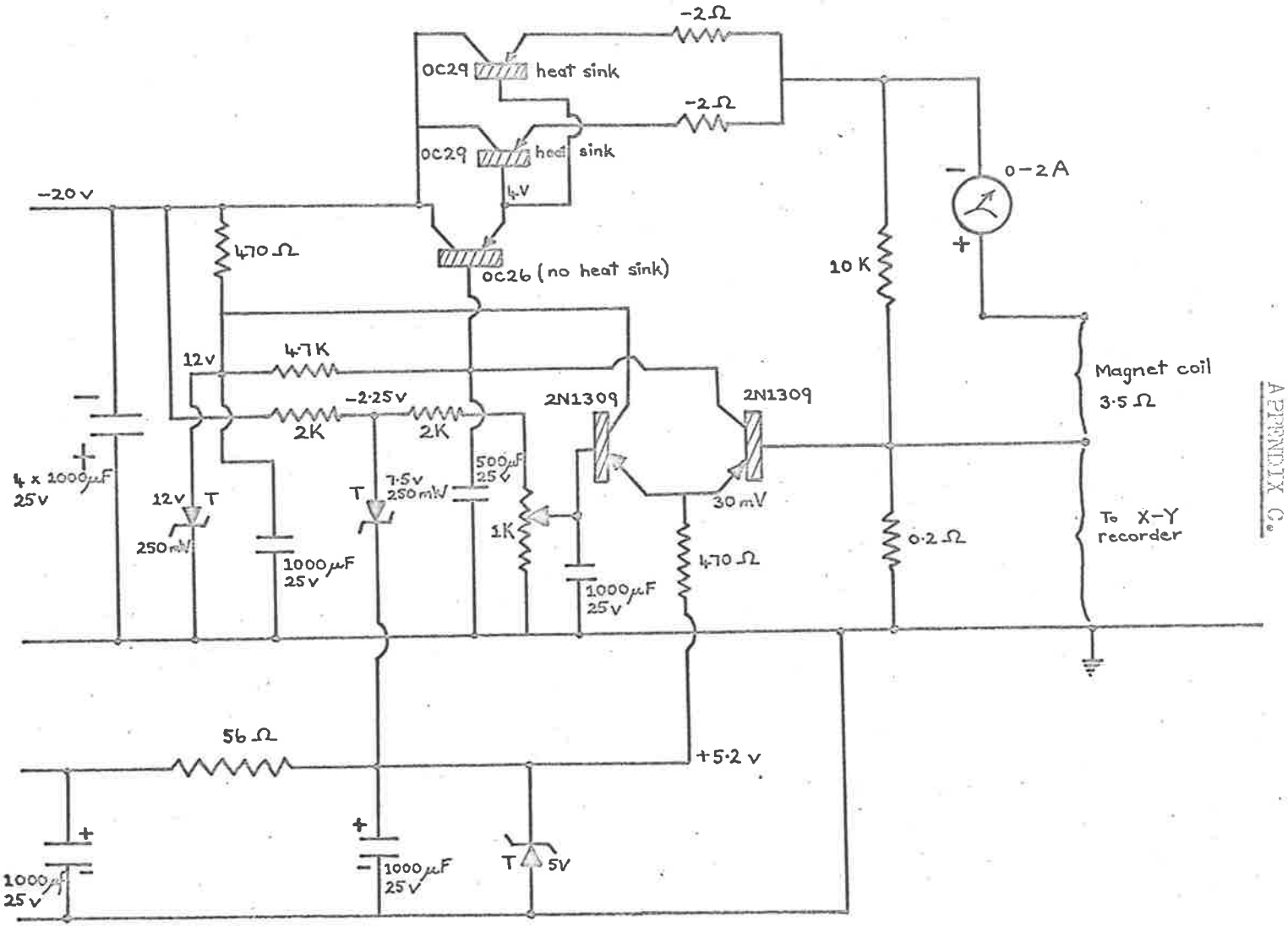

Current supply for Mass Spectrometer Magnet.

Arnot, F.L. (1931).

Proc.Roy.Soc. (A), 133, 615.

Ausburn, K. (1964).

Brit.J.App.Phys., 34, 111.

Banerjee, S.N., Jha, R., and Sil, N.C. (1966).

Ind.J.Phys., 40, 489.

Bederson, B., Malamud, M., and Hammer, J. (1957).

Bull. Am.Phys.Soc., 2, 122.

Born, M. (1926).

Z.Physik., 38, 803.

Boyd, R.L.F., Boksenburg, A. (1959).

Proceedings of the Fourth International Conference on Ionization Phenomena in Gases (Uppsala) p.529.

Boyd, R.L.F., and Green, G.A. (1958).

Proc.Phys.Soc., (London), 71, 351.

Brackmann, R.T., Fite, W.L., and Neynaber, R.H., (1958).

Phys.Rev., 112, 1157.

Bullard, E.C., and Massey, H.S.W. (1931).

Proc.Roy.Soc., A, 130, 637.

Burke, P.G., Ormonde, S., and Whitaker, W. (1966).

Phys.Rev.Lettera, 17, 800.

Burke, P.G., Schey, H.M., and Smith, K. (1963).

Phys.Rev., 129, 1258.

Burke, P.G., and Smith, K. (1962).

Revs. Modern Phys., 34, 458.

Castillejo, L., Percival, I.C., and Seaton, M.J. (1960).

Proc.Roy.Soc., A, 254, 259.

Chamberlain, G.E., Heideman, H.G.M., Simpson, J.A., and Kuyatt, C.E.(1965)

Abstracts of Fourth International Conference on the Physics of Electronic and Atomic Collisions (Quebec) p.378.

Currie, M.R. (1958).

Proc.Inst.Radio Engrs., 46, 911.

Danielson, W.E., Rosenfeld, J.L., and Saloom, J.A. (1956).

Bell Systems Tech.Journal, 35, 375.

Dushman, S., and Lafferty, J.M. (1963).

Scientific Foundations of Vacuum Technique (Wiley - New York, London).

Faxen, H., and Holtsmark, J. (1927).

Z.Physik, 45, 307.

Fite, W.L. (1962).

"Atomic and Molecular Processes", Ed. Bates. (Academic Press - New York and London.)

Fite, W.L., and Brackmann, R.T. (1958).

Phys.Rev., 112, 1141.

Fite, W.L., and Brackmann, R.T. (1958a).

Phys.Rev., 112, 1151.

Fite, W.L., Brackmann, R.T., and Snow, W.R. (1958).

Phys.Rev., 112, 1161.

Fite, W.L., Gerjuoy, E. (1965).

Science, 150, 516.

Fite, W.L., Stebbings, R.F., and Brackmann, R.T. (1959).

Phys.Rev., 116, 356.

Foner, S.N., Hudson, R.L. (1962).

J.Chem.Phys., 36, 2681.

Fox, R.E., Hickam, W.M., Grove, D.J., and Kjeldaas, T. (1955).

Rev.Sci.Inst., 26, 1101.

Franck, J., and Hertz, G., (1914).

Deutsche Physikalische Gesell Schraft, 16, 457.

Frost, L.S., Furl, O.T., and Johnson, R.E., (1962).

Proc.Inst.Radio Engrs., 50, 1800.

Gerjuoy, E., (1965).

Physics Today, 18, No. 45, page 24.

Gilbody, H.B., and Ireland, J.V. (1963).

Proc.Roy.Soc., A, 277, 137.

Gilbody, H.B., Stebbings, R.F., and Fite, W.L. (1961).

Phys.Rev., 121, 794.

Green, L.C., Mulder, M.M., Lewis, M.N., and Woll, J.W. (1954).
Phys.Rev., 93, 757.

Handbook of Chemistry and Physics (1958). Hodgman C.D. (ed.)
Chemical Rubber Publishing Co., Cleveland, Ohio.

Harrower, G.A., (1955).
Rev.Sci.Inst., 26, 850.

Hendrie, J.M. (1954).
J.Chem.Phys., 22, 1503.

Hils, D., Kleinpoppen, H., and Koschmider, H. (1966).
Proc.Phys.Soc., (London), 89, 35.

Holtzmark, J. (1929).
Z.Physik, 55, 437.

Hughes, A.L., and McMillen, J.H. (1932).
Phys.Rev., 39, 585.

Hughes, A.L., McMillen, J.H., and Webb, G.M. (1932).
Phys.Rev., 41, 154.

Hughes, R.C., Coppola, P.P. (1957).
Philips Technical Review, 19, 179.

Hummer, D.G., and Seaton, M.J. (1961).
Phys.Rev.Letters, 6, 471.

Khare, S.P., Moiseiwitsch, B.L. (1965).
Proc.Phys.Soc., (London), 85, 821.

Kingston, A.E., Moiseiwitsch, B.L., and Skinner, B.G. (1960).

Proc.Roy.Soc., A, 258, 237.

Kingston, A.E., and Skinner, B.G. (1961).

Proc.Phys.Soc., (London), 77, 724.

Klemperer, O., (1953).

"Electron Optics" (Cambridge University Press).

Kroll, N.A., and Gerjuoy, E. (1961).

Second International Conference on the Physics of Electronic and Atomic Collisions (W.A. Benjamin Inc. New York) p.23.

Kuyatt, C.E., and Simpson, J.A. (1964).

"Atomic Collision Processes", (Ed. M. McDowell, North Holland Publishing Company), p.191.

Lamb, W.E., and Retherford, R.C. (1950).

Phys.Rev., 79, 549.

Langmuir, I., (1915).

J.Amer.Chem.Soc., 37, 442.

Lassettre, E.N., Berman, A.S., Silverman, S.M., and Krasnow, M.E.(1964).

J.Chem.Phys., 40, 1232.

Lichten, W., and Schultz, S. (1959).

Phys.Rev., 116, 1132.

Lockwood, G.J., Helbig, H.F., and Everhart, E. (1964).

J.Chem.Phys., 41, 3820.

Mac Dougall, J. (1932).

Proc.Roy.Soc., A, 136, 549.

McGowan, J.W., and Fineman, M.A., (1965).

Abstracts of Fourth International Conference on Physics of Electronic and Atomic Collisions (Quebec) (Science Bookcrafters Inc., New York) p.429.

Massey, H.S.W. (1956).

Handbuch Der Physik, 36, 307. S. Flügge - ed. (Springer Verlag, Berlin).

Massey, H.S.W. (1956a).

Revs. Modern Phys., 28, 199.

Massey, H.S.W. (1964).

Atomic Collision Processes. Edited by M.R.C. McDowell (North Holland Publishing Co. Amsterdam) p.3.

Massey, H.S.W., and Burhop, E.H.S. (1952).

"Electronic and Ionic Impact Phenomena" (Oxford Clarendon Press).

Massey, H.S.W., and Mohr, C.B.O., (1932).

Proc.Roy.Soc., A, 136, 289.

Massey, H.S.W., and Mohr, C.B.O. (1934).

Proc.Roy.Soc., A, 146, 880.

Mehr, J. (1967).

Z.Physik, 198, 345.

Mohr, C.B.O., and Nicoll, F.H. (1932).

Proc.Roy.Soc., A, 138, 229.

Moiseiwitsch, B.L. (1962).

"Atomic and Molecular Processes", Edited by Bates

(Academic Press, New York, London).

Moiseiwitsch, B.L., and Williams, A. (1959).

Proc.Roy.Soc., A, 250, 343.

Moore, C.E., (1949).

"Atomic Energy Levels", U.S. Dept. of Commerce; National

Bureau of Standards.

Mott, N.F., and Massey, H.S.W. (1965).

"Theory of Atomic Collisions" (Oxford University Press,

London) Third Edition.

Neynaber, R.H., Marino, L.L., Rothe, E.W., and Trujillo, S.M. (1961).

Phys.Rev., 124, 135.

Ochkur, V.I., (1964).

Soviet Physics. J.E.T.P., 18, 503.

Oppenheimer, J.R. (1928).

Phys.Rev., 32, 361.

Perteus, J.O., (1964).

"Atomic Collision Processes" edited by M.R.C. McDowell

(North Holland Publishing Co. Amsterdam) p.537.

Pierce, J.R. (1949).

"Theory and Design of Electron Beams" (D. Van Nostrand Co. Inc. Toronto, New York, London).

Ramsey, N.F. (1956).

"Molecular Beams" (Oxford Clarendon Press).

Rothe, E.W., Marino, L.L., Neynaber, R.H., and Trujillo, J.M. (1962).

Phys.Rev., 125, 582.

Scott, B.L. (1965).

Phys.Rev., 140, A, 699.

Scott, B.L. (1967).

Private Communication.

Simpson, J.A. (1964).

Rev. Sci.Inst., 35, 1698.

Simpson, J.A., and Kuyatt, C.E. (1963).

Rev.Sci.Inst., 34, 265.

Smith, S.J. (1965).

Abstracts of the Fourth International Conference on the Physics of Electronic and Atomic Collisions (Science Bookcrafters New York), p.377.

Stebbings, R.F., Fite, W.L., Hummer, D.G., and Brackmann, R.T. (1960).

Phys.Rev., 119, 1939.

Spangenburg, K.R. (1948).

"Vacuum Tubes", McGraw-Hill Book Co. Inc. (New York, Toronto, London).

Spangenburg, K.R., Field, L.M., and Helm, R., (1942).
"The Production and Control of Electron Beams",
(Federal and Telephone Radio Corp. - New York).

Trodden, W.G., (1959).
Proc. I.E.E., 106B, 389.

Wallmark, J.T. (1955).
Brit.J.App.Phys., 2k, 590.

Webb, G.M., (1935a).
Phys.Rev., 47, 379.

Webb, G.M. (1935b).
Phys.Rev., 47, 384.

Yarnold, G.D., and Bolton, H.C. (1949).
J.Sci.Inst., 26, 38.